Chemical Reviews

Volume 82, Number 5 October 1982

Aqueous Oxidation of Pyrite by Molecular Oxygen

RICHARD T. LOWSON

Environmental Science Division, Australian Atomic Energy Commission, Lucas Heights Research Laboratories, Sutherland, NSW 2232, Australia

Received February 15, 1982

Contents

Richard Lowson was born and educated in the United Kingdom. Prior to his undergraduate studies he spent two years working as a laboratory assistant with ICI. He graduated in 1965 with a B.Sc. (Hons) in Applied Chemistry from the University of Aston in Birmingham, U.K.; he then moved to Imperial College, London, for his postgraduate work under Professor Barrer. In 1968 he was awarded a Ph.D. for research on the flow of gas mixtures through microporous media. He emigrated to Australia in 1969 and joined the staff of the Chemistry Division of the Australia Atomic Energy Commission's Research Establishment. Initially his work was divided between environmental studies associated with uranium mines and the corrosion of nuclear materials. In 1978 he transferred to the recently formed Environmental Science Division of the A.A.E.C. His research effort is now centered around the kinetics and electrochemistry of the aqueous oxidation of pyrite and the physical chemistry of geochemical transport with application to the nuclear industry.

I. Introduction

La pyrite est à l'industrie chimique ce que le pain est à l'alimentration de l'homme (P. Truchot, 1907).[1]

One of the surprising features of modern chemistry is that the chemistry of the new glamor compounds is often known more precisely than the chemistry of iron; the oxidation of pyrite (iron disulfide, FeS_2, fool's gold) is a typical example. Yet there have been references to pyrite as far back as Dioscorides[2] (ca. 75 AD) and Pliny[3] (ca. 77 AD), which can possibly be traced back to Theophrastus in a work written about 315 BC.[4] A ubiquitous material, referred to by Henckel[5] as "The Jack-in-every-street-Pyrite", this compound was used extensively throughout the Middle Ages and in the early days of modern chemistry as the source of vitriol and sulfuric acid. The basic chemistry was defined during

0009-2665/82/0782-0461$06.00/0

the 19th century as a contribution to the general interest in iron and its compounds, an interest that had begun to wane by the beginning of the 20th century. Since this was before the introduction of chemical abstracting services, much of the early definitive chemistry would have been lost but for an encyclopedic treatise by Mellor,[6] who referred extensively to work carried out in the 19th and early 20th centuries.

With the gradual development of alternative sources and processes for the production of sulfuric acid, interest in pyrite had declined to the extent that it was more frequently regarded in mining enterprises as a nuisance, principally because it may present an environmental hazard. This factor has led recently to an increased funding of basic and technical research on pyrite and in a renewed commercial interest.

Pyrite is a common material, which occurs in the most ancient magmatic rocks and in more recent sedimentary deposits. The environmental hazard usually arises during the mining of a sedimentary sulfide deposit with either pyritic overburden or pyritic gangue (gangue is unwanted material contained within an ore body). The hazard occurs at coal mines which have an inorganic sulfur content in the coal of greater than 1%. The value of 1% should be treated with reservation since coals containing pyritic sulfur at levels greater than 1% do not necessarily pose an environmental hazard; on the other hand, the value of 1% does not represent an absolute lower limit below which there will be no environmental hazard. Pyrite also occurs in soils which have been deposited recently under anaerobic conditions such as abandoned rice paddies in Thailand.

The hazard is due to the oxidation of pyrite to ferrous and ferric iron and sulfuric acid following exposure of the pyrite to air. Uncontrolled and frequently unrecognized, at least initially, discharge of the products of oxidation causes extensive environmental damage. In the coal industry this is known as acid mine drainage. If the products are not drained, the basic ferric sulfate (jarosite) precipitates, resulting in an increase in material volume which can cause disastrous soil heave under structures built on pyritic shale. At heavy metal sulfide mines, the ferric ion and sulfuric acid form an ideal acid oxidizing leach solution, which will leach out the below economic grade heavy metals contained within an overburden heap. Uncontrolled discharge of the heavy metal leachate will exacerbate the environmental hazard, particularly in the case of copper, which is the most toxic of the common heavy metals for many species of fish.

Although considerable effort has been expended on attempts to curtail the reaction at mine sites, it is now recognized that enhancement of the reaction will allow commercial recovery of heavy metals from ores and overburdens that are normally considered to have a metal content below economic recovery grade. The method that is known as heap leaching has been used quite extensively to recover copper from low grade ores[7] and, to a limited extent, for the recovery of uranium.[8] Studies have also been carried out on the recovery of other heavy metals by this method.[9] Currently the method is being investigated as a possible means of coal[10] desulfurization.

Early investigations indicated that the chemical oxidation of pyrite is very slow. Subsequently, it was shown that the reaction can be catalyzed by autotrophic bacteria, *Ferrobacillus ferrooxidans*, *Ferrobacillus thiooxidans*, and *Thiobacillus thiooxidans*; recent work on the oxidation of pyrite has concentrated on this aspect. The nomenclature, taxonomy, type, and number of these bacterial species are being constantly revised, and the complexity of the problem has been increased further by the discovery of thermophilic bacteria that can oxidize sulfides at 60 or even 80 °C.[11]

At first the chemistry was viewed as a series of simple chemical reactions that can be observed individually under controlled laboratory conditions. This has been questioned by Bailey and Peters, who, in 1976, demonstrated that the oxidation of pyrite, at least under the conditions of their experiment, namely 110 °C and 6.7 MPa, was electrochemical.[12] This observation has thrown into doubt the conventional wisdom about the chemistry of a leaching heap. A proper understanding of the chemistry is required if the means of controlling the environmental hazard or enhancing the reaction for commercial exploitation are to be devised. Accordingly, the chemistry of the oxidation of pyrite is reviewed here to identify those areas of definitive knowledge and those in which there is need for further work. The environmental hazard is a multidisciplinary problem requiring elucidation by biologists, chemists, and physicists. In this review I address myself strictly to its chemical aspects, at the same time recommending that biological and physical factors be similarly reviewed.

II. Physical Properties of Pyrite and Marcasite

A. The Sulfide Minerals

In general, sulfides are known by their mineralogical names. Unfortunately, this terminology usually bears little relationship to the chemical stoichiometry and is not standardized. Table I, which lists the better known sulfide minerals and is by no means exhaustive, indicates the extensive and, in some cases, complex nature of the sulfide system. This complexity is well illustrated by the iron sulfides. Table II is a compilation of some of the physical and crystallographic properties of iron sulfides taken from tabulations by a number of workers. In addition to the sulfides listed in Table II, a number of subsulfides, Fe_8S, Fe_4S_3, and Fe_7S_6, have been reported as precipitates from various synthetic melts.[6] Since these subsulfides have not been found in nature, they will not be considered further.

Ferric sulfide, Fe_2S_3, was discussed at length by Mellor;[6] although not known to occur naturally, it is the product of the classic schoolboy experiment of heating iron filings with sulfide in a nonoxidizing atmosphere, at a temperature between 450 and 500 °C, until the excess sulfur is expelled. It is also formed by the adsorption of hydrogen sulfide onto ferric oxide at ~40 °C, which was the basis of the technique for removing hydrogen sulfide from coal gas in the early 19th century.

The system is in a delicate state of equilibrium. Hydrated ferric sulfide is formed when hydrated ferric oxide is moistened or suspended in water and treated with an excess of hydrogen sulfide for several hours in the absence of air. If the moistened ferric sulfide is then exposed to hydrogen sulfide in the absence of air, it is transformed to a mixture of ferrous sulfide and ferrous disulfide. Dry ferric sulfide is stable in dry air, but

when moist, it soon converts to ferric oxide and sulfur. Although unstable in the pure state, ferric sulfide occurs in the mineral form as a complex copper ferric sulfide series

chalcopyrite	$CuFeS_2$
barhardite	$Cu_4Fe_2S_5$
bornite	$CuFeS_3$
barracanite	$CuFe_2S_4$
chalcopyrrhotite	$CuFe_4S_6$
chalmersite (rhombic), cubanite (cubic)	$CuFe_2S_3$

Mellor[6] discussed these and other copper iron sulfides that may be added to the above list; the series also includes complex compounds of other heavy metals, including arsenic, nickel, and antimony. Although not discussed further, it should be remembered that chalcopyrite frequently occurs in pyritic seams and that its chemical composition makes it an ideal reagent for galvanic reactions either within itself or as a half-cell to another mineral; as such, this reaction may provide a significant or even dominant leaching mechanism.

B. Appearance and Habit

1. Euhedral Material

There are two forms of iron disulfide, pyrite and marcasite. Pyrite is opaque, of a pale brass yellow color, and irridescent when tarnished. Its streak has been variously reported as greenish black, brownish black, pale brown, and violet. It has a metallic lustre, splendent to glistening. In polished section it is creamy white, isotropic, and sometimes anisotropic and may display pleochroism. It may exhibit zonal growth banding.[6,13]

The crystal form, or habit of pyrite has been discussed by Mellor[6] and, in more detail, Gait;[14] an in-depth study, including 691 drawings of pyrite crystals, was made by Goldschmidt.[15] The most common forms are the cube and the pentagonal dodecahedron; the latter is so characteristic of pyrite that the crystal is also known as the pyritohedron. Other common forms are the octahedron and the diploid. The pyritohedral and cubic faces are almost invariably striated with fine lines caused by oscillatory growth between the cube and the pyritohedron. This is a form of penetration microtwinning.

The direction of twinning controls the sign of the thermoelectric properties; crystals with striae parallel to the cubic edge are thermoelectrically positive with respect to copper whereas those with striae orthogonal to the cubic edge are negative. Crystals are usually extensively twinned, both on a macro- and microscale, with penetration twinning along parallel axes. Microtwinning leads to the formation of repetitive minute crystal faces, which form a large rounded face. Macrotwinning is also the cause of the conchoidal to uneven fracture and the indistinct cleavage at the 100 and 111 plane. A 121 gliding plane has been reported but not confirmed. The crystalline material may be found in massive, fine granular, subfibrous, radiated, reniform, globular, and stalactitic forms.

Marcasite is opaque, of a pale bronze yellow color with a tinge of green, and it has a metallic luster. When newly fractured the color is tin-white. On exposure the color deepens, and owing to the inherent instability of marcasite, a white ferrous sulfate powder develops on the surface. The streak may be greyish black, brownish black, or greenish grey. In the polished section it is strongly anisotropic and pleochroic and varies from creamy white on the 100 face to light yellowish white on the 010 face and white with a rose-brown tint on the 001 face.[6,13]

The common habit of marcasite is pyramidal and tabular, parallel to the 001 face. The brachydomes and pinacoids tend to be deeply striated parallel to the 010/001 edge. Mellor[6] reported that twinning occurs about the 110 plane and less frequently about the 101 plane, the crystals crossing at an angle of nearly 60°; Dana[13] reported the frequency of twinning in the reverse order. Mellor observed that cleavage on the 110 face is rather distinct but that on the 011 face appears in traces, whereas Dana noted that cleavage is distinct on the 101 face and only appears as a trace on the 110 face. Fracture is uneven and/or radiating. Marcasite occurs in stalactitic forms with a radiating internal structure; it also occurs in globular, reniform, and other imitative shapes, which has led to a number of special names, some of which have been discussed by Mellor.[6]

2. Framboidal Pyrite

Discussion up to this point has been about material with a well-developed crystal form. However, the low-grade pyritic material associated with overburden heaps, coal measures, and mine tailings is not graced with such beauty, but more usually is dispersed heterogeneously through a host rock as either massive or granular material. Attempts have been made to classify this material on morphological grounds. In a study by The Ohio State University Research Foundation,[16] the following classification was proposed for pyritic material in coal.

Primary Pyrite	Secondary Pyrite
sulfur ball	secondary replacement pyrite
disseminated pyrite	fracture-filling pyrite
primary replacement pyrite	

Primary pyrite was considered to be deposited contemporaneously with the peat that was subsequently converted to coal. This material was subdivided into three self-descriptive categories. Sulfur ball occurs as large lenses of primary pyrite ranging from 2.5 to 75 mm thick by 30 to 300 mm long and wide, and comprised of 90 to 98% pyrite. The mass is formed from small grains ranging in size from 2 to 5 μm in diameter. These grains tend to agglomerate in spheres, of between 10 and 30 μm diameter. Few crystal faces are evident in the grains, and the agglomerates resemble strawberries, hence the term framboidal after the French *framboise* (strawberry). The Ohio State University workers did not use this term, although Gray and co-workers[17] had earlier called attention to this form in coal.

Disseminated pyrite is, as the name implies, material that is dispersed throughout the host material. It is seldom visible to the naked eye because of its low occurrence and minute size. Its morphology is framboidal, with a grain size of 1–5 μm diameter and an agglomerate size of 5–25 μm diameter. Primary replacement pyrite is a descriptive title for pyritic material that has replaced plant parts such as leaves or even tree trunks and branches. Masses up to 5 kg can occur and are

comprised of individual grains varying in diameter from 50 μm to 1 mm. Many of the grains have well-developed crystal faces that clearly distinguish them from the framboidal agglomerates found in sulfur ball and disseminated pyrite.

Secondary replacement pyrite commonly replaces sulfur ball and primary plant replacement pyrite. The mass is comprised of grains ranging from 0.25 to 2 mm diameter with well-developed crystal faces. Fracture-filling pyrite is descriptive of secondary pyrite that has penetrated and filled fractures in the coal. The material forms flakes, 0.1–0.3 mm thick and up to 0.7–15 mm diameter. Secondary pyrite is not framboidal.

Caruccio and co-workers[18] employed a slightly different classification of

primary massive
plant replacement pyrite
primary euhedral pyrite
secondary cleat (joint) coats
framboidal pyrite

Primary massive pyrite consists of crystalline masses, commonly in the range 150–600 μm diameter, encapsulated by the coal. Plant replacement pyrite is similar to the primary replacement pyrite described by Stiles. Primary euhedral pyrite refers to a small grain (0.5–2 μm diameter) crystalline pyrite that is dispersed through the host coal. The grains may occur discretely, in layers, or in spherical agglomerates. Caruccio[18] referred to the spherical agglomerates as "framboidal pyrite"; however, it would seem preferable to reserve this term specifically to noncrystalline grains and agglomerates of noncrystalline grains. Secondary cleat (joint) coats are equivalent to the fracture-filling pyrite given in The Ohio State University classification. Framboidal pyrite is eqivalent to the disseminated pyrite, although Caruccio and co-workers included crystalline agglomerates within the term. Caruccio did not employ the term "sulphur ball".

In environmental studies, it is simpler to classify pyrite generally as euhedral and framboidal and retain the term framboidal for noncrystalline pyrite having grain sizes typically in the range 0.05–1.0 μm diameter. The grain, termed microcryst by Rickard,[25] is in the form of a bead with no or few crystal faces. The grains may agglomerate to form a small mass, typically 50 μm in diameter, resembling a strawberry or framboid. This classification is based on the observation that framboidal pyrite is very much more reactive than euhedral pyrite.[19-21]

The literature on framboidal pyrite is associated principally with coal and its relationship with acid mine drainage. However it readily occurs in other formations such as the Kupferschiefie in Europe[22] and the barite deposits at Kempfield, NSW, Australia.[23] Grain size may be correlated with the type of host rock, with larger grains occurring in the coal measures. This is probably due to the environmental factors that existed at the time of deposition rather than to a direct interaction by the host rock.

Framboidal pyrite has been discussed by a number of authors.[23-28] Czyscinski[29] showed that framboidal material was formed during the past 30 years beneath abandoned rice paddies in Thailand. It has been suggested that in some cases framboidal pyrite is a necessary precursor to the euhedral form;[28,30] this is supported by the discovery of framboidal cores in euhedral pyrite grains,[31] framboidal cores in euhedral cobaltite,[32] and euhedral overgrowths on dispersed framboids.[33] Caruccio[18,34] observed that in coal seams formed in a brackish marine paleoenvironment a higher proportion of the total sulfur was framboidal rather than euhedral pyrite compared to that associated with coal seams formed in a freshwater paleoenvironment. However, it is not clear whether the brackish marine paleoenvironment favored the formation and retention of framboidal pyrite or prevented the subsequent transformation to euhedral pyrite.

There have been no reports of synthetic framboidal pyrite, but there are several reports of a natural colloidal iron disulfide that occurs in specimens of marcasite.[35-37] Doss[38] reported on a natural iron disulfide hydrogel that occurs in a number of localities. Doss named the gel melnikoffite (or melnikowite, melnikovite) and considered it to be a stage in a series of reactions, troilite gel → melnikoffite gel → melnikoffite → pyrite. Feld[39] showed that the hydrogel of ferrous sulfide passes through a similar series of reactions. Allen and co-workers[40-42] reported the formation of an amorphous iron disulfide from the action of an alkali polysulfide on a solution of ferric sulfate. Melnikoffite does not resemble pyrite; it is black with a steel grey luster and has a specific gravity of 4.2–3 and a hardness of 2–3. Berner[43] has questioned whether these gels should be considered as separate compounds. Rickard[44] discussed the relationship between pyrite genesis, sulfide ion, and metastable ferrous sulfides and ferrous polysulfides in sedimentary iron sulfide formations. The kinetics for pyrite formation have been reported.[45]

C. Crystal Structure

The crystallographic data of the iron sulfides are listed in Table II; however, this listing does not do justice to the extensive discussions that have appeared in the literature on the crystallography of the iron sulfides. Pyrite was first studied by W. L. Bragg in the early days of crystallography. Because of its distinctive structure, pyrite has been allocated its own place in crystal structure typology. Wyckoff[47] grouped pyrite under miscellaneous structures. It is isomorphic with the natural mineral chalcogenides of manganese, cobalt, and nickel and with the synthetic chalcogenides of copper, zinc, and cadmium.[47] Chalcogenides of osmium, ruthenium, and rhodium, a number of salts of the platinum group, and phosphorus, arsenic, antimony, and bismuth also have the same structure. Pyrite crystallizes in the cubic system. The space lattice resembles that of sodium chloride, with Fe^{2+} replacing the sodium and S_2^{2-} replacing the chloride. Although the structure of pyrite cannot be classified as essentially close packed, it is still a very dense material. The four molecules in the unit cube are in special positions T_h^6 ($Pa3$); the following interatomic distances have been collated from Table II and other sources:[6,48]

spacing of the unit cell a_o	0.54175 nm
between two iron atoms on the 110 face	0.382 nm
between two sulfur atoms of the sulfur pair on the 111 axis	0.206 nm
between iron and the center of a sulfur pair on the 001 face	0.270 nm

TABLE I. Mineral Metal Sulfides

name	composition	structure	ref
acanthite	Ag_2S III	monoclinic	50, 208a
alabandite	MnS	cubic	50, 208a
andorite	$PbAgSb_3S_6$	rhombic	208a
argentite	Ag_2S I & II	cubic	50, 208a
argentopyrite	$AgFe_2S_3$	orthorhombic	50
arsenopyrite	FeAsS	triclinic[b]	50
bismuthinite	Bi_2S_3	orthorhombic	50, 208a
bornite	Cu_3FeS_4	high and meta, cubic; low, tetragonal	50, 208a
boulangerite	$Pb_5Sb_4S_{11}$	monoclinic	208a
bouronite	$PbCuSbS_3$	rhombic	208a
braggite	Pts	tetragonal	208a
bravoite	$(Ni,Fe)S_2$	cubic	208a
cattierite	CoS_2	cubic	50
chalcocite	Cu_2S II & III	II hexagonal; III orthorhombic	50, 208a
chalcopyrite	$CuFeS_{1.9}$	tetragonal	50, 208a
cinnabar	HgS	hexagonal	50, 208a
cobaltite	CoAsS	cubic	50, 208a
cooperite	PbS	tetragonal	50
covellite	CuS	hexagonal	50, 208a
cubanite	$CuFe_2S_3$	orthorhombic	50, 208a
daubreelite[a]	Cr_2FeS_4	cubic	50, 208a
digenite	Cu_2S I	cubic	50, 208a
emplectite	$CuBiS_2$	orthorhombic	208a
enargite	Cu_3AsS_4	orthorhombic	208a
famatimite	Cu_3SbS_4	tetragonal	50
galena	PbS	cubic	50, 208a
galenabismuthite	$PbBi_2S_4$	rhombic	208a
gersdorfite	NiAsS	cubic	50
glaucodot	(Co,Fe)AsS	orthorhombic	50
greenockite	CdS	hexagonal	50, 208a
greigite	Fe_3S_4	cubic	50
gudmundite	FeSbS	monoclinic	50
hauerite	MnS_2	cubic	50
hawleyite	CdS	cubic	50
heazelwoodite	Ni_3S_2	rhombohedral	50
herzenbergite	SnS	orthorhombic	50
jalpaite	$Ag_{1.55}Cu_{0.45}S$ III	tetragonal	50
laurite	RuS_2	cubic	50
linnaeite	Co_3S_4	cubic	50
luzonite	Cu_3AsS_4	tetragonal	50
marcasite	FeS_2	orthorhombic	50, 208a
metacinnabar	HgS	cubic	50, 208a
miargyrite	$AgSbS_2$	monoclinic	50
millerite	NiS	hexagonal	50, 208a
molybdenite	MoS_2	hexagonal	50, 208a
oldhamite	CaS	cubic	50, 208a
orpiment	As_2S_3	monoclinic	50, 208a
pentlandite	$Fe_{5.25}Ni_{3.75}S_8$	cubic	50, 208a
polymidite	Ni_3S_4	cubic	50
proustite	Ag_3AsS_3	rhombohedral	50, 208a
pyrargyrite	Ag_3SbS_3	rhombohedral	50, 208a
pyrite	FeS_2	cubic	50, 208a
pyrrhotite	$Fe_{1-0.8}S$	hexagonal	50, 208a
realgar	AsS	monoclinic	50, 208a
shandite	β-$Ni_3Pb_2S_2$	rhombohedral	50
sphalerite	ZnS	cubic	50, 208a
sternbergite	$AgFe_3S_3$	orthorhombic	50
stibnite	Sb_2S_3	orthorhombic	50, 208a
stromeyerite	$Ag_{0.93}Cu_{1.07}S$ III	orthorhombic	50
teallite	$PbSnS_2$	orthorhombic	50
tennantite	$Cu_2As_2S_{13}$	cubic	50
tetrahedrite	$Cu_2Sb_4S_{13}$	cubic	50, 208a
troilite	FeS	hexagonal	50
tungstenite	WS_2	hexagonal	50
ullmannite	NiSbS	cubic	208a
vaesite	NiS_2	cubic	50
violarite	$FeNi_2S_4$	cubic	50
wurtzite	ZnS	hexagonal	50, 208a

[a] Daubreeite. [b] Monoclinic in ref 208a.

between adjacent sulfur atoms	0.226 nm
S–Fe–S bond angle	85.66 and 94.34°
Fe–S–Fe bond angle	115.5°
S–S–Fe bond angle	102.4°

Each Fe atom is surrounded by six S atoms in a distorted octahedral array and each S atom has one nearest-neighbor S atom and three nearest-neighbor Fe atoms.[48]

TABLE II. Physical Properties of Iron Sulfides

name or phase	chemical name	composition	mol wt	structure	structure type	Fe valence	color	density g cm^{-3}	Mohr hardness	mp, °C[f]	temp of dec, °C
pyrite[a]	ferrous disulfide	FeS_2	119.98	cubic	pyrite	2+	brass-yellow[b]	5.0[b]	6-6.5[b]	1171[d]	<687[c]
marcasite[a]	ferrous disulfide	FeS_2	119.98	orthorhombic	marcasite	2+	bronze-yellow[b]	4.88[b]	6-6.5[b]	tr 450[d]	227?[c]
troilite[a]	ferrous sulfide	FeS	87.91	hexagonal	nicolite	2+	black-brown[d]	4.74[d]		1193-1199[d]	>137[c]
amorphous[c]	ferrous sulfide	FeS	87.91			2+					?[c]
mackinawite[c]	ferrous sulfide	$Fe_{1+x}S$, ($x < 0.12$)	variable	tetragonal		2+					135[c]
hexagonal pyrrhotite[c]	ferrous sulfide	$Fe_{1-x}S$, ($x < 0.11$)	variable	hexagonal	defective nicolite	2+	bronze-yellow[b]	~4.74[b]	6-6.5[b]	1195[c]	
monoclinic pyrrhotite[c]	ferrous sulfide	Fe_7S_8	647.36	monoclinic		2+					217-297
A/hypothetical[a]	ferrous sulfide	FeS	87.91	hexagonal	zincite	2+					
B/hypothetical[a]	ferrous sulfide	FeS	87.91	cubic	sphalerite	2+					
smythite[a]	ferro-ferric sulfide	Fe_3S_4	295.8	hexagonal		2+					~77
greigite[a]	ferro-ferric sulfide	Fe_3S_4	295.8	cubic	spinel	2+	sooty-black[e]				~77
amorphous[c]	ferric sulfide	Fe_2S_3	207.86			3+					?
crystalline[c]	ferric sulfide	Fe_2S_3	207.86	tetragonal ?	spinel ?	2+	yellow-green[d]				<77-177

name or phase	molecules per unit cell[a]	cell dimensions[a] a_0	b_0	c_0	cell volume,[a] 10^{-24} cm^3	molar volume[a] cm^3	molar volume[a] cal bar^{-1}	X-ray density,[a] g cm^{-3}
pyrite	4	5.4175			159.000	23.940	0.57221	5.0116
marcasite	2	4.443	5.423	3.386	81.622	24.579	0.58749	4.8813
troilite	2	3.446		5.877	60.439	18.20	0.4350	4.830
amorphous								
mackinawite								
hexagonal pyrrhotite	2	3.446		5.848	60.14	18.11	0.4329	4.793
monoclinic pyrrhotite		11.9108[e]	6.8673[e]	22.7898[e]				
A/hypothetical	2	3.872		6.345	82.38	24.81	0.5930	3.544
B/hypothetical	2	5.455			162.36	24.44	0.5842	3.597
smythite								
greigite	8	9.876			963.26	72.57	1.733	4.079
amorphous								
crystalline								

[a] Reference 50. [b] Reference 208a. [c] Reference 454. [d] Reference 208b. [e] Reference 46. [f] More recent work indicates decomposition at ~800 °C, see section IID. [g] β for monoclinic pyrrhotite = 90.5769, ref 46.

Marcasite crystallizes in the orthorhombic system with a distinctive structure, which, like pyrite, gives it a self-identified position in the structure typology. Wyckoff[47] lists seven isomorphs—iron diarsenide, diphosphide, diantimonide, diselenide, and ditelluride, cobalt ditelluride, and nickel diarsenide. This list could most likely be extended. Most of the data on marcasite and its isomorphs indicate a dimolecular unit, but faint reflections have suggested a tetramolecular cell. The structure is less dense than pyrite; Mellor[6] reports the following interatomic distances:

between two iron atoms	0.552 nm
between two sulfur atoms of a sulfur pair	0.225 nm
between unpaired sulfur atoms	0.295 nm
between a sulfur and an iron atom	0.221 nm

The atomic separations are those to be expected from neutral radii.

The crystal structure of the iron monosulfides was reviewed in detail by Ward.[46]

D. Properties Associated with Mass and Volume

Analysis of a large number of samples from various sources has shown that pyrite has a variable sulfur deficiency within the range $FeS_{2.00}$ to $FeS_{1.94}$.[49] The density of pyrite varies over the range d^{20}_4 = 4.6–5.2, the density of the pure material being d^{20}_4 5.02.[49] The X-ray density is 5.0116.[50] Defining the thermal expansion α as

$$\alpha = \frac{10^6 \Delta l}{l \Delta T} \tag{1}$$

and the rate of change of α with temperature T as

$$\Delta = 10^9 \frac{\Delta \alpha}{\Delta T} \tag{2}$$

produces the following values for α:[51] [temperature (K), α] 268.7, 8.43; 237.4, 7.73; 214.8, 7.09; 155.0, 5.16; 129.7, 3.92; 108.0, 2.95. α^{40} = 9.1 and $\Delta(20°–70°)$ = 18. Defining the compressibility β as

$$\beta = -\frac{1}{V_0}\left(\frac{\partial V}{\partial P}\right)_T \tag{3}$$

with a temperature dependence given by

$$A_p = \frac{1}{\beta_0}\left(\frac{\partial \beta}{\partial T}\right)_p \tag{4}$$

and a pressure dependence

$$A_T = \frac{1}{\beta_0}\left(\frac{\partial \beta}{\partial P}\right)_T \tag{5}$$

the following values have been reported for pyrite and marcasite at 25 °C and 1 × 10^5 Pa:[51]

	$10^6\beta$	$10^4 A_p$	$-10^4 A_T$
pyrite	0.70	1	0.06
marcasite	0.82		

Recent studies disagree with the standard texts on the melting point of pyrite. Gupta et al.[52] report that in an inert atmosphere or vacuum pyrite decomposes in the temperature range 825–850 °C before it melts. Horita and Suzuki[53] reported a decomposition temperature of 715 °C.

E. Magnetic, Mössbauer, Electrical, and Optical Properties

The Mössbauer, magnetic, electrical, and optical properties of pyrite and marcasite are interrelated and defined by the 3d valence electrons of iron and the 3p valence electrons of sulfur. In recent years, these properties have been studied in considerable detail because the Fe^{2+} valence electrons of pyrite and marcasite straddle the localization–delocalization regime for 3d electrons. This work has been extended to similar transition-metal dichalcogenides and related compounds.

Studies by a number of workers[54–63] indicate that the magnetic susceptibility is very small, positive, and slightly temperature dependent; the general conclusion is that pyrite has no magnetic moment, and there is a small paramagnetic (or Van Vleck) component that is temperature dependent. Stevens et al.[64] cited an unreferenced diamagnetism for pyrite. Konig[65] has reported a collated value of $\chi_{Fe} = 60 \times 10^{-6}$ emu mol^{-1} and Burgardt and Seehra[63] a value of $\chi = 19.8 \times 10^{-6}$ cm^3 mol^{-1} for the temperature limit T = 0 K; these very low values are most sensitive to trace impurities. Gupta and Ravindra[66] considered the band gap energy of pyrite to be the principal contributor to the temperature dependence of the Van Vleck susceptibility. Marusak et al.[67,68] reported that the paramagnetic susceptibility was independent of pressure up to 1100 kPa.

Conclusions on the electronic structure of pyrite, based on magnetic susceptibility studies, have been verified by Mössbauer spectroscopy,[48,62,63,69–77] Walker et al.[69] assumed that the iron was present in the Fe^{3+} state, but the absence of a magnetic moment discounts this assumption. Failure by later workers to duplicate earlier work is usually attributed to the sensitivity of the spectrum to trace impurities. Framboidal material exhibits a slightly different isomer shift and quadrupole splitting compared to the crystalline material.

The consensus[78] is that iron in pyrite is present as Fe^{2+}. The six d electrons are paired and occupy the t_{2g} ground state. This is also referred to as the low-spin state or d_E state. Consequently the Fe^{2+} ion in pyrite has no magnetic moment. Further splitting of the t_{2g} orbitals is produced by trigonal distortion of the octahedral electrostatic crystal field. Sulfur is present as the S_2^{2-} moiety. The ten electrons completely fill the bonding p_σ and p_π orbitals and the p_π^* antibonding orbital; consequently S_2^{2-} also has no magnetic moment.[62,64,76,79] The occurrence of quadrupole splitting of the Mössbauer spectra indicates the presence of an electric field gradient (EFG), unexpected in view of the high symmetry of the Fe site. Explanations for the source of the EFG in terms of molecular orbital terms,[48] symmetry terms,[80] or trigonal distortion through the axis of the S_2^{2-} moiety[64] are still being investigated.

Magnetic susceptibilities for marcasite have been reported.[56,58,81] The measurements are very sensitive to impurities; this has led to the high erroneous values collated by Konig[65] and the report of a diamagnetic component.[58,79] The only reliable values are those of Seehra and Jagadeesh,[81] who obtained a value of χ = 64 cm^3/mol at T = 0 K. The χ vs. temperature be-

havior for marcasite is qualitatively similar to that observed for pyrite Mössbauer spectra.[73,82,83] The small paramagnetic value and temperature dependence indicate that the 3d electrons of Fe^{2+} are in a similar low-spin state to pyrite. Marcasite, with its orthorhombic crystal structure, has a lower symmetry than pyrite, leading to modified crystal-field splitting with the band gap, E_g, being smaller for marcasite than pyrite.[79] The band gap is inversely proportional to the paramagnetic susceptibility. Consequently, marcasite has a greater paramagnetic susceptibility than pyrite mainly because of the difference in their band gaps.[84]

Values for the electrical resistivity or the reciprocal of the resistivity, conductivity, for pyrite and marcasite are listed in the International Critical Tables.[51] These values should be treated with caution since Smith[49] demonstrated that for a given crystal the value could vary by a factor of 20 depending on direction, and for a given crystal face the value could vary by a factor of 10 000 depending on the source of the sample. The resistivity is also pressure dependent.[51]

Part of the complexity is due to the occurrence of pyrite as both n- and p-type semiconductors, and even as p–n junction material.[85] For p-type material the resistivity decreases with temperature, but for n-type it increases. The variation over the temperature range 0–800 K does not fit a simple relationship, and the variation is specific to each specimen. Measurements indicate a common value for the resistivity of ~0.2 Ω cm for all specimens of pyrite at 500 °C.[86,49] At room temperatures, n-type material has a low resistivity, ρ, of the order of 0.10 Ω cm, a negative Hall coefficient, R_H, and a high Hall mobility, $\mu_H = |R_H|/\rho$, of about 100–200 $cm^2\ V^{-1}\ S^{-1}$. The p-type material has a higher resistivity (about 2 Ω cm), a positive Hall coefficient, and a low Hall mobility (~1–2 $cm^2\ V^{-1}\ S^{-1}$). The exhaustion region appears near room temperature, and the exhaustion carrier concentration, which is independent of carrier type, is of the order of 1×10^{18} cm^3.[61,86-88]

The variable nature of the semiconducting properties of pyrite has been attributed to the sulfur content,[89] the lead content,[90] the nickel and cobalt content,[91] and a range of heavy metals.[92] The low Debye temperature limit for pyrite semiconductor, θ_D, has been reported as 703 K[93] and 610 K.[94] Husk and Seehra[95] reported a value of 10.9 ± 0.5 for the dielectric constant e'. The value was independent of frequency within the range 500 Hz to 100 kHz, and temperature range 77 to 297 K. The $\epsilon'(\infty)$ value was calculated to be 8.9. A value for the high frequency dielectric constant of 19.6 at 5 eV has been reported.[61] Smith[49] noted that the sign of the thermoelectric potential with respect to copper was related to the sign of the temperature coefficient of resistivity and hence to the semiconductor type, so p-type material has a positive thermoelectric potential and n-type a negative one. A Seebeck coefficient of $-500\ \mu V\ deg^{-1}$ was reported for a synthetic sample of n-type material.[61]

Information on the electrical properties of marcasite is extremely limited. Hulliger and Mooser[79] referred to the work of Wesely[96] to identify marcasite as a semiconductor. Some values for the electrical resistivity are listed in the International Critical Tables.[51] Jagadeesh and Seehra[84] reported electrical resistivity measurements over the temperature range 53–370 K for a natural crystal of p-type material, and a value of 13.9 was calculated for the high frequency dielectric constant.

TABLE III. Band Gap, E_g, for Pyrite and Marcasite

material	band gap, eV	temp, K	method	ref
pyrite	1.2	300	resistivity	86
	1.12	300	resistivity	87
	1.0	300		455
	0.92	300	optical	61
	0.77	550		53
	0.9	77	photoconductivity	456
	0.92	300	theoretical	52
	0.96	300	dielectric	95
	0.95	300	optical	105
	0.835	0	optical	106
marcasite	0.34	300	resistivity	84

Optical anisotropism has been observed in a number of samples of pyrite,[49] but it could not be directly related to the degree of sulfur deficiency. It tended to occur in p-type material or material formed below a critical temperature of less than 135 °C and could be removed from some specimens by heat treatment. Optical anisotropism could not be related to electrical anisotropism. In contrast, Revyakin and Revyakina[92] reported sedimentary pyrite to be n-type and hydrothermally altered pyrite to be p type.

The real and imaginary parts for the complex refractive index of pyrite over the range 0.5–5.0 eV have been reported for specular, near normal incidence, reflectance spectra measurements.[61,97] Ultraviolet photoemission spectra (UPS)[98] and X-ray photoemission spectra (XPS)[99] have also been reported. A fairly complete series of X-ray emission spectra are available.[100-102] Sharp peaks in the region of 1 eV have been attributed to the 3d t_{2g} level.[103] Infrared reflectivity has been reported by Verble and Wallis[104] and Schlegel and Wachter.[105] Optical absorption in the 0.7–1-eV range has been reported by a number of authors.[105-108] The UV specular reflectance spectrum has been reported by Schlegel and Wachter,[105] and more recently, photoconduction spectra have been identified by Horita and Suzuki.[109] Saz has recently published the only optical data for marcasite.[97]

Most of the work described above sought to confirm the electron structure previously deduced from the magnetic studies. A direct result from this work is a value for the band or energy gap, E_g, between the valence and conduction bands of the semiconductor; Table III summarizes the reported values. The temperature dependence of the energy gap has been reported by Kou and Seehra[106] and the range extended by Seehra and Seehra[107] to cover 0–400 K. The latter authors treated E_g as a thermodynamic variable so that

$$\left(\frac{\partial E_g}{\partial T}\right)_P = \left(\frac{\partial E_g}{\partial T}\right)_V - \frac{\beta}{K_s}\left(\frac{\partial E_g}{\partial P}\right)_T \qquad (6)$$

where β is the volume expansivity and K_s the compressibility. Thus E_g is a function of T and T^2. Accordingly, the equation

$$E_g(T) = E_g(0) + aT + bT^2 \qquad (7)$$

was fitted successfully to the data with the parameters $E_g(0) = 8.835$ eV, $a = 4.9 \times 10^{-5}$ eV K^{-1}, and $b = -7.4$

$\times 10^{-7}$ eV K^{-2} obtained from the best fit.

The reduced energy gap for marcasite reflects the enhanced splitting of the t_{2g} orbitals to e_g and a_g components.[79]

III. Thermodynamic Properties of the Iron Sulfide Minerals

A. $\Delta G_f°$, $\Delta H_f°$, S, and C_p

The thermodynamic values for $\Delta H_f°_0$, $\Delta H_f°$, $\Delta G_g°$, $H°_{298} - H°_0$, $S°$, $C_p°$, and the constants a, b, and c of the equation $C_p = a + bT + cT^{-2}$ are listed in Table IV for the more common iron sulfide minerals. The listing was compiled from a number of primary and secondary sources but should not be considered an exhaustive survey. Most of the primary sources were identified by a computer search of the literature, a method of searching that is restricted to the more recent publications. Publications before 1950 were not consulted as it was assumed that all of the older papers have been identified and critically reviewed in the secondary sources. Where there is a choice the more recent measurements of Grønvold et al.[110-112] are preferred. This is not because the most recent results are necessarily the best but rather because these measurements were made with a better understanding of the phase relationships between the iron sulfides and because this work was part of an overall study of the thermochemistry of the transition-metal chalcogenides and thus allowed intercomparison between compounds. Such intercomparisons are needed to identify any serious errors in the results.

All original source data were quoted in calories and have been converted to SI units by using the factor 1 cal = 4.1840 J. The constants a, b, and c for the C_p data of Grønvold et al.[110,112] were determined by using a linear-least-squares computer program. The temperature range was confined to that given in Table IV to enable a reasonable fit of the empirical equation to the experimental data. For values outside the temperature range quoted, readers are advised to consult the original papers. The upper temperature limit for pyrite was set by the experiment; Grønvold and Westrum[112] set the limit at 780 K and Coughlin[113] set it at 980 K. Agreement between these workers was 4.8% at 400 K but improved to 0.3% at 700 K. The upper temperature limit for the C_p data for marcasite and the iron-rich and sulfur-rich pyrrhotite was set by the occurrence of the temperature at which a phase transition occurred. The above results were obtained by adiabatic calorimetry. Mraw and Naas[114] determined the C_p of pyrite over the temperature range 100 to 800 K using a differential scanning calorimeter; this method is generally regarded as being less accurate. However, the results of Mraw and Naas were usually within 1% of those of Grønvold et al., with the difference rising to 2% at the very lowest and highest temperatures.

The specific heat data for pyrite and marcasite reveal that the specific heat of marcasite is slightly higher than that of pyrite over the entire temperature range of mutual existence. The transformation of marcasite to pyrite is significantly exothermic at 700 K with a heat transformation of ΔH_t (700 K) = -4.9 ± 0.2 kJ mol^{-1}, so $H°$ (T = 0, marcasite) − $H°$ (T = 0, pyrite) = 4.1 ± 0.2 kJ mol^{-1}. Consequently, marcasite is metastable

TABLE IV. Thermodynamic Properties for Iron Sulfides

compound	$\Delta H_f°_0$, kJ mol^{-1}	$\Delta H_f°$, kJ mol^{-1}	$\Delta G_f°$, kJ mol^{-1}	$H°_{298} - H°_0$, kJ mol^{-1}	$S°$, J deg^{-1} mol^{-1}	C_p, J deg^{-1} mol^{-1}	$C_p = a + bT + cT^2$, J deg^{-1} mol^{-1}			T, K	$-[G°(T) - H°_0]/T$, J deg^{-1} mol^{-1}
							a	$b \times 10^{-3}$	$c \times 10^5$		
pyrite, FeS_2	−174.56[a]	−178.24[a]	−166.94[a]	9.63[a,b]	52.93[a,b,g,h]	62.17[a,b,g]	68.58[c]	13.64[c]	−9.05[c]	200–780[c]	20.61[c]
pyrite, FeS_2		−173.64[c]	−162.34[c]			62.09[d,e,h]	74.81[d,e,g]	5.52[d,e,g]	−12.76[d,e,g,h]	298–1000[e]	
pyrite, FeS_2		−174.05[g]	−162.76[g]			62.17[h]					
pyrrhotite, FeS_2		−171.54[h]									
marcasite, FeS_2		−169.45[c]	−158.57[c]	9.74[c]	53.89[c]	62.43[c]	67.57[c]	16.11[c]	−8.77[c]	200–700[c]	21.21[c]
marcasite, FeS_2		−154.81[a]									
marcasite, FeS_2		−150.62[g]				58.95[h]					
troilite, $Fe_{1.00}S$						54.64[d,e]	21.72[d,e,g]	110.46[d,e,g]		298–411	
troilite, $Fe_{1.00}S$					60.31[a,f-h]	50.54[a,f,g]	10.13[f]	124.73[f]	3.39	200–350	
troilite, $Fe_{1.00}S$	−100.46[a]	−99.99[a,g]	−100.42[a,g,h]	9.35[a]	60.79[f,g]	49.87[f,g]	38.58[f]	46.82[f]	−2.36	200–350	
pyrrhotite as $Fe_{0.877}S$											
pyrrhotite as Fe_7S_8	−743.41[a]	−736.38[a]	−748.52[a]	73.72[a]	485.76[a]	398.57[a]					
Fe_2S_3	−279.91[g]	−280.75[g]			152.29[g]						

[a] Reference 400. [b] Reference 111. [c] Reference 112. [d] Reference 456. [e] Reference 113. [f] Reference 110. [g] Reference 458. [h] Reference 459.

over the entire temperature region and owes its formation and presence to kinetic factors.

B. E_h–pH Diagrams

Potential–pH diagrams may be constructed from the thermochemical data of the reactants and products. This allows regimes of stability to be defined beyond which the system is thermodynamically unstable. Whether the system remains in an unstable condition or reverts to a stable state within the confines of the adjusted variables is a question that may only be answered by examining the kinetics of the reaction and the associated activation energies.

A number of potential–pH diagrams for the iron–water–sulfur system at 25 °C have been reported.[115-118] Biernat and Robins constructed diagrams for the iron–water–sulfur system up to 300 °C and conveniently included all working equations and thermodynamic data in their paper. Application of these diagrams to pyrite oxidation has been considered by Linkson, Nobbs, and Robins.[119] The iron–water–sulfur system consists of a large number of compounds and dissolved species. Posnjak and Merwin[120] identified experimentally at room temperature seven crystalline phases of hydrated ferric sulfate and three more phases at elevated temperatures. Table II lists ten mineral iron sulfides but excludes the gel materials. There are a number of ferrous and ferric oxides: FeO, Fe_3O_4, Fe_2O_3, $Fe(OH)_2$, $Fe(OH)_3$, FeOOH; and Biernat and Robins[118] listed eight aqueous iron species. Consequently, the complete potential–pH diagram for the iron–water–sulfur system is exceedingly complex, and it is usual to select compounds and species that are specific to the problem. Accordingly, the following species are selected: FeS_2 (pyrite), FeS (trolite), Fe_3O_4 (magnetite), FeOOH (goethite), $KFe_3(SO_4)_2(OH)_6$ (jarosite), Fe^{3+}, Fe^{2+}, H_2S(aq), HS^-, S^{2-}, SO_4^{2-}, and K^+. The selection of most of these compounds and species is self-explanatory, but selection of the ferric oxides and jarosite warrants discussion.

The simple ferric oxides consist of Fe_2O_3 as hematite and a red radial fibrous form (turgite), the hydrated form $Fe_2O_3 \cdot H_2O$ or FeOOH (goethite or lepidocrocite), an indefinite amorphous form with a considerable excess of water known as limonite, and the hydroxide $Fe(OH)_3$. The potential–pH diagrams of Biernat and Robins[118] indicated that the hydroxide is the stable form at room temperature, goethite is stable between 90 and 130 °C, and hematite is the stable form at high temperatures. The temperature of transformation between solid forms can change by 25 °C per pH unit. These calculations are supported by experimental observation of the phase equilibria of iron oxides in acid media[121] and neutral and alkaline media.[122-125] Mineralogically, the ferric hydroxide occurs as goethite, so this is the preferred material for the calculations.

Ferric sulfate is readily hydrolyzed to a series of basic hydrates, which, in turn, form a series of complex basic ferric sulfate salts. This is the form in which ferric sulfate usually occurs as a mineral; a common form associated with iron–sulfur oxidizing ores is jarosite, $KFe_3(SO_4)_2(OH)_6$, first named by Breithaupt[126] from a sample collected at Barranco Jaroso, Spain.

Jarosite belongs to the alunite–jarosite group of minerals, which are isostructural with the beudanite, $Fe_3(AsO_4,SO_4)_2(OH)_6$, and plumbogummite groups, $PbFe_3(PO_4,CO_3)(OH)_6$. The general formula for these minerals is $AB_3(XO_4)_2(OH)_6$. The A position may be filled by one-, two-, or three-valent cations such as Na, K, H_3O, Ca, Pb, Sr, or Ce. The B position is usually filled by Al or Fe; in some minerals this position contains some copper. Usually XO_4 is SO_4, PO_4, AsO_4, (AsO_4, SO_4), or (PO_4, SO_4), but some analyses indicate CO_3 or SiO_4 substituted in this position. A few analyses have indicated that halogens substitute in part for $(OH)_6$.[127] Dana[13] separated these minerals into groups according to the nature of the anion. Alternative grouping based on iron and aluminum content has been suggested.[128] A single group with aluminum and iron members has been suggested by Larsen and Berman.[129]

Some mineral names are superfluous, and McKie[130] described some complex mixtures by using percentages of end members, as is commonly employed for feldspars. Brophy[131] demonstrated that for the alunite group, which has the general composition $AB_3(SO_4)_2(OH)_6$, where A may be K^+, Na^+, Pb^{2+}, NH_4^+, or Ag^+ and B may be either Fe^{3+} or Al^{3+}, there is a solid solution between the end members alunite $KAl_3(SO_4)_2(OH)_6$ and jarosite $KFe_3(SO_4)_2(OH)_6$. He concluded that there may be an alunite–jarosite solution series in nature but that minerals intermediate between the end members are rare. At 105 °C and 0.2 N sulfuric acid, Fe^{3+} rather than Al^{3+} is taken up by the solid. If the temperature is increased and acidity reduced, the preference of Fe^{3+} over Al^{3+} is reduced.

Jarosite is frequently associated as a product of the oxidation of pyrite.[132-137] The formation of jarosite from pyrite causes a 115% increase in molar volume. This has contributed to a 9.45-cm vertical heave of a building sited on a pyritic shale in Canada.[138-143] However, there are reports of preferential formation of alunite from pyritic zones,[131,144-149] but this has not been satisfactorily explained. General indications are that the major parameters are pH and oxidizing potential. In view of the co-occurrence of jarosite and alunite with pyrite, these two end members should be included in the potential–pH diagram. A further restriction on available thermodynamic data limits the choice to jarosite.

Figure 1 is the resulting potential–pH diagram based on the equations listed in Table V. As indicated in the table, with the exception of the jarosite equations (eq 18–20), the equations were taken directly from published work. The jarosite equations were obtained by using the following values for the Gibbs free energy of formation: $\Delta G°$, K^+ = −251.2 kJ;[150] $\Delta G°$, $KFe_3(SO_4)_2(OH)_6$ = −3322 kJ.[151] Slight variations between diagrams constructed by different authors are due to the chosen limiting activity. Thus Biernat and Robins,[118] whose diagrams were for hydrometallurgical considerations, set the activity of all dissolved species at unity. This formed a sulfur regime as a long finger over a pH range of −1 to 8 and at an E_h of ~0.2 V. However, by reducing the limiting activity to 10^{-6} mol, as is done in Figure 1, the sulfur regime can be removed, so depending on the solution conditions, pyrite may or may not be in equilibrium with oxidation to sulfur.

A five-dimensional diagram is required to illustrate adequately the variation of the jarosite regime with the variables E_h, pH, $a_{(K^+)}$, $a_{(Fe^{3+},Fe^{2+})^3}$, and $a_{(HSO_4^-,SO_4^{2-})^2}$. This was discussed by Brown,[152] who used three-dimensional

TABLE V. Equations for the Iron-Water-Sulfur-Jarosite System[a]

eq	equation	ref	ref eq
	Reactions Involving Water Stability		
A	$2H^+ + 2e^- \rightarrow H_2$ $E_h = 0 - 0.05917pH$	339	a
B	$O_2 + 4H^+ + 4e^- \rightarrow 2H_2O$ $E_h = 1.23 - 0.05917pH$	339	b
	Reactions Involving the Iron-Water System		
1	$Fe^{3+} + e^- \rightarrow Fe^{2+}$ $E_h = 0.770 + 0.05917 \log (a_{Fe^{3+}}/a_{Fe^{2+}})$	118	3a
2	$Fe^{2+} + 2e^- \rightarrow Fe$ $E_h = -0.409 + 0.296 \log a_{Fe^{2+}}$	118	15a
3	$Fe^{3+} + 2H_2O \rightarrow FeOOH + 3H^+$ $3pH = -1.85 - \log (Fe^{3+})$	118	13a
4	$FeOOH + 3H^+ + e^- \rightarrow Fe^{2+} + 2H_2O$ $E_h = 0.66 - 0.177pH - 0.05917 \log a_{Fe^{2+}}$	118	17d
	Reactions Involving the Sulfur-Water System		
5	$H_2S(aq) \rightarrow HS^- + H^+$ $pH = 7.00 + \log (a_{HS^-}/a_{H_2S_{aq}})$	460	3
6	$HS^- \rightarrow S^{2-} + H^+$ $pH = 12.92 + \log (a_{S^{2-}}/a_{HS^-})$	460	4
7	$HSO_4^- \rightarrow SO_4^{2-} + H^+$ $pH = 1.99 + \log (a_{SO_4^{2-}}/a_{HSO_4^-})$	460	6
8	$SO_4^{2-} + 9H^+ + 8e^- \rightarrow HS^- + 4H_2O$ $E_h = 0.249 - 0.067pH + 0.0074 \log (a_{SO_4^{2-}}/a_{HS^-})$	460	10
9	$SO_4^{2-} + 8H^+ + 8e^- \rightarrow S^{2-} + 4H_2O$ $E_h = 0.153 - 0.059pH + 0.0074 \log (a_{SO_4^{2-}}/a_{S^{2-}})$	460	11
10	$HSO_4^- + 9H^+ + 8e^- \rightarrow H_2S_{aq} + 4H_2O$ $E_h = 0.286 - 0.067pH + 0.0074 \log (a_{HSO_4^-}/a_{H_2S(aq)})$	460	33
11	$SO_4^{2-} + 10H^+ + 8e^- \rightarrow H_2S_{aq} + 4H_2O$ $E_h = 0.301 - 0.074pH + 0.0074 \log (a_{SO_4^{2-}}/a_{H_2S(aq)})$	460	34
	Reactions Involving the Iron-Water-Sulfur System		
12	$Fe^{2+} + H_2S_{aq} \rightarrow FeS + 2H^+$ $2pH = 1.11 - \log (a_{Fe^{2+}} a_{H_2S(aq)})$	118	19a
13a	$FeS + 2H^+ + 2e^- \rightarrow Fe + H_2S$ $E_h = -0.376 - 0.05917pH - 0.0296 \log a_{H_2S(aq)}$	118	20a
13b	$FeS + H^+ + 2e^- \rightarrow Fe + HS^-$ $E_h = -0.583 - 0.0296pH - 0.0296 \log a_{HS^-}$	118	20b
13c	$FeS + 2e^- \rightarrow Fe + S^{2-}$ $E_h = -0.965 - 0.0296 \log a_{S^{2-}}$	118	20c
14a	$FeS_2 + 2H^+ + 2e^- \rightarrow FeS + H_2S_{aq}$ $E_h = -0.165 - 0.05917 - 0.0296 \log [H_2S_{aq}]$	118	22a
14b	$FeS_2 + H^+ + 2e^- \rightarrow FeS + HS^-$ $E_h = -0.372 - 0.029pH - 0.0296 \log a_{HS^-}$	118	22b
14c	$FeS_2 + 2e^- \rightarrow FeS + S^{2-}$ $E_h = -0.754 - 0.0296 \log a_{S^{2-}}$	118	22c
15	$FeS_2 + 4H^+ + 2e^- = Fe^{2+} + 2H_2S$ $E_h = -0.133 - 0.118pH - 0.0296 \log (a_{Fe^{2+}} a^2_{H_2S(aq)})$	118	23a
16a	$Fe^{2+} + 2SO_4^{2-} + 16H^+ + 14e^- = FeS_2 + 8H_2O$ $E_h = 0.362 - 0.068pH + 0.0042 \log (a_{Fe^{2+}} a^2_{SO_4^{2-}})$	118	25a
16b	$Fe^{2+} + 2HSO_4^- + 14H^+ + 14e^- = FeS_2 + 8H_2O$ $E_h = 0.345 - 0.05917pH + 0.0042 \log (a_{Fe^{2+}} a^2_{HSO_4^-})$	118	25c
17	$FeOOH + 2SO_4^{2-} + 19H^+ + 15e^- = FeS_2 + 10H_2O$ $E_h = 0.382 - 0.075pH + 0.0039 \log a^2_{SO_4^{2-}}$	118	26g
	Reactions Involving the Iron-Water-Sulfur-Jarosite System		
18	$K^+ + 3Fe^{3+} + 2HSO_4^- + 6H_2O \rightarrow KFe_3(SO_4)_2(OH)_6 + 8H^+$ $8pH = -21.1 - \log (a_{K^+} a^3_{Fe^{3+}} a^2_{HSO_4^-})$		
19a	$KFe_3(SO_4)_2 \cdot (OH)_6 + 8H^+ + 3e^- \rightarrow K^+ + 3Fe^{2+} + 2HSO_4^- + 6H_2O$ $E_h = 0.354 - 0.0197 \log (a_{K^+} a^3_{Fe^{2+}} a^2_{HSO_4^-}) - 0.157pH$		
19b	$KFe_3(SO_4)_2 \cdot (OH)_6 + 6H^+ + 3e^- \rightarrow K^+ + 3Fe^{2+} + 2SO_4^{2-} + 6H_2O$ $E_h = 0.275 - 0.0197 \log (a_{K^+} a_{Fe^{2+}} a^2) - 0.1566pH$		
20	$KFe_3(SO_4)_2 \cdot (OH)_6 \rightarrow K^+ + 3FeOOH + 2SO_4^{2-} + 3H^+$ $3pH = +19.53 + \log (a_{K^+} a^2_{SO_4^{2-}})$		

[a] E_h is the reduction potential with reference to SHE (volts). The equations are written as reduction equations left to right.

drawings. Only the jarosite boundaries for unity solution activities are shown in Figure 1. Jarosite will start to precipitate at pH 1.28, above an E_h of 0.69, and at a limiting concentration of 5.9×10^{-6} mol L^{-1} for each species. The limiting concentration for any species may be reduced, provided that the concentrations of the other species are increased to maintain the equilibrium conditions required by the jarosite equations. Increasing the concentrations of all species increases the regime of jarosite stability on either side of the limiting pH of 1.28 but with a disproportionate increase in favor of the area above pH 1.28. At unit activity of all species,

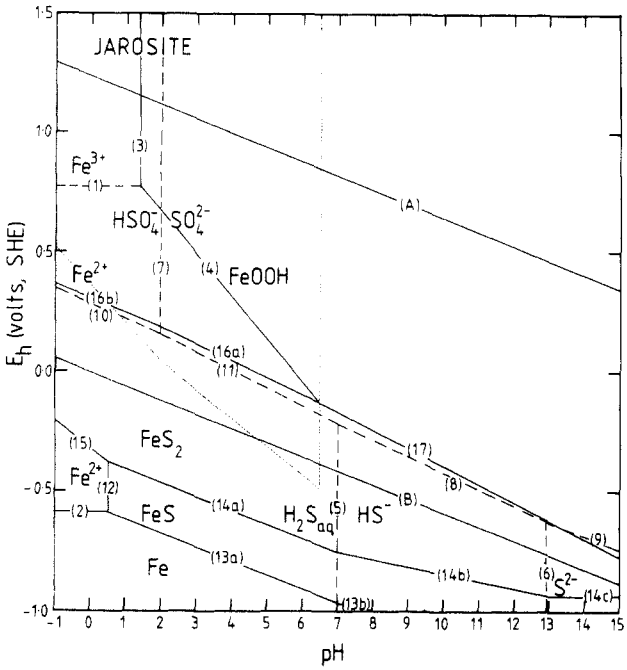

Figure 1. E_h–pH diagram for the iron–sulfur–water system at 25 °C: (—) boundary of solid regimes with limiting solution activity 10^{-6} mol L^{-1}; (- - -) boundary of regime of predominant ion; (···) boundary of jarosite regime with solution activities 1 mol L^{-1}.

the regime is bounded by pH −2.63 to 6.51, and there is a reduction of the limiting E_h as indicated by the diagram.

Alunite replacement is probably favored by solutions of pH greater than 4.5 and high ionic strength, i.e., solutions in which extensive pyritic oxidation has taken place and which have subsequently been partially neutralized. Such solutions would be displaced from the center of the jarosite regime toward the hydrargillite, $2Al_2O_3 \cdot 3H_2O$, regime, which has a pH region of stability between 4.5 and 9.5,[153] and therefore favors iron replacement by aluminum. The alunite–jarosite minerals are chemical buffers and will maintain a system at a set pH. The exact pH will be a function of the mineral composition and the influent ion concentrations. Miller[154,155] reported an effluent stream as having a pH of 3.19 ± 0.17 and a pSO_4 of 3.46 ± 0.14. This is fairly typical of acid mine drainage solutions in which the pH and pSO_4 can vary by 1 or 2 log units.[136,156,157]

IV. Chemical Oxidation of Pyrite

A. Introduction

Howie[158] pointed out that studies have shown three possible pathways for the aqueous oxidation of pyrite. These are (i) through bacterial catalysts, which will not be discussed in detail in this review; (ii) through a sequence of chemical reactions; and (iii) through an electrochemical reaction, although this has only been demonstrated under the hydrometallurgical conditions of 110 °C and 2–7 MPa[12]. Although the possibility of bacterial action may be discounted above 100 °C, reasonable care must be exercised to exclude bacterial activity from any experiments designed to identify the reaction path below 100 °C, particularly with the recent discovery of autotrophic bacteria that have an optimum living environment of 80 °C.[9] Howie[158] reported a case of chemical oxidation at ambient temperatures of pyritized museum fossils based on the following observations:

(i) The application of bactericides[159,160] failed to protect pyritic specimens from further oxidation. In addition, test material which had been sterilized by washing with acetone continued to degrade.

(ii) Degradation continued despite very high local acidity (pH <1.0) and a sulfate concentration of >1.0 M.[161] These concentrations inhibit bacterial activity.

(iii) Bacteria could not be cultured in various thiobacilli culture media from several actively oxidizing pyritic fossils.

A number of chemical reaction sequences have been proposed. Although there are differences in the fine detail, in essence the overall reaction paths are similar in that oxygen reacts fully by a molecular path, designated an atom transfer reaction, and ends up in the product sulfate. McKay and Halpern[162] proposed the following reaction sequence:

$$2O_2 + FeS_2 \rightarrow FeS_2(O_2)_{ads} \rightarrow Fe^{2+}{}_{aq} + SO_4{}^{2-}{}_{aq} + S^0 \quad (8)$$

Although the reaction accounts for the observation of elemental sulfur as a minor product, it fails to account for the observed production of Fe^{3+}. Singer and Stumm[163,164] and Stumm and Morgan[165] proposed the following sequence of chemical steps for the reaction path in the context of acid mine drainage:

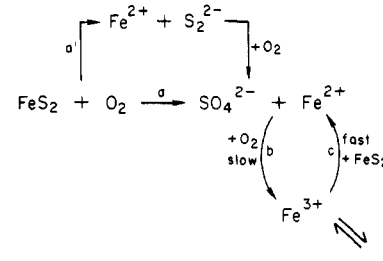

(9)

The model bears the hallmarks of electron-transfer processes in biochemical systems and is, in fact, derived from the bacteriological work of Temple and Delchamps.[166] The model consists of three reactions:

(i) The oxidation of pyrite by molecular oxygen to Fe^{2+} and sulfate via reaction a or a′. This is viewed as the necessary primary step.

(ii) The oxidation of Fe^{2+} to Fe^{3+} by molecular oxygen, step b. Singer and Stumm[164] regarded this as the rate-determining step.

(iii) The oxidation of pyrite by ferric ion, step c. This is viewed as a fast step.

Each of these reactions may be observed individually and may occur in an environmental situation independently of the overall reaction. Steger and Desjardins[167] and Goldhaber[465] observed a thio compound as a minor product. Formulation of both sulfate and thiosulfate in sterilized solutions has been reported by Sorokin.[168]

In comparison, the electrochemical mechanism is an electron-transfer reaction in which the pyrite reacts with water at an anodic site to produce Fe^{3+}, $SO_4{}^{2-}$, H^+, and electrons:

$$FeS_2 + 8H_2O \rightarrow Fe^{3+} + 2SO_4{}^{2-} + 16H^+ + 15e^- \quad (10)$$

The electrons are transferred via an external circuit to a cathodic site where oxygen will be reduced to water:

$$O_2 + 4H^+ + 4e^- \rightarrow 2H_2O \quad (11)$$

Using ^{18}O as a marker, Bailey and Peters[12] demonstrated that 100% of the reactant oxygen becomes product water for the oxidation of pyrite at 110 °C and between 2 and 7 MPa, thus indicating that under their operating conditions the reaction is predominantly electrochemical. A similar mechanism by which sulfate oxygen is derived from water has been described for the anaerobic oxidation of sulfur by sulfur-oxidizing bacteria.[169]

B. Aqueous Oxidation of Pyrite by Molecular Oxygen

1. Stoichiometry and Order

Aqueous oxidation of pyrite by molecular oxygen has attracted scientific interest for more than 100 years.[6,170,171] Stumm and co-workers[163-165] regarded the reaction as the initial step in the chemical sequence of pyritic oxidation in acid mine drainage. There are two oxidizable species, the ferrous iron and the sulfidic sulfur. Nelson, Snow, and Keyes[172] established that, irrespective of the mechanism, during the initial solubilization only the sulfidic sulfur is oxidized and the iron passes into solution in the ferrous state. The ferrous iron may be oxidized in a subsequent slow step.

The overall stoichiometry may be represented as

$$2FeS_2 + 7O_2 + 2H_2O \rightarrow 2FeSO_4 + 2H_2SO_4 \quad (12)$$

This scheme was derived by Allen and co-workers[40-42] and subsequently employed by Burke and Downs,[173] Cornelius and Woodcock,[174] and Mathews and Robins.[175] There are at least two side reactions, neither of which has been properly identified. Gmelin[176] reported sulfur as a side product during the oxidation of marcasite, and there have been similar observations reported for pyrite.[172,177-184] The percentage sulfur reported depends in part on the operating conditions, method of analysis, and whether it is specifically sought. The yield is usually low, which accounts for claims by some investigators that the pyritic sulfur is oxidized exclusively to sulfate.[185-188] A second side reaction is the possible formation of thiosulfate and sulfite intermediates.[189,465] Steger and Desjardins[167] reported the presence of an "$S_2O_3^{2-}$" compound. Their method of analysis failed to distinguish between thiosulfate, sulfite, or polythionate for the "$S_2O_3^{2-}$" moiety, but it was considered that thiosulfate was the most likely candidate.

The principal reaction is a heterogeneous surface reaction between a dissolved gas and a solid surface. The reaction rate is not normally limited by the oxygen solubility provided that an adequate rate of mass transfer from the gas phase to the liquid phase is maintained. This transfer can become a rate-controlling factor.[191] The solubility of oxygen in water at 25 °C and an air pressure of 1 atm is 0.0085 g of O_2 L^{-1} and in 1 atm of pure oxygen is 0.04 g of O_2 L^{-1}. For a given temperature, the variation of solubility with pressure obeys Henry's law for linear absorption

$$P_{O_2}/M_{O_2} = k_H \quad (13)$$

where P_{O_2} is the gas pressure, M_{O_2} is the dissolved oxygen concentration, and k_H = 0.45 Pa M^{-1} at 25 °C. The solubility decreases with increasing temperature to a minimum value at ~ 100 °C and then increases again.[192-194] At pH 7 the solubility is reduced by only 10% on addition of up to 1 mol of sodium chloride.[193] In the absence of carbon dioxide, the solubility is independent of pH except in strongly alkaline solutions.[195,196] In the presence of carbon dioxide the sum of the partial pressures is given by

$$P_{CO_2} + P_{O_2} + P_{H_2O}(0.03 \text{ atm}) = 1 \text{ atm}$$

The partial pressure of the carbon dioxide is a function of pH according to

$$\text{pH} = 5.82 - \log P_{CO_2} \quad (14)$$

Any fluctuation in the partial pressure of the carbon dioxide will be mirrored by a fluctuation of the partial pressure of oxygen to maintain a total pressure of 1 atm. Tamura, Goto, and Nagayama[197] have listed the dissolved oxygen concentrations in the pH range 6–7 for a number of carbonic acid–bicarbonate solutions.

With a linear solubility isotherm, the reaction order with respect to oxygen may be determined either from the rate of sulfate production, ferrous iron production, or pyrite dissolution as a function of oxygen partial pressure. A variety of reaction orders have been reported. Pressure-leaching studies with the temperature range 60 to 150 °C, at 0–0.5 MPa, and in an acid environment indicate a first-order reaction.[162,177,179-184,198] As the temperature is increased beyond 150 °C and the pressure is increased past 1 MPa, the order becomes increasingly fractional.[12,185] Cornelius and Woodcock[174] reported the order to be $(P_{O_2})^{1/2}$ at 165 °C and up to 2.5 MPa, and Woodcock[199] interpreted Warren's results[185] to be $(P_{O_2})^{1/2}$ also.

For acid mine drainage environments, Clark[200] proposed a fractional order of $(O_{2(aq)})^{2/3}$ for the dissolved oxygen, Mathews and Robins[175] reported a value of $(O_{2(aq)})^{0.81}$ that becomes approximately first order when converted to oxygen partial pressures, and Smith and Shumate[16] reported a complex fractional order based on a summation of terms.

The observation of first-order kinetics is central to any mechanism in which the rate-determining step is an atom-transfer reaction. Deviation into fractional order kinetics is usually viewed as evidence that the rate-determining step is an adsorption or desorption process, with the surface concentrations being defined by a nonlinear, typically Langmuir, isotherm. In his proposal for an electrochemical model, Woodcock[199] eliminated the need to define the reaction order because the reaction now became a zero-order reaction. Nagai and Kiuchi[183] and Bailey and Peters[12] reached a similar conclusion.

2. Activation Energies

Table VI lists a number of reported activation energies for the oxidation of pyrite by molecular oxygen. Individual reports claim reasonable agreement with previous work, yet this compilation indicates a wide spread of the results. The range of values is independent of oxygen partial pressure. Bailey and Peters[12] noted a possible correlation with temperature, but there may also be a correlation with pH or sulfate concentration. It should be noted that no experimental condition has been duplicated by another worker and the method for determining the rate of reaction was dif-

TABLE VI. Activation Energies for the Oxidation of Pyrite by Oxygen

activation energy, kJ M^{-1}	O_2 pressure, MPa	temp, range, °C	conditions: media	conditions: species monitored	ref
84	1.4	90-170	1 M NaOH	O_2	186
88		120-250	NaOH		205
84	0.17	130-190	water	SO_2	185
77	0.620	130-165	water	SO_2	174
69	0.620	130-165	water	Fe^{2+}	174
57	0.4	100-130	0.075 H_2SO_4	FeS_2	162
55					179
50	6.7	85-130	1 M H_2SO_4	O_2	12
42					180
39	0.1	25-70	1 M H_2SO_4	Fe	175
1979[a]			20% NaCl	SO_4^{2-}	461

[a] Reported in abstract as 473 kcal mol^{-1}. Incorrect units may have been assigned.

ferent in most cases. In one case, a difference of 8 kJ mol^{-1} was noted, depending on whether the rate was measured in terms of SO_4^{2-} produced or Fe^{2+} produced in the same experiment.[174] Even the lowest activation energy significantly exceeds that expected for a diffusion-controlled process, normally ~10 kJ mol^{-1},[201] so it is unlikely that the rate of pyrite oxidation in aqueous solution is controlled by transport of oxygen to the pyrite surface or by the diffusion of products away from the surface.

3. Source of Sample and Morphology

Only marginal differences in the rate of leaching of pyrite by oxygen have been observed for specimens sampled from different sulfide ores. Warren[185] observed no difference in the leach rates of pyrite from three Australian ores. Bailey and Peters[12] classified their set of specimens collected from the United States, Canada, and Japan into two groups, one being slightly more reactive than the other. The more reactive group came from a common location (Sullivan, Cominco Mines). Scanning electron micrographs indicated that the more reactive specimens had a rougher fractured surface. All the specimens discussed above would be categorized as primary euhedral material and occurred either as large crystals or as a crystalline mass.

The influence of morphology on the reaction rate has been studied by a number of workers. Leathen et al.[202] reported a fivefold increase for the bacterially catalyzed oxidation of marcasite compared with that of sulfur ball pyrite. Caruccio and co-workers[18-21] reported that framboidal pyrite is significantly more reactive than euhedral pyrite. Pugh[203] obtained the following order: massive pyrite < framboidal pyrite < museum pyrite < marcasite, for bacterially catalyzed oxidation of material crushed or sieved to a common size. The high reaction rate for the museum grade pyrite was attributed to the production of fresh surfaces during crushing. Mathews and Robins[175] considered that the bacterial oxidation rate of pyrite and marcasite is similar to the chemical oxidation of these two materials and independent of crystal form.

4. Surface Area and Pulp Density

There are a number of reports in the literature indicating that the rate of reaction is linearly related to the surface area. However, inspection of the experimental data indicates that the evidence is not really sufficient to substantiate these claims.

Stenhouse and Armstrong[186] concluded from four results that the rate of oxidation of pyrite by oxygen in caustic soda is inversely proportional to the square of the average particle size over a size range of 11–120-μm diameter. Warren[185] noted that the leach rate in water increases with reducing particle size. Cornelius and Woodcock,[174] using ground pyrite (in the range −270 mesh + 325 mesh Tyler) with a theoretically calculated surface area of 0.024 $m^2 g^{-1}$, concluded from three experiments in which the pulp density was changed from 16.7 g L^{-1} to 33.3 g L^{-1} that the rate of reaction is directly proportional to the surface area of the pyrite. Similarly, McKay and Halpern[162] observed a linear relationship between reaction rate and surface density on varying the pulp density of their solutions. The materials used were an unsieved ground material (surface area 0.053 $m^2 g^{-1}$) one sized in the range −150 mesh + 200 mesh Tyler (0.5 wt % of the unsieved material; surface area 0.0275 $m^2 g^{-1}$) and another in the range −270 mesh + 325 mesh Tyler (64.3 wt % of the unsieved material; surface area 0.053 $m^2 g^{-1}$). The surface area was estimated by microscopic examination and was approximately double the theoretical estimate of Cornelius and Woodcock[174] for the same size fraction of ground pyrite. Mathews and Robins[175] reported the rate to be linearly related to the surface area. These workers used two samples in the range −36 mesh + 52 mesh British Standard (surface area 0.66 $m^2 g^{-1}$) and −85 mesh + 120 mesh British Standard (surface area 0.76 $m^2 g^{-1}$). The surface area was determined by B.E.T. krypton adsorption.

Bailey and Peters[12] studied the effect of particle size on the rate of reaction, using four sieved fractions and samples from two sources. The surface area, which ranged from 0.01 to 0.03 $m^2 g^{-1}$, was calculated assuming spherical particle geometry. These authors reported a loss of linearity between reaction rate and apparent surface area and suspected that a roughness factor should be included for the coarser material.

In summary the following rate equations have been reported for surface area effects: rate $\propto 1/d^2$, d = average particle diameter;[186] rate $\propto$ SA, SA = surface area;[167,174-175] rate $\propto SA^n$.[12]

5. pH

The influence of pH on the rate of pyrite leaching by dissolved oxygen has been variously reported as nil to significant. Smith and Shumate[16] demonstrated that the rate of reaction for the oxidation of pyrite in water at 25 °C and 0.1-MPa oxygen partial pressure increases nonlinearly, possibly as the exponential or square, as the pH is raised from 1 to 10. This is the only study over the complete pH range. Stenhouse and Armstrong[186] observed the rate to be pH dependent for the pressure leaching of pyrite at 120 °C and 1.4-MPa oxygen partial pressure in caustic solutions. Gray[204] and then Warren[185] observed that the addition of calcium carbonate during the pressure leaching of pyrite in water at 190 °C and 0.17 MPa would drastically reduce the oxidation rate. Bunn[205] reported that the reaction rate is linear with sodium hydroxide concentration for a packed-bed reactor operating between 120 and 215 °C. Kostina and Chernyak[206] discussed the kinetics of

leaching pyrite in sodium and potassium hydroxide at 50 °C.

Kim and Choi[180] found that the pressure leaching rate of pyrite is independent of pH at elevated temperatures and pressures and in strong acid solutions. Similarly, Mathews and Robins[175] concluded that the leaching rate was independent of pH over the range −0.7 to 1.2 for coal pyrite (a pyrite–marcasite mixture) at 25 to 70 °C. McKay and Halpern[162] explored the system in more detail to determine the pressure leaching rate of pyrite in acid at 110 °C and 0.4-MPa oxygen partial pressure. In the absence of any H_2SO_4 present, all the sulfur in the pyrite was converted to sulfate and no elemental sulfur was formed. On the other hand, when the solution contained 0.15 M H_2SO_4 initially, no additional free acid was formed and the sulfur was oxidized to elemental sulfur and ferrous and ferric sulfate. With intermediate initial acid concentrations, the products were distributed between free acid, sulfate as ferrous and ferric sulfate, and elemental sulfur. Bailey and Peters[12] demonstrated that if the acid strength is increased beyond 0.17 M H_2SO_4, the leaching reaction becomes an acid consumer rather than an acid generator. This was elegantly explained in terms of competing anodic reactions:

$$FeS_2 + 8H_2O \rightarrow Fe^{3+} + 2SO_4^{2-} + 16H^+ + 15e^- \quad (15)$$

and

$$FeS_2 \rightarrow Fe^{2+} + S^0 + 2e^- \quad (16)$$

These are half-cell reactions; to apply these to an operating system, the stoichiometries have to be modified to

$$FeS_2 + 4yH_2O \rightarrow xFe^{3+} + ySO_4^{2-} + 8yH^+ + (x + 7y)e^- \quad (17)$$

and

$$FeS_2 \rightarrow (1 - x)Fe^{2+} + (2 - y)S^0 + (2 - y)e^- \quad (18)$$

where the stoichiometric coefficients x and y reflect the relative proportions of the two half-cell reactions. The overall stoichiometry of the anodic reaction is then given by the sum

$$FeS_2 + 4yH_2O \rightarrow (1 - x)Fe^{2+} + xFe^{3+} + ySO_4^{2-} + (2 - y)S^0 + 8yH^+ + (2 + x + 6y)e^- \quad (19)$$

The complementary cathodic reaction

$$0.5O_2 + 2H^+ + 2e^- \rightarrow H_2O \quad (20)$$

is modified to

$$(0.5 + 0.25x + 1.5y)O_2 + (2 + x + 6y)H^+ + (2 + x + 6y)e^- \rightarrow (1 + 0.5x + 3y)H_2O \quad (21)$$

and the overall stoichiometry for the oxidation of pyrite becomes

$$FeS_2 + (0.5 + 1.5y + 0.25x)O_2 + (2 + x - 2y)H^+ \rightarrow (1 - x)Fe^{2+} + xFe^{3+} + (2 - y)S^0 + ySO_4^{2-} + (1 - y + 0.5x)H_2O \quad (22)$$

The push–pull effect of x and y within the stoichiometric term for the hydrogen ion $(2 + x - 2y)$ predicts a pH maximum. This was confirmed experimentally by Bailey and Peters,[12] who found that acid production during the pressure leaching of pyrite becomes zero at an acid concentration of 0.17 M H_2SO_4 (pH 1) and that further increase in acid strength causes acid consumption. The acid is consumed by the ferrous ion which is produced by the oxidation of pyrite to ferrous ion and elemental sulfur. Consequently, the system becomes self-buffering at about pH 1.

6. Humidity in Undersaturated Systems

The role of water is germane to identifying the controlling mechanism. In the atom-transfer model of Singer and Stumm,[163,164] water is relegated to the role of solvent, whereas in the electrochemical model of Bailey and Peters,[12] it is a reactant. In saturated systems, the role of water is not obvious, and it is necessary to resort to the isotopic marking techniques of Bailey and Peters.[12] However, in undersaturated systems the role of water may be readily identified by examining the influence of water concentration, i.e., humidity, on the reaction rate.

The earliest report on the instability of pyrite in moist air is that of Berzelius[207] although, according to Mellor,[6] the phenomenon was already well-known and used to prepare ferrous sulfate solutions as a precursor to vitriolic acid by exposing pyrites in heaps to moist air and collecting the drainage water in tanks for evaporation. The reaction was discussed widely during the 19th century and then, except for the reference in Mellor's encyclopedic work, was forgotten.

The partial pressure of water in the gas phase of an undersaturated system is termed the absolute humidity, but usually it is measured as a relative humidity. The relative and absolute humidities are related by

$$\text{rh} = \frac{P}{P_{sat}} \times 100 \quad (23)$$

where rh is the relative humidity percentage, P is the partial pressure of water, P_{sat} is the vapor pressure of water at the given temperature, and

$$\text{ah} = \frac{(\text{rh})P_{sat}M}{100RT} \text{ g per unit volume} \quad (24)$$

where ah is absolute humidity, M is the molecular weight of water, R is the gas content, and T is the temperature in K. The relative humidity is usually measured by determination of the dew point, and the vapor pressure of water as a function of temperature is listed in tables of physical chemical constants.[208] Howie[158] presented a simplified hygrometric chart that showed the relationship between absolute and relative humidity as a function of temperature.

Kim[209] reported that over a limited absolute humidity range at 25 °C the rate varied linearly with the absolute humidity. Morth and Smith[210] extended this work to 45 °C. Their results showed that (i) with increasing temperature, the reaction order increased beyond first order; (ii) for a given absolute humidity, the reaction rate decreased with temperature; (iii) for a given relative humidity, the reaction rate decreased with temperature; and (iv) at 100% relative humidity, the reaction rates in the vapor phase and liquid phase were very similar.

Smith and Shumate[16] thought that the reaction was controlled by the degree of water adsorption on the pyrite surface. Vapor phase oxidations of pyrite have been reported by a number of workers who did not develop a kinetic expression.[158,167,211-214]

7. Catalysts

The oxidation of pyrite is insensitive to small amounts of additives, although some effect is noticed with gross amounts in ~1 M concentrations. Small additions of copper have minimal effect on the pressure leaching of pyrite.[12,162] Additions of up to 1 M concentrations of $CaSO_4$, $ZnSO_4$, and $NiSO_4$ depress the leach rates by up to 30%. The pressure-leaching rates are insensitive to heavy addition of sulfate.[185]

Additions considerably in excess of normal environmental levels of humic acids, chromium, copper, manganese, and nickel cations, and nitrate, chloride, phosphate, and sulfate anions have no effect on the atmospheric leaching rate of coal pyrite, and an inhibitory effect occurs with phosphate at concentrations greater than 200 mg L^{-1}.[16]

Under laboratory conditions the rate of reaction at low or high temperatures appears to be independent of low ferrous and ferric ion concentrations.[16,162,215] Increasing the ferric concentration to >0.1 M introduces a competing oxidation reaction which leads to an increase in the overall rate.[176,216] Inhibition of pyrite weathering can be achieved by recycling mine effluent with an Fe concentration of 100 mg L^{-1} at pH 4.5 onto the spoil heaps.[217] Diev and Pavlov[211] reported that peat water or xylenols inhibit the oxidation.

8. Mechanisms

Identification of the rate-determining step must take into account the following observations:

(i) The rate is between fractional and first order with respect to oxygen and is independent of solution composition, i.e., the concentrations of H^+, Fe^{2+}, Fe^{3+}, Cu^{2+}, SO_4^{2-}, except for gross variations of composition, and then only marginally.

(ii) The activation energy indicates a chemical rather than physical rate-determining step.

(iii) The rate is first order or greater with respect to water in undersaturated systems.

(iv) Production of elemental sulfur reaches a maximum at about 100–150 °C; overall production is reduced above 150 °C and is minimal at ambient temperatures.

(v) Formation of elemental sulfur is favored by high acidities.

(vi) Formation of a thiosulfate intermediate is possible.

(vii) Pyrite can be oxidized by an electrochemical reaction.

Early theories favored an oxygen adsorption mechanism followed by a chemical reaction.[185,186] This approach was developed by McKay and Halpern,[162] who proposed that oxygen is chemisorbed rapidly on the pyrite surface. Consequently, the surface is always covered by a monolayer of oxygen with one oxygen molecule at each FeS_2 site; i.e.,

$$FeS_2 + O_{2_{aq}} \xrightarrow{\text{fast}} FeS_2{\cdot}O_2 \qquad (25)$$

Oxidation occurs through further adsorption by a second oxygen molecule on an O_2-covered site; this is viewed as the slow step:

$$FeS_2{\cdot}O_2 + O_{2_{aq}} \xrightarrow{\text{slow}} FeS_2{\cdot}2O_2 \rightarrow FeSO_4 + S^0 \qquad (26)$$

The experimentally determined apparent entropy of activation is −75 J M^{-1} K^{-1}, which is not unreasonable for a rate-determining process involving adsorption of a reactant from solution onto a solid surface. The ultimate distribution of products between Fe^{2+}, Fe^{3+}, S^0, and SO_4^{2-} is determined by the subsequent oxidation reactions:

$$8FeSO_4 + 2O_2 + 2H_2SO_4 \rightarrow 8Fe_2(SO_4)_3 + 4H_2O \qquad (27)$$

and

$$2S + 3O_2 + 2H_2O \rightarrow 2H_2SO_4 \qquad (28)$$

These reactions are not involved in the rate-determining process.

Mathews and Robins,[175] quoting from a conference paper by Majima and Peters,[189] reviewed a modified adsorption–chemical reaction path via the formation of thiosulfate. In the first step, oxygen is adsorbed to form atomic oxygen:

$$O_{2_{aq}} \rightarrow 2O_{ads} \qquad (29)$$

The slow step is the oxidation of the pyritic sulfur to adsorbed thiosulfate:

$$3O_{ads}{\cdot}FS_2 \xrightarrow{\text{slow}} FeS_2O_{3_{ads}} \qquad (30)$$

The thiosulfate will then desorb and disproportionate to sulfite and elemental sulfur:

$$FeS_2O_3 + 2H^+ \rightarrow Fe^{2+} + H_2SO_3 + S^0 \qquad (31)$$

and the sulfite is further oxidized to sulfate

$$H_2SO_3 + {}^1/_2O_2 \rightarrow HSO_4^- + H^+ \qquad (32)$$

The rate-controlling step is a function of the surface area and the adsorption isotherm, leading to a theoretical rate equation:

$$\frac{d[FeS_2]}{dt} = KA\frac{K_2[P_{O_2}]^{1/2}}{1 + K_2[P_{O_2}]^{1/2}} \qquad (33)$$

An alternative mechanism recognized by McKay and Halpern[162] is one in which elemental sulfur is not an intermediate in the formation of sulfate but elemental sulfur and sulfate are produced by simultaneously competing paths via a common intermediate:

$$FeS_2 + O_2 \xrightarrow{\text{slow}} FeS_2{\cdot}O_2 \text{ (a)}$$

$$FeS_2{\cdot}O_2 \rightarrow FeSO_4 + S \text{ (b)}$$

$$FeS_2O_2 + H_2O \rightarrow FeSO_4 + H_2SO_4 \text{ (b')} \qquad (34)$$

with the formation of the intermediate as the slow step.

This adsorption mechanism requires, at least initially, a 50:50 distribution of elemental sulfur and sulfate as product. This is only observed experimentally at approximately 120 °C. Although higher temperatures favor subsequent oxidation of elemental sulfur to sulfate, oxidation of elemental sulfur below the melting point of sulfur (112.8 °C)[208] is exceptionally slow;[218] consequently, all elemental sulfur produced during the low temperature oxidation of pyrite should appear as a final product and be in the region of 50% of pyritic sulfur oxidized. This is not observed in practice. In fact, minimal to nil elemental sulfur is produced in the low-temperature experiments.

The adsorption mechanisms are effectively chemical reactions at the pyrite surface involving adsorbed oxygen. An alternative approach is an electrochemical

mechanism with separate anodic reactions (eq 15 and 16) and a cathodic reaction (eq 20).

An important difference between these two approaches is that whereas the oxygen in the products via the adsorption mechanism is derived from dissolved molecular oxygen, the oxygen in the products via the electrochemical mechanism is derived from water, and the dissolved molecular oxygen is employed in a separate cathodic reaction.

The electrochemical mechanism does not require a 50:50 distribution of elemental sulfur and sulfate in the product because, in contrast to the absorption mechanism, the elemental sulfur and sulfate occur through separate independent reactions which would be expected to have different reaction rates. Bailey and Peters[12] suggested that the production of elemental sulfur is self-inhibitive owing to the formation of a passive sulfur film. Because of the increase in volume of solids as pyrite is oxidized to monoclinic sulfur (24 $cm^3\ mol^{-1}\ FeS_2 \rightarrow 32.7\ cm^3\ mol^{-1}\ S^0$), this film remains intact if less than 27% of the pyrite decomposes simultaneously to form sulfur. If sulfur production increases above 27%, it would lead to less protection, through strain and cracking of the film, and to higher decomposition rates, whereas raising the temperature above the melting point of monoclinic sulfur (120 °C) would destroy the passive film completely. An objection to this argument is that unless the two reactions 15 and 16 are site specific, there should be an accumulation of sulfur over the total surface below 120 °C and this accumulating film should inhibit both reactions. Bailey and Peters[12] were able to derive a rate equation in terms of the Tafel parameters of eq 15 and 20 and the oxygen adsorption isotherm:

$$\log \text{rate} = K_1 + \frac{b}{b_c + b_a} \log \frac{K_2 P_{O_2}}{1 + K_3 P_{O_2}} \qquad (35)$$

where b_a and b_c are the Tafel parameters of the anodic and cathodic reactions. Although this theoretical equation is similar to the experimental rate equation, more conclusive evidence is required in the form of the oxygen adsorption isotherm.

C. Oxidation of Ferrous Iron

As indicated in section IVA, the oxidation of ferrous iron to ferric iron by molecular oxygen is one of a series of reactions that may occur in acid mine drainage. Singer and Stumm[164] suggested that this can become the rate-limiting step. Although conditions can be envisaged where this is certainly true, it is also true that conditions may be adjusted to more favorable kinetics so that the reaction is no longer rate limiting. Specific variables on the reaction rate are discussed below.

1. Reaction Order

The reaction order for the oxidation of ferrous iron by molecular oxygen is a function of the media, pH, ferrous iron concentration, oxygen concentration, temperature, and certain catalytic materials. Changes in molecularity also occur when some conditions are varied. It is necessary, therefore, in both experiment and review to define clearly the operating conditions. The extensive range of rate equations is summarized in Tables VII, VIII, and IX.

In Sulfuric Acid, Nitric Acid, and Perchloric Acid, pH <2, ~25 °C. Knowledge of the chemistry of ferrous sulfate, vitriol, dates back to classical times. Mellor[6] has briefly reviewed its interesting history and also provided a detailed review of work during the late 19th and early 20th century on the kinetics of the air and molecular oxygen oxidation of ferrous sulfate. These and subsequent studies indicated that at ambient temperatures and in sulfuric acid solutions below pH 2, the rate of reaction was very slow, independent of pH, first order with respect to the partial pressure of oxygen and second order with respect to ferrous iron,[162,174,219-225] resulting in the rate equation

$$-\frac{d[Fe^{2+}]}{dt} = K[Fe^{2+}]^2 P_{O_2} \qquad (36)$$

Mathews and Robins[226] reported a slight drop in reaction rate with increasing acidity over the pH range 2–0.5 with a fractional order of $[H^+]^{-1/4}$. A slight increase in reaction rate has been observed for concentrated sulfuric acid solutions.[227,228] The rate is independent of dissolved ferric ion,[229] provided that additional sulfuric acid is added; otherwise the products slow down the reaction rate.[230] Huffman and Davidson[231] observed a dependence of the reaction rate on the sulfate concentration at a fixed pH and ionic strength. The above reaction order also applies to the oxidation of ferrous iron by oxygen in nitric acid[227,232] and in perchloric acid.[227,233,234] For both acids, the reaction rate increased as the acid strength was increased from pH ~1 to more concentrated solutions. There is some evidence that the ClO_4^- ion will contribute to the oxidation at 70 °C.[235]

Kinetics have also been reported for a relatively fast reaction in oxalic acid at pH 1.0.[232]

In Sulfuric Acid, pH <2, >100 °C. As the temperature is raised, the reaction order changes.[236-239] Huffman and Davidson[231] demonstrated that the kinetics of ferrous iron oxidation by molecular oxygen in 1 M sulfuric acid at 140–180 °C proceeds simultaneously by second-order and first-order paths with respect to ferrous iron, giving an overall rate equation:

$$\frac{d[Fe^{2+}]}{dt} = K_1[Fe^{2+}]P_{O_2} + K_2[Fe^{2+}]^2 P_{O_2} \qquad (37)$$

and that the reaction reverts to the single second-order reaction with respect to ferrous iron at 30 °C. This was contrary to the result predicted from the high-temperature activation energies. The high-temperature experiment results have been independently confirmed.[240,241] Cornelius and Woodcock[174] considered the reaction to be solely second order with respect to ferrous iron over the temperature range 110–165 °C, pH 1.4–1.2, and between 1 and 3 g L^{-1} Fe^{2+}. Saprygin and Gusar[242] considered the reaction path to have variable dependence on the ferrous ion concentration. At concentrations below 0.05 mol of Fe^{2+} L^{-1} in sulfuric acid and between 90 and 150 °C, the oxidation is first order with respect to ferrous ion; above 0.1 g of mol of Fe^{2+} L^{-1}, the reaction is second order. In addition, it was considered that Fe^{3+} inhibits the rate of formation of Fe^{2+}. Deviation from simple-order kinetics with increasing dilution of ferrous ion had previously been reported.[243-245]

TABLE VII. Kinetics of Ferrous Iron Oxidation by Molecular Oxygen in Various Pure Media

rate equation, $-\frac{d[Fe^{2+}]}{dt} =$	temp, °C	pH	media: anion	media: concn	Fe^{2+} concn	constant	activation energy: ΔH^*, kJ	activation energy: temp range, °C	ref
$K[Fe^{2+}]^2P_{O_2}$	30	~0	H_2SO_4	1 M	0.45-0.02 M	$K = 1.1 \times 10^{-6}$ M^{-1} atm^{-1} s^{-1}			219
$K[Fe^{2+}]^2P_{O_2}$	30	~0	H_2SO_4	1 M	0.2-0.15 M	$K = 4.0 \times 10^{-6}$ M^{-1} atm^{-1} s^{-1}			223
$K[Fe^{2+}]^2P_{O_2}$	30	~0	H_2SO_4	1 M	0.025-0.001 M	$K = 2.78 \times 10^{-6}$ M^{-1} atm^{-1} s^{-1}			231
$K[Fe^{2+}]^2P_{O_2}$	80	~0	H_2SO_4	1 N	~1.2 N		73.6	40-80	236
$K[Fe^{2+}]^2P_{O_2}[H^+]^{-1/4}$	30	~1	H_2SO_4	1 N	0.01-1.0 M	$K = 5.1 \times 10^{-7}$ $M^{-1.25}$ atm^{-1} s^{-1}	74	20-80	226
$K_b[Fe^{2+}]P_{O_2} +$ $K_t[Fe^{2+}]^2P_{O_2}$	159	~1	H_2SO_4	1 M	0.025-0.001 M	$K_b = 1.93 \times 10^{-5}$ atm^{-1} s^{-1}	56 ± 8	140-180	231
						$K_t = 1.60 \times 10^{-3}$ M^{-1} atm^{-1} s^{-1}	68 ± 8	140-180	
$K[Fe^{2+}]^2P_{O_2}$	100	~1	H_2SO_4	0.08 M	0.05 M	$K = 4.2 \times 10^{-4}$ M^{-1} atm^{-1} s^{-1}	69	100-130	162
$K[Fe^{2+}]^2P_{O_2}$	130	~1	H_2SO_4	0.05 M	0.05 M	$K = 3.0 \times 10^{-3}$ M^{-1} atm^{-1} s^{-1}	62	130-165	174
$K[Fe^{2+}]P_{O_2}$	150	~1	H_2SO_4	0.1 N	0.1 N	$K = 2.0 \times 10^{-5}$ atm^{-1} s^{-1}	56	100-150	240
$K[Fe^{2+}]^2P_{O_2}$	30	~0	$HClO_4$	1 N	0.3-0.01 M	$K = 9.7 \times 10^{-7}$ M^{-1} atm^{-1} s^{-1}	73	25-40	233
$K[Fe^{2+}]^2P_{O_2}$	30	~0	$HClO_4$	1 N		$K = 2 \times 10^{-6}$ M^{-1} atm^{-1} s^{-1}	65	30-60	234
$K[Fe^{2+}]^2P_{O_2}$	30	~0	HCl	1 N		$K = 6.5 \times 10^{-7}$ M^{-1} atm^{-1} s^{-1}			219
$K[Fe^{2+}]P_{O_2}$	150	~1	HCl	0.1 N	0.1 M	$K = 9.2 \times 10^{-6}$ atm^{-1} s^{-1}			240
$K[Fe^{2+}]P_{O_2}f[HCl]$	18	<1	HCl	8 N	0.055 N	$K = 1.3 \times 10^{-3}$ atm^{-1} s^{-1}	61.1	0-36	255
$K[Fe^{2+}]P_{O_2}f[HCl]$	45	<1	HCl	6 N	0.2 M	$K = 3.1 \times 10^{-4}$ atm^{-1} s^{-1}	78.2	35-60	261
$K_1 + K_2[Cl^-]$	30	<0	HCl	0-3 M		$K_1 = 2.7 \times 10^{-6}$, $k_2 = 8.9 \times 10^{-7}$	71.9	30-60	257
$K[Fe^{2+}]P_{O_2}[H_3PO_4]$	30	~2	H_3PO_4	1 N	0.02-0.005 M	$K = 1.25 \times 10^{-3}$ M^{-2} atm^{-1} s^{-1}	83	20-30	250
$K_1[Fe^{2+}]P_{O_2}[H_3PO_4]^2 +$ $K_2[Fe^{2+}]P_{O_2}[H_4P_2O_7]$	30	1-2	H_3PO_4 + $H_4P_2O_7$	0.2-0.4 M 0.2-0.8 M	0.02-0.005 M	$K_1 = 1.08 \times 10^{-3}$ M^{-2} atm^{-1} s^{-1}	88	20-30	251
						$K_2 = 2.13 \times 10^{-3}$ M^{-1} atm^{-1} s^{-1}	25	20-30	
$K[Fe^{2+}]P_{O_2}[H_4P_2O_7^{2-}]$	30	2-3	$H_4P_2O_7$	5×10^{-3} M	0.01 M	$K = 2.2 \times 10^{-5}$ M^{-1} atm^{-1} s^{-2}			253
$K[Fe^{2+}]P_{O_2}$	25	3-5	H_2SO_4	0.0005 M	$\sim 7 \times 10^{-4}$ M	$K = 1.7 \times 10^{-9}$ atm^{-1} s^{-1}			164
$K[Fe^{2+}]P_{O_2}[OH^-]^2$	20	6-7	HCO_3^-	0.01 N	3×10^{-5} M	$K = 2.5 \times 10^{11}$ M^{-2} atm^{-1} s^{-1}	96	20-50	298
$K[Fe^{2+}]P_{O_2}[OH^-]^2$	25	6-7	HCO_3^-	0.01 N	5×10^{-5} M	$K = 3.5 \times 10^{11}$ M^{-2} atm^{-1} s^{-1}			276
$K[Fe^{2+}]P_{O_2}[OH^-]^2$	21	7-7.5	HCO_3^-	0.01 N	5×10^{-5} M	$K = 9.5 \times 10^{11}$ M^{-2} atm^{-1} s^{-1}			280
$K[Fe^{2+}]P_{O_2}[OH^-]_2\beta^n$	25	6-7	HCO_3^-	0.01 N	5×10^{-5} M	$K = 8.3 \times 10^{11}$ M^{-2} atm^{-1} s^{-1}			462
$K[Fe^{2+}]P_{O_2}[OH^-]^2$	25	6-7	HCO_3^-	0.01 N	5×10^{-5} M	$K = 8.3 \times 10^{11}$ M^{-2} atm^{-1} s^{-1}			463
$K[Fe^{2+}]P_{O_2}[OH^-]^2$	25	6-7				$K = 2.3 \times 10^{12}$ M^{-2} atm^{-1} s^{-1}			281
$K[Fe^{2+}]P_{O_2}[OH^-]^2$		~8	sea water			$K = 1.6 \times 10^{10}$ M^{-2} atm^{-1} s^{-1}			283
$K[Fe^{2+}]P_{O_2}[OH^-]^2$		~8				$K = 1.5 \times 10^{10}$ M^{-2} atm^{-1} s^{-1}			284
$K[Fe^{2+}]P_{O_2}[OH^-]^2$		6-7	HCO_3^-	0.01 M	3×10^{-5} M	$K = 4.0 \times 10^{11}$ M^{-2} atm^{-1} s^{-1}			285

TABLE VIII. Kinetics of Ferrous Iron Oxidation by Molecular Oxygen in the Presence of Possible Catalysts

rate equation	temp, °C	pH	Media: anion	Media: concn	Fe^{2+} concn	catalyst: ion	catalyst: concn	rate constant	ref
$K_t[Fe^{2+}]^2P_{O_2} +$ $K_{Cu}[Fe^{2+}][Cu^{2+}]$	30	~1	SO_4^{2-}	0.5 M	0.001 M	Cu	1.1×10^{-5} M	$K_t = 1.5 \times 10^{-5}$ M^{-1} atm^{-1} s^{-1} + $K_{Cu} = 7.6 \times 10^{-3}$ M^{-1} s^{-1}	231
$K[Fe^{2+}][Z]P_{O_2}$	25	~2	ClO_4^-	1 M	2.9×10^{-5} M	HEDTA	$\sim 10^{-5}$ M	$K = 1.6$ M^{-1} atm^{-1} s^{-1}	337
$K[Fe^{2+}][Z]P_{O_2}$	25	~2	ClO_4^-	1 M	2.9×10^{-5} M	EDTA	$\sim 10^{-5}$ M	$K = 0.06$ M^{-1} atm^{-1} s^{-1}	337

$K[Fe^{2+}][Z]P_{O_2}$	25	~2	ClO_4^-	1 M	2.9×10^{-5} M	NTA	$\sim 10^{-5}$ M	$K = 0.02\ M^{-1}\ atm^{-1}\ s^{-1}$	337
$K[Fe^{2+}][Z]P_{O_2}$	25	~2	ClO_4^-	1 M	2.9×10^{-5} M	HDTPA	$\sim 10^{-5}$ M	$K = 0.004\ M^{-1}\ atm^{-1}\ s^{-1}$	337
$K[Fe^{2+}][Z]P_{O_2}$	25	~2	ClO_4^-	1 M	2.9×10^{-5} M	DTPA	$\sim 10^{-5}$ M	$K = 0.002\ M^{-1}\ atm^{-1}\ s^{-1}$	337
$K[Fe^{2+}][Z]P_{O_2}$	25	~2	ClO_4^-	1 M	2.9×10^{-5} M	EDTAOH	$\sim 10^{-5}$ M	$K = 0.02\ M^{-1}\ atm^{-1}\ s^{-1}$	337
$K[Fe^{2+}][Z]P_{O_2}$	25	~2	ClO_4^-	1 M	2.9×10^{-5} M	EDTP	$\sim 10^{-5}$ M	$K = 0.02\ M^{-1}\ atm^{-1}\ s^{-1}$	337
$K[Fe^{2+}][Z]P_{O_2}$	25	~2	ClO_4^-	1 M	2.9×10^{-5} M	CyDTA	$\sim 10^{-5}$ M	$K = 0.02\ M^{-1}\ atm^{-1}\ s^{-1}$	337
$K[Fe^{2+}]^2[Cu]^{1/2}P_{O_2}$	100	~1	SO_4^{2-}	0.08 M	0.05 M	Cu	$\sim 10^{-5}$ M	$K = 1.3 \times 10^{-2}\ M^{-1.5}\ atm^{-1}\ s^{-1}$	162
$K[H^+][Fe^{2+}]P_{O_2}[C][Fe]^{-1}$	35	~0	HCl	2 N	0.061 N	C	89 g L^{-1}	$K = 0.39\ M^{-2}\ atm^{-1}\ s^{-1}$	301
$K[Fe^{2+}]P_{O_2}[OH^-]^2$	25	6.5	HCO_3^-	0.01 M	1×10^{-4} M	ClO_4^-	0.1 M	$K = 3.02 \times 10^{11}\ M^{-2}\ atm^{-1}\ s^{-1}$	197
$K[Fe^{2+}]P_{O_2}[OH^-]^2$	25	6.5	HCO_3^-	0.01 M	1×10^{-4} M	NO_3^-	0.1 M	$K = 2.59 \times 10^{11}\ M^{-2}\ atm^{-1}\ s^{-1}$	197
$K[Fe^{2+}]P_{O_2}[OH^-]^2$	25	6.5	HCO_3^-	0.01 M	1×10^{-4} M	Cl^-	0.1 M	$K = 2.07 \times 10^{11}\ M^{-2}\ atm^{-1}\ s^{-1}$	197
$K[Fe^{2+}]P_{O_2}[OH^-]^2$	25	6.5	HCO_3^-	0.01 M	1×10^{-4} M	$H_3SiO_4^-$	0.0012 M	$K = 2.07 \times 10^{11}\ M^{-2}\ atm^{-1}\ s^{-1}$	197
$K[Fe^{2+}]P_{O_2}[OH^-]^2$	25	6.5	HCO_3^-	0.01 M	1×10^{-4} M	Br^-	0.1 M	$K = 1.73 \times 10^{11}\ M^{-2}\ atm^{-1}\ s^{-1}$	197
$K[Fe^{2+}]P_{O_2}[OH^-]^2$	25	6.5	HCO_3^-	0.01 M	1×10^{-4} M	I^-	0.1 M	$K = 1.73 \times 10^{11}\ M^{-2}\ atm^{-1}\ s^{-1}$	197
$K[Fe^{2+}]P_{O_2}[OH^-]^2$	25	6.5	HCO_3^-	0.01 M	1×10^{-4} M	SO_4^{2-}	0.033 M	$K = 1.73 \times 10^{11}\ M^{-2}\ atm^{-1}\ s^{-1}$	197
$K[Fe^{2+}]P_{O_2}[OH^-][F^-]^2$	25	6.5	HCO_3^-	0.01 M	1×10^{-4} M	F^-	<0.1 M	$K = 1.73 \times 10^{7}\ M^{-3}\ atm^{-1}\ s^{-1}$	197
$K[Fe^{2+}]P_{O_2}[OH^-][H_2PO_4^-]^2$	25	4.5–4	HCO_3^-	0.01 M	1×10^{-4} M	$H_2PO_4^-$	0.1 M	$K = 6.38 \times 10^{6}\ M^{-3}\ atm^{-1}\ s^{-1}$	197
$(K[P_{O_2}][OH^-]^2 + K_{Si^-}$ $[H_4SiO_4]^{1/2}[OH^-]^{1/2})[Fe^{2+}]$	25	6.5	HCO_3^-	~0.01 M	$\sim 5 \times 10^{-5}$ M	H_4SiO_4	10^{-3} M	$K = 3.3 \times 10^{11}\ M^{-1}\ atm^{-1}\ s^{-1}$ $K_{Si} = 30\ M^{-1}\ s^{-1}$	276

Agde and Schimmel[246] reported an anomalous observation: when air at 105 atm was substituted for oxygen at 20 atm, a more rapid oxidation took place in the pressure oxidation of ferrous sulfate in acid and neutral solutions. Nicol[247] derived empirical expressions for an industrial process at elevated temperature (60–110 °C) and pressures (200–600 kPa). Tiwari, Kolbe, and Hayden[248] reported on recent studies employing oxygen–sulfur dioxide gas mixtures as the oxidant. Depending on the operating conditions, the following reactions could be favorably carried out: (i) oxidation of ferrous ion, (ii) reduction of ferric ion, and (iii) generation of sulfuric acid.

In Phosphoric Acid. Initial work by Spoehr[249] indicated that ferrous iron solutions are rapidly oxidized by molecular oxygen in the presence of pyrophosphate at ambient temperatures. Smith and Spoehr[243] subsequently determined the kinetics of the reaction and reported the rate to be first order with respect to ferrous iron:

$$-\frac{d[Fe^{2+}]}{dt} = K[Fe^{2+}]P_{O_2} \qquad (38)$$

This was discounted in a later study by Lamb and Elder,[223] who demonstrated that, under the experimental conditions employed, the rate is diffusion controlled and that Smith and Spoehr's observations were a function of the rate of stirring. Subsequent work[250,251] demonstrated that the reaction rate is first order with respect to ferrous iron for the oxidation of ferrous sulfate by molecular oxygen in phosphoric acid and pyrophosphoric acid solutions at pH ~1–2, with the ionic strength adjusted to 1.0–1.1 with sodium perchlorate, and at 30 °C. The rate is also second order with respect to phosphate, yielding an overall rate law

$$-\frac{d[Fe^{2+}]}{dt} = K[Fe^{2+}]P_{O_2}[H_2PO_4^-]^2 \qquad (39)$$

and first order to pyrophosphate with a rate law

$$\frac{d[Fe^{2+}]}{dt} = K_1[Fe^{2+}]P_{O_2}[H_2PO_4^-]^2 + K_2[Fe^{2+}]P_{O_2}[H_2P_2O_7^{2-}] \qquad (40)$$

King and Davidson[251] considered that phosphate and pyrophosphate species act as independent catalysts and that the second-order dependence on phosphate is not due to the equilibrium

$$2H_2PO_4^- = H_2P_2O_7^{2-} + H_2O \qquad (41)$$

Sokol'skii and co-workers[252] studied the oxidation of ferrous sulfate by molecular oxygen in both sulfuric acid and phosphoric acid solutions using a potentiometric technique and developed a working equation which is first order with respect to ferrous iron and oxygen; this is effectively a series relationship with either sulfate or phosphate truncated to the second power. The kinetics of ferrous iron oxidation in mixtures of perchloric and pyrophosphoric acid have been studied.[253,254]

In Hydrochloric Acid. Pound[227] reported that the rate of oxidation of ferrous chloride solutions by air is a function of acid strength, the rate increasing with increasing concentration of hydrochloric acid. At ambient temperatures, the effect is slight up to 1 M concentrations, but thereafter rises at an increasing rate.

TABLE IX. Catalytic Effect of Various Materials on the Oxidation of Ferrous Iron by Molecular Oxygen (Rate Laws Not Reported)

media		Fe^{2+}	temp,		catalyst			
anion	concn, M	concn, M	°C	pH	ion	concn, M	effect	ref
SO_4^{2-}	0.52	0.15	30	~0	Na	0.1	1.087	223
SO_4^{2-}	0.52	0.15	30	~0	Zn	0.1	1.153	223
SO_4^{2-}	0.52	0.15	30	~0	Mn	0.1	0.895	223
SO_4^{2-}	0.52	0.15	30	~0	Cr	0.1	0.676	223
SO_4^{2-}	0.52	0.15	30	~0	acetate	0.1	0.979	223
SO_4^{2-}	0.52	0.15	30	~0	PO_4^-	0.1	1.003	223
SO_4^{2-}	0.23	0.15	30	~0	K	0.1	0.815	223
SO_4^{2-}	0.23	0.15	30	~0	Mg	0.1	1.125	223
SO_4^{2-}	0.23	0.15	30	~0	Ni	0.1	1.254	223
SO_4^{2-}	0.23	0.15	30	~0	Cu	0.1	44	223
SO_4^{2-}	0.5	0.15	30	~0	C	0.2 g cm^{-3}	857	223
SO_4^{2-}	0.5	0.15	30	~0	Pt	0.01 g cm^{-3}	1198	223
SO_4^{2-}	0.5	0.15	30	~0	SiO_2	0.02 g cm^{-3}	3	223
SO_4^{2-}	1.0	0.005	140	~0	glass wool		Nil	231
ClO_4^-	0.51	0.1	35	~0	Cu	0.2	2.5	233
$H_2PO_4^-$	0.2	0.2	30	1-2	glass wool		Nil	251
SO_4^{2-}	0.05	0.2	50	1.45	glass wool		1.04	226
SO_4^{2-}	0.05	0.2	50	1.45	Ni	0.001	1.14	226
SO_4^{2-}	0.05	0.2	50	1.45	Zn	0.001	1.07	226
SO_4^{2-}	0.05	0.2	50	1.45	Cu	0.01	2.8	226
SO_4^{2-}	0.05	0.2	50	1.45	Mn	<0.001	1	226
SO_4^{2-}	0.05	0.2	50	1.45	Co	0.001	1.06	226
SO_4^{2-}	0.05	0.2	50	1.45	Hg	0.001	0.98	226
SO_4^{2-}	0.05	0.2	50	1.45	Mo	0.001	1.092	226
SO_4^{2-}	0.05	0.2	50	1.45	As	<0.001	1.06	226
SO_4^{2-}	0.05	0.2	50	1.45	Cr	0.001	1.019	226
SO_4^{2-}	0.05	0.2	50	1.45	Na	0.001	1.17	226
SO_4^{2-}	1×10^{-2}	0.001	50	4.0	Al_2O_3	8000 m^2 L^{-1}	30	163, 330
SO_4^{2-}	1×10^{-2}	0.001	50	4.0	SiO_2	3000 m^2 L^{-1}	12	163, 330
SO_4^{2-}	1×10^{-2}	0.001	50	4.0	bentonite	10 g L^{-1}	12	163, 330
SO_4^{2-}	1×10^{-2}	0.001	50	4.0	Mn^{2+}	?	nil	163, 330
SO_4^{2-}	1×10^{-2}	0.001	50	4.0	Al^{3+}	?	nil	163, 330
SO_4^{2-}	1×10^{-2}	0.001	50	4.0	$Fe(OH)_3$	?	nil	163, 330
SO_4^{2-}	1×10^{-2}	0.001	50	4.0	kaolinite	?	nil	163, 330
SO_4^{2-}	1×10^{-2}	0.001	50	4.0	C	?	nil	163, 330
SO_4^{2-}	1×10^{-2}	0.001	50	4.0	FeS_2	?	nil	163, 330

Posner[255] and other workers[256,257] confirmed this observation and determined the kinetics in 4.0–8.0 M hydrochloric acid. The reaction is first order with respect to ferrous ion and oxygen but has a complex function with the hydrochloric acid. Astanina and Rudenko[232] reported that whereas hydrochloric acid is an accelerant, sodium chloride is a retardant. Leipina and Macejevskis[224] observed that potassium salts are accelerants. Other workers reported that the oxidation of ferrous chloride solutions in hydrochloric acid by molecular oxygen is second order with respect to ferrous ion and independent of pH or ferric ion as product.[258,259] Nikishova and co-workers[260] reported that, for the same system, there is a deviation from first-order kinetics owing to accumulation of ferric ion and variation in pH. A more recent study by Iwai and co-workers[261] identified the rate of reaction as first order with respect to ferrous ion, oxygen concentration, hydrogen ion activity, and chloride activity. These authors suggested that a reanalysis of earlier work with their analytical method might resolve the controversy.

In Near Neutral Waters (pH 3–7). The principal media in acid mine drainage is acid sulfate, but the presence of other anions should not be dismissed out of hand. Chlorides may be present due to seawater or brackish water or as effluent from a solvent extraction plant. Phosphates may be present either through normal agricultural use or as part of a rehabilitation program which includes extensive addition of phosphate fertilizer. Complexing organics may be present from natural sources or as industrial effluent. Rehabilitation programs normally include a lime treatment, and a knowledge of the oxidation kinetics under neutral and alkaline conditions is necessary for defining a liming program.

As the solution pH is raised from 2 toward 5, the reaction rate changes and there is a change in reaction order with respect to hydroxyl to give[262-266]

$$-\frac{d[Fe^{2+}]}{dt} = K[Fe^{2+}]P_{O_2}[OH^-] \qquad (42)$$

at pH <5. Sysoeva and Nikishova[267] reported a modified version of the above equation involving forward and backward rate constants. The pH of acid mine drainage is typically between 3 and 4, and is in the midrange in the change of reaction order with respect to hydroxyl. Consequently, an exact equation describing the kinetics of ferrous iron oxidation with respect to hydroxyl in acid mine drainage cannot be derived. Oxidation rates of ferrous iron in acid mine drainage field conditions have been measured, and a generalized empirical equation has been fitted to the results to describe the oxidation rate as a function of pH and ferrous iron concentration. The rate constants are site specific, indicating that on-site measurements are necessary.[268]

Equation 42 is only an intermediate condition because as the pH is raised above 5 to neutral, the reaction rate increases and the order changes to second order with respect to hydroxyl.[163,269-284]

$$-\frac{d[Fe^{2+}]}{dt} = K[Fe^{2+}]P_{O_2}[OH]^2 \quad (43)$$

at pH > 5.

The rate constant is a function of ionic strength, with high concentrations of NaCl or Na_2SO_4 or seawater reducing the rate constant by factors up to 100 over freshwater conditions.

In Alkaline Media. Increasing the pH into the alkaline region causes precipitation of ferrous hydroxide, which causes the rate of oxidation to change from a homogeneous to a heterogeneous reaction and leads to a further increase in the rate.[286,287] Room temperature studies by Roig and co-workers[288] suggested that oxidation of solid ferrous sulfate heptahydrate by molecular oxygen in the presence of solid calcium hydroxide proceeds via ferrous hydroxide as an intermediate. The heterogeneity of the reaction is indicated by the presence of an induction period that decreases with particle size, shaking, and the addition of calcium chloride. The rate of oxidation is a function of excess calcium hydroxide and the addition of calcium chloride. However, oxidation of dry powders by molecular oxygen at 100–150 °C[289] or 205–265 °C[290] is independent of the presence of alkali and proceeds in two steps. This high-temperature reaction has a low value for the energy of activation, which indicates that the oxidation process is essentially diffusion controlled.

Gluud and Reise[286] reported that the rate of oxidation of ferrous hydroxide suspensions is favored by the presence of ammonia hydroxide, whereas it is retarded by sodium hydroxide and sodium carbonate when they are present in high concentrations. It was suggested that this may be due to the reduced solubility of oxygen in sodium hydroxide. Emets and Bogdanov[291] observed that the rate decreases in the order LiOH > NaOH > KOH and confirmed Gluud and Reise's report[286] that the rate passes through a maximum with increasing alkali concentration. Macejevskis and Liepina[292] found that in a ferrous sulfate–ferrous hydroxide mixture there is a rapid and almost uniform autoxidation of ferrous hydroxide but that the ferrous sulfate is only oxidized slowly. A subsequent study with hydrated iron oxide indicated that the reaction is diffusion controlled.[293]

Gorshkov and Reibakh[294] reported that the oxidation of ferrous hydroxide is first order with respect to oxygen. Emets and Bogdanov[291] reported that the addition of sulfate ions during precipitation actually decreases the rate. This was confirmed by Prasad and Ramasastry[295] for the oxidation of ferrous hydroxide by air with a 5% excess of calcium hydroxide and varying additions of ferrous sulfate over the range 1.25–5%. These workers also showed that the rate of oxidation of ferrous hydroxide is dependent on air flow but independent of the amount of calcium hydroxide added over the range 10–30% excess; however the extent of oxidation depends on the amount of calcium hydroxide added. Very similar results were obtained with sodium carbonate as the alkali but with the rates increased by a factor of 2.

2. Catalysts

Mellor[6] summarized the early work on possible catalysts for the oxidation of acid solutions of ferrous sulfate by air or oxygen. The rate is accelerated by the surface catalysts palladium, platinum, gold, and coconut charcoal and the solution catalyst Cu^{2+}. The rate is not influenced by the presence of powdered silica gel, arsenic trioxide, ammonia, and the dissolved salts of uranium, vanadium, silver, zirconium, nickel, cerium, beryllium, Sn^{2+}, or Co^{2+}.

Surface Catalysts. The rate of oxidation of ferrous sulfate in sulfuric acid at pH 0 by molecular oxygen may be increased 1000-fold by the addition of freshly prepared platinum black,[296] but the catalyst is quickly poisoned.[223] The catalytic action of platinum was also reported for air oxidation of acidic ferrous sulfate solutions,[297] acidic ferrous chloride solutions,[227] and neutral ferrous iron solutions.[298]

A number of workers have reported on the air oxidation of acid ferrous sulfate solutions catalyzed by activated carbon.[297] Lamb and Elder[223] reported that the accelerating effect is approximately proportional to the amount of carbon up to 1 g per 50 cm^3 with the comment that the loss of linearity may have been due to inefficient stirring. Thomas and Ingraham[299] found the rate to be first order in oxygen and carbon and a complex function of the sulfuric acid, ferrous, and ferric concentrations and fineness of carbon. Saito[300] also reported the rate to be unimolecular with respect to carbon within the range 0.1–1 g per 50 cm^3 but found that the rate varies considerably with the type of activated carbon. Stumm and Lee[298] found that activated carbon catalyzes the air oxidation of neutral ferrous solutions.

Posner[301] studied the autoxidation of ferrous iron in dilute hydrochloric acid (0.1–4 N) by charcoal catalysis and found the reaction rate to be first order with respect to oxygen, hydrogen ion, and catalyst concentration but a more complex function of ferrous and ferric ion concentration, as would be expected for a heterogeneous surface reaction, to yield the rate equation

$$\frac{d[Fe^{2+}]}{dt} = \frac{K[H^+][Fe^{2+}]P_{O_2}[C]}{\sum Fe} \quad (44)$$

Lamb and Elder[223] reported a threefold increase in the oxidation rate following the addition of 1 g of silica gel to 50 cm^3 solution of 0.15 M ferrous sulfate in 1 M sulfuric acid. Although insoluble in strong acids, dissolved silica is a major constituent in most natural waters, principally as the monomeric orthosilicic acid H_4SiO_4.[302] This dissolved silica can form a moderately strong complex with ferric iron[303] and will affect the oxidation kinetics of ferrous iron in natural water. Schenk and Weber[276] obtained the following rate equation for the catalytic oxidation of ferrous iron by dissolved silica in a bicarbonate buffered system:

$$-\frac{d[Fe^{2+}]}{dt} = (KP_{O_2}[OH^-]^2 + K_{Si}[H_2SiO_4]^{1/2}[OH^-]^{1/2})[Fe^{2+}] \quad (45)$$

The effect of silica has also been studied by Stankevicius.[304]

A product of ferrous iron oxidations in neutral solutions is precipitated ferric hydroxide.[305] A number of workers have reported ferric hydroxide to be a catalyst for the oxidation of ferrous iron in neutral solution.[283,306–310] Bond and Bernard[311] reported that ferric

hydroxide retarded the oxidation whereas Stumm and Lee[275] found that addition of up to 5 mg L^{-1} Fe as ferric hydroxide had no appreciable effect on the reaction. Takai[312-314] pointed out that of the several types of ferric hydroxide, only γ-FeOOH, goethite, is an effective catalyst. A detailed study by Tamura, Goto, and Nagayama[315] indicated that in the presence of ferric hydroxide, either as a reaction product or as an additive, the reaction proceeds along two paths: (i) the normal homogeneous reaction that is first order with respect to oxygen and second order with respect to hydroxide; and (ii) a heterogeneous reaction that is first order with respect to ferrous iron and precipitated ferric hydroxide. The overall rate equation is

$$-\frac{d[Fe^{2+}]}{dt} = (K_0 P_{O_2}[OH^-]^2 + K_1[Fe(OH)_3])[Fe^{2+}] \quad (46)$$

Copper(II) Catalyst. The slow oxidation of ferrous sulfate in acid solution by air or molecular oxygen may be catalyzed by Cu^{2+}.[220,296,316-320] A reduction in oxidation rate has been reported by Banerji.[321] Unlike the uncatalyzed system, the rate is proportional to acid strength and logarithmically proportional to copper concentration, with a slight saturation effect toward 0.1 M $CuSO_4$. The rate is somewhat retarded in 1.0–4.0 M H_2SO_4 solutions and has a nonlinear function with H^+ ion activity.[322] The rate is also retarded by ferric ion either as a reaction product or as an additive.[323,324]

The saturation effect was noted by Kobe and Dicky[325] during high temperature (100–150 °C), copper-catalyzed, molecular oxygen oxidation of ferrous sulfate in sulfuric acid for the industrial recovery of spent acetylene absorber catalysts; an optimum concentration of 0.01 M copper sulfate was recommended. Huffman and Davidson[231] observed a change in reaction order for the oxidation of ferrous sulfate at room temperature by molecular oxygen at pH 1. Below 1×10^{-5} M Cu^{2+}, the rate is first order with respect to ferrous iron and cupric copper but zero order with respect to molecular oxygen; no dependence on acid strength was reported:

$$-\frac{d[Fe^{2+}]}{dt} = K[Fe^{2+}][Cu^{2+}] \quad (47)$$

Above what was termed "a relatively high" total cupric ion concentration of 1.1×10^{-5} M, the rate equation is also first order with respect to oxygen to yield an overall rate equation:

$$-\frac{d[Fe^{2+}]}{dt} = K[Fe^{2+}]P_{O_2} + K_1[Fe^{2+}][Cu^{2+}] \quad (48)$$

In contrast, McKay and Halpern,[162] working at 100 °C with 0.08 M H_2SO_4, reported that the catalytic contribution is of the form

$$-\frac{d[Fe^{2+}]}{dt} = K[Fe^{2+}][Cu^{2+}]^{1/2}P_{O_2} \quad (49)$$

Mathews and Robins[226] reported a fractional order of $[Cu]^{0.28}$ with respect to copper at 50 °C. A definitive investigation has yet to be made.

The rate of oxidation of ferrous chloride in hydrochloric acid by oxygen at 40 °C and catalyzed by Cu^{2+} is complex. The order of reaction varies with time. The initial rate is proportional to the square root of the copper concentration and linearly proportional to the H^+ ion activity.[326] Colborn and Nicol[259] noted the catalytic effect of Cu^{2+} in acidic ferrous chloride solutions.

George[233] reported that in perchlorate media cupric copper is a poor catalyst, yielding only a 2.5-fold increase in reaction rates for the oxidation of ferrous iron in perchloric acid between pH 0 and 2 with up to 0.2 M Cu^{2+}. In contrast, there is a complex catalytic effect by cupric copper on the oxidation of ferrous iron by molecular oxygen at room temperature in phosphoric acid.[250] This system has a saturation effect with significant catalysis at $\sim 10^{-5}$ M Cu^{2+} and minimal increase above 10^{-3} M Cu^{2+}. The reaction rate, which is first order for ferrous iron, oxygen, and phosphate concentration in the absence of copper, changes to a complex order approximately proportional to $(Fe^{2+})^2/(Fe^3)$. The final equation is

$$-\frac{d[Fe^{2+}]}{dt} = \frac{K_1[Fe^{2+}]P_{O_2}\left[1 + K_1\frac{P_{O_2}}{[Fe^{3+}]}\right] + K_3\frac{[Fe^{2+}][Cu^{2+}]P_{O_2}}{[Fe^{3+}]}}{1 + K_2\frac{P_{O_2}}{[Fe^{3+}]} + K_4\frac{[Cu^{2+}]}{[Fe^{2+}]}} \quad (50)$$

Copper as Cu^{2+} also catalyzes the oxidation of near neutral and neutral ferrous salts.[298,327-329]

Possible Catalysts. In addition to their work with copper, Lamb and Elder[223] examined the catalytic effect of Na_2SO_4, K_2SO_4, $MgSO_4$, $ZnSO_4$, $MnSO_4$, $Cr_2(SO_4)_3$, NaOAc, Na_3PO_4, $NiSO_4$, Ag_2SO_4, and Hg_2SO_4 on the oxidation of ferrous iron in acid solution, and found it to be minimal to nil. Mathews and Robins[226] repeated the work at 50 °C, extended the list to include $CoSO_4$, $(NH_4)_6Mo_7O_{24}$, As_2O_3, and glass wool, and reported no catalytic effect. Singer and Stumm[163,330] observed a significant catalytic effect with alumina, silica, and bentonite and no effect with kaolinite, precipitated ferric hydroxide, or pyrite for oxidation in near neutral and neutral waters. Pound[227] noted that although the ferrous salts of the weak acids acetate, borate, or succinate are oxidized more rapidly than the corresponding salts of sulfuric, hydrochloric, or phosphoric acid, addition of a weak acid to the ferrous salts of a strong acid has no effect on the oxidation; conversely, when a strong acid is added to the ferrous salts of the weak acid there is a decreased oxidation rate.

Although oxalic and citric acids behave in a similar manner to the weak acids listed above, the formation of insoluble ferrous oxalate and the influence of light introduces complications with these two acids. The effect of light on the oxidation of neutral solutions of ferrous citrate was reported by Starkenstein and Steiger,[305] who also noted the rapid oxidation of ferrous lactate and ferrous gluconate. Yamamoto[331] noted the catalytic effect of citrate and tartrate. Gilroy and Mayne[332] reported that the rate increased for the following order of anions $SO_4^{2-} < Cl <$ formate < benzoate ≡ acetate over the pH range 6–8.

The aerial oxidation of ferrous chloride solutions may be catalyzed by acetic acid and the acetate salts of sodium, calcium, manganese, and vanadium, and by va-

TABLE X

1st order	2nd order
$H_2P_2O_7$ at 1 M and 25 °C	HCl at <1 M and 25 °C
$H_2P_2O_4$ at 1 M and 25 °C	H_2SO_4 at 1 M and 25 °C
HCl at 5 M and 25 °C	HNO_3 at 1 M and 25 °C
H_2SO_4 at 1 M and 150 °C	$HClO_4$ at 1 M and 25 °C

nadium lactate.[333] Solid manganese dioxide has been employed as a catalyst for the air and molecular oxygen oxidation of both acid and neutral solution of ferrous sulfate,[275,334-336] and the use of Mn^{2+} has been briefly considered.[223,275] Singer and Stumm[163,330] observed no catalytic effect with Mn^{2+}.

Stumm and Lee[275] mentioned a catalytic effect by Co^{2+} and zeolite on the oxidation by molecular oxygen of ferrous sulfate at pH 6.92 and ambient temperatures. The oxidation of ferrous iron by molecular oxygen at room temperature in sulfate solutions at the intermediate pH 2.3 is catalyzed by the chelating agents ethylenediaminetetraacetic acid (EDTA), nitrilotriacetic acid (NTA), diethylenetriaminepentaacetic acid (DTPA), 1,2-cyclohexanediaminetetraacetic acid (CyDTA), *N*-hydroxyethylenediamine-*N*,*N*′,*N*′-triacetic acid (EDTAOH), and ethylenediaminetetrapropionic acid (EDTP); the following rate equation is obtained:[337]

$$-\frac{d[Fe^{2+}]}{dt} = K_1[Fe^{2+}HZ]P_{O_2} + K_2[Fe^{2+}Z]P_{O_2} \quad (51)$$

where $Fe^{2+}HZ$ is the protonated chelate and $Fe^{2+}Z$ is the normal chelate.

Kauffmann[338] reported that the oxidation of ferrous iron by molecular oxygen in water is retarded by minute quantities of hydrogen sulfide, thiosulfate, colloidal sulfur, ferrocyanide, ferricyanide, cystine, and glutathione. The reagents sulfanilamide, sulfathiazole, and sulfate had no effect, but sulfite at 30 mg L^{-1} accelerates the reaction.

Nitric oxide has been reported as a catalyst for the oxidation of ferrous chloride solutions by molecular oxygen.[339] α- and β-amino acids have been reported to have a catalytic effect on the oxidation of ferrous ion by molecular oxygen,[340,341] although cystine has an inhibiting effect.

3. Reaction Mechanism

The following observations should be taken into account when drawing up a reaction mechanism for the oxidation of ferrous ion in solution:

(i) Under all conditions the reaction rate is first order with respect to the partial pressure of oxygen.

(ii) At concentrations of about 1 M Fe^{2+}, the reaction rate order with respect to ferrous iron varies with the media anion according to Table X.

(iii) In sulfuric acid, at concentrations less than 0.5 M Fe^{2+}, the order with respect to ferrous ion is fractional and, below 0.09 M Fe^{2+}, oxidation ceases.

(iv) Above pH 2 in any medium, the reaction rate has a functional relationship with pH and, above pH 5, is second order with respect to hydroxide.

(v) The reaction is catalyzed by Cu^{2+}.

(vi) In acid solutions below pH 2 and for a given pH, the rate decreases in the order $H_2P_2O_7^{2-} > H_2PO_4^- > Cu^{2+} > SO_4^{2-} > NO_3^- > ClO_4^-$.

Reaction mechanisms for the oxidation of ferrous ion were first suggested for the autoxidation of neutral solutions of ferrous bicarbonate. This reaction was observed to be first order with respect to ferrous ion and oxygen, and the effect of pH was not investigated. Drawing on other work, Just[269] proposed the reaction sequence:

$$Fe(HCO_3)_2 = Fe(OH)_2 + 2CO_2 \quad (52)$$

$$Fe(OH)_2 + O_2 + H_2O = HO_2 + Fe(OH)_3 \quad (53)$$

the HO_2 radical being derived from the O_2^- ion formed by the oxidation of the O_2 molecule by the ferrous ion. This approach was subsequently developed in more detail by Weiss[342] for the oxidation of ferrous ion in acid media:

$$Fe^{2+} + O_2 \rightarrow Fe^{3+} + O_2^- \quad (54)$$

$$H^+ + O_2^- = HO_2 \quad (55)$$

$$Fe^{2+} + HO_2 \rightarrow Fe^{3+} + O_2H^- \quad (56)$$

$$H^+ + O_2H^- = H_2O_2 \quad (57)$$

$$Fe^{2+} + H_2O_2 \rightarrow Fe^{3+} + OH^- + OH \quad (58)$$

$$Fe^{2+} + OH \rightarrow Fe^{3+} + OH^- \quad (59)$$

This may be simplified to

$$Fe^{2+} + O_2 + H^+ \rightarrow Fe^{3+} + HO_2 \quad (60)$$

$$Fe^{2+} + HO_2 + H^+ \rightarrow Fe^{3+} + H_2O_2 \quad (61)$$

$$2Fe^{2+} + H_2O_2 + 2H^+ \rightarrow Fe^{3+} + 2H_2O \quad (62)$$

and the reaction may be catalyzed by copper through the reaction sequence:

$$Fe^{2+} + Cu^{2+} = Fe^{3+} + Cu^+ \quad (63)$$

$$Cu^+ + O_2 + H^+ = Cu^{2+} + HO_2 \quad (64)$$

again represented as simplified equations.[250] Reaction 60 was considered to be the slow step, so the overall reaction is bimolecular and first order with respect to ferrous ion and oxygen. Although this is in accord with Just's results,[269] it fails to explain the termolecular reactions observed in dilute hydrochloric acid, sulfuric acid at room temperature, nitric acid, and perchloric acid. In addition, George[233] considered that the proposed reaction sequence for the catalytic action by copper (eq 63 and 64) would be dominated by the reverse reactions, resulting in a decrease in oxidation rate.

Subsequently, Weiss[343] modified his proposed reaction sequence to include a ferrous ion–oxygen complex, stabilized by the media anion, e.g., $H_2PO_4^-$, Cl^-, SO_4^{2-}, etc., and the oxidation proceeding through a transition state:

$$[X\text{---}Fe^{2+}\text{---}O_2] = [X\text{---}Fe^{3+}\text{---}O_2^-] \quad (65)$$

Huffman and Davidson[231] extended this approach by arguing that the change from a termolecular to a bimolecular reaction was directly related to the complexing strength of the anion with the ferric ion; see Table XI. However, there is no correlation between the reaction rate and the ligand stability when the product ferric ion is strongly chelated to ligands such as EDTA, CyDTA, etc.[337]

George[233] also developed a reaction sequence based on the formation of a ferrous ion–oxygen complex. He

TABLE XI

bimolecular strong complexing anion	termolecular moderate or weak complexing anion
$H_2P_2O_7^{2-}$, 1 M at 25 °C	HCl, <1 M at 25 °C
$H_2PO_4^-$, 1 M at 25 °C	H_2SO_4, 1 M at 25 °C
HCl, >1 M at 25 °C	HNO_3, 1 M at 25 °C
H_2SO_4, 1 M at 150 °C	$HClO_4$, 1 M at 25 °C

considered that the product $[Fe^{3+}O_2^-]$ is thermodynamically a less favored structure than $Fe^{2+}O_2$; consequently he proposed the following reaction sequence:

$$Fe^{2+} + O_2 = Fe^{2+}O_2 \quad (66)$$

$$Fe^{2+}O_2 + H_2O + Fe^{2+} = FeO_2H^{2+} + HOFe^{2+} \quad (67)$$

$$FeO_2H^{2+} + HOFe^{2+} = 2Fe^{3+} + H_2O_2 \quad (68)$$

$$2Fe^{2+} + H_2O_2 + 2H^+ = 2Fe^{3+} + 2H_2O \quad (69)$$

where eq 68 is the rate-determining step. The existence of the ion-pair complexes FeO_2H^{2+} and $HOFe^{2+}$ had previously been established by Evans, George, and Uri.[344]

The Weiss model and its modifications by Weiss and other workers fails to account for the second-order dependence of the rate on hydroxyl concentrations in neutral solutions. Consequently, Abel[272] proposed an entirely new mechanism based on the suggestion that the oxygen molecule may undergo a two-stage hydrolysis reaction to form O_3^{2-}, termed "peroxide-like-oxygen", according to the following sequence:

$$O_2 + OH^- = O_2OH^- \quad (70)$$

$$O_2OH^- + OH^- = O_3^{2-} + H_2O \quad (71)$$

The ferrous ion is then oxidized by the O_3^{2-} ion according to

$$Fe^{2+} + O_3^{2-} \rightarrow Fe^{3+} + 3O^- \quad (72)$$

$$3O^- + 3H^- \rightarrow 3OH \quad (73)$$

$$3Fe^{2+} + 3OH \rightarrow 3Fe^{3+} + 3OH^- \quad (74)$$

with reaction 75 as the rate-determining step. This approach was subsequently generalized with the proposal that the oxygen molecule could form an anionic complex of the general form

$$O_2 + A^- \rightarrow {}^-O{\cdot}OA \quad (75)$$

with a subsequent oxidation sequence

$$^-O{\cdot}OA + X \rightarrow 2O^- + X^+ + A \quad (76)$$

$$A + X \rightarrow X^+ + A^- \quad (77)$$

when suitable anions would include OH^-, CN^-, HSO_3^-, HSO_4^-, $HS_2O_3^-$, $H_2PO_4^-$, and $C_2O_4^{2-}$.[345,346] This approach has been criticized on the grounds that the O_3^{2-} concentration must be very small yet the O_3^{2-} concentration required in the rate-determining step must be large and approximately equal to the normal solubility of molecular oxygen.[280,347,348]

Hydrolysis reactions are attractive because they introduce a pH dependence for the reaction. Consequently, Goto, Tamura, and Nagayama[280,348] modified Abel's approach by considering the reactant species to be hydrolyzed ferrous ion, $FeOH^+$, and first-stage hydrolyzed oxygen, O_2HO^-. These species then followed a modified Weiss sequence:

$$FeOH^+ + O_2HO^- \rightarrow Fe(OH)_2^+ + O_2^- \quad (78)$$

$$O_2^- + H^+ = HO_2 \quad (79)$$

$$Fe^{2+} + HO_2 \rightarrow Fe^{3+} + HO_2^- \quad (80)$$

$$HO_2^- + H^+ = H_2O_2 \quad (81)$$

$$Fe^{2+} + H_2O_2 \rightarrow Fe^{3+} + OH^- + OH \quad (82)$$

$$Fe^{2+} + OH \rightarrow Fe^{3+} + OH^- \quad (83)$$

where eq 78 is the rate-determining step. When observed rates and the measured stability constant for $FeOH^+$ are used, the value for the stability constant of O_2OH^- is in the range $10^{-2.5} < K_{O_2OH^-} < 10^{-0.3}$. This produces a rate constant for eq 78 in the range $4.6 \times 10^9 < K < 1.4 \times 10^{11}$ M^{-1} s^{-1} and an activation energy of 7 kJ mol^{-1}. Such a large value for K and small activation energy indicate that the rate-determining step is controlled by the diffusion of $FeOH^+$ and O_2OH^-.

The actual reaction path has only recently been discussed. Goto, Tamura, and Nagayama[280] proposed an S_N2 process in which the hydrolyzed oxygen makes a nucleophilic attack on the hydrated–hydrolyzed ferrous ion with its OH^- group:

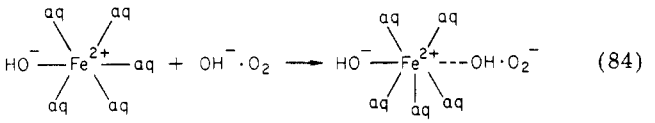

(84)

The transition complex ejects a water molecule and subsequently the O_2^- ion before the ferrous ion oxidizes up to the 3+ state:

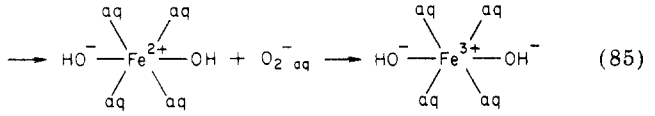

(85)

An alternative was advanced by Astanina and Rudenko[245] for oxidation in moderate acid solutions, where the ferrous ion is present as the hexaaquo complex. These authors argued for the initial formation of mixed aquo complexes involving water from the solvent sheaths as dinuclear complexes of iron linked either through single water bridges or diwater bridges:

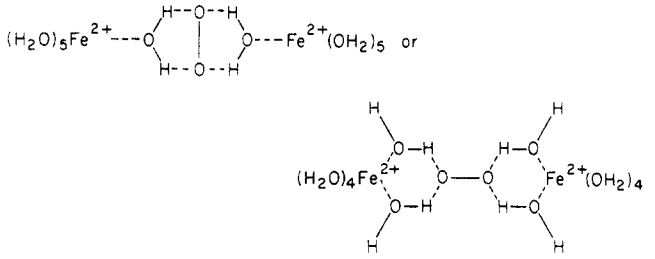

Oxidation of the ferrous iron then occurs via intramolecular electron transfer:

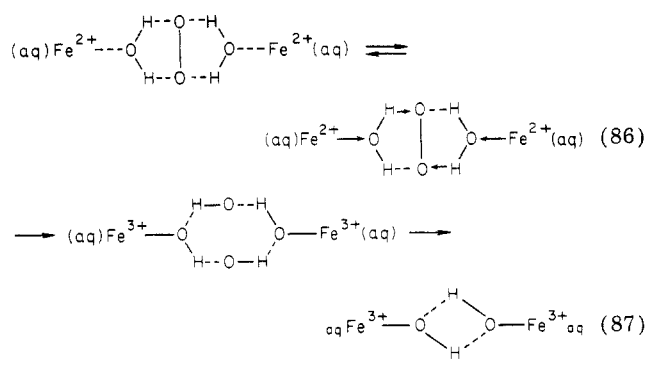

(86)
(87)

to yield hydrolyzed ferric ion and hydrogen peroxide. Similar mechanisms were derived for the diwater bridge complexes and hydroxo aquo complexes of ferrous ion. Macejevskis and Liepina[349] considered the aquo complexes to be generally less reactive than hydroxy and acidσ complexes.

D. Oxidation of Pyrite by Ferric Ion

In 1960, Woodcock[199] was only able to give three references on the use of ferric ion as a leaching agent for sulfides in a review of the oxidation of sulfide minerals in aqueous suspension. Since then, the use of ferric ion as a leaching agent has gained increasing popularity, and Dutrizac and MacDonald[350] listed 209 references in their review of this subject. Most of this work was associated with the economic minerals, and only a small number of studies have been carried out on pyrite, although there are several references to bacterial catalysis. More recently the commercial use of ferric ion has been considered for the desulfurization of coal. In many high sulfur coals, sulfur is present predominantly as pyrite, and an ideal cleaning process would be to remove this sulfur as soluble sulfate without oxidizing the coal.

Ideality has to be sacrificed for operation at the optimum economic conditions. Thus the Kennecott copper process[351] operates with an acid ferric sulfate leach at 130 °C and applied oxygen pressure to obtain a fast conversion to 100% sulfate. In contrast, the Meyers process[352] operates with an acid ferric sulfate leach at 90 °C. Although this eliminates the necessity for an autoclave, up to 40% of the pyritic sulfur may be converted to elemental sulfur, and the product requires further refining. A low-temperature (25 °C) leach with ferric chloride at pH 1 and ~1 M Fe^{3+} has been recommended.[119] It is claimed that the relatively slow reaction rate is more than compensated by the saving in fuel. Bryner, Walker, and Palmer[216] demonstrated that ferric ion will oxidize about one-third more pyrite in a nitrogen atmosphere than in air. King and Lewis[353] recently reported a synergistic effect when leaching with oxygen and ferric ion.

The kinetics of the reaction have not been fully derived. Thomas and Whalley[354] studied the leaching of pyrite at 90 °C with ferric sulfate solutions. The reaction rate was reported to be faster than either the air oxidation of pyrite to ferric sulfate in air or the oxidation of ferrous ion to ferric ion under the same conditions; the following stoichiometry was proposed:

$$FeS_2 + 7Fe_2(SO_4)_3 + 8H_2O \rightarrow 15FeSO_4 + 8H_2SO_4 \quad (88)$$

In contrast, McKay and Halpern[162] made a brief study of the oxidation of pyrite at 110 °C by ferric ion in 0.075 M sulfuric acid and, from the relative amounts of pyrite oxidized, concluded that ferric ion was a poor oxidizer compared to molecular oxygen. However, the experiments were not identical with those of Thomas and Whalley. Although the operating pH and temperature were the same, the oxidant concentrations were not. For oxidation by oxygen, "the partial pressure of oxygen was held constant throughout each experiment by means of a standard diaphragm regulating valve"; i.e., the oxidant concentration was kept constant at the initial value throughout the experiment. For oxidation by ferric ion, the ferric ion concentration was monitored but not adjusted to the initial value as it became depleted. These are two entirely different experiments; hence the relative rates may only be compared by deriving the rate equations.

Garrels and Thompson[355] studied the reaction rate by monitoring the redox potential and assuming that it is controlled by the Fe^{2+}/Fe^{3+} redox couple. A stoichiometry of

$$FeS_2 + 8H_2O + 14Fe^{3+} \rightarrow 15Fe^{2+} + 2SO_4^{2-} + 16H^+ \quad (89)$$

was postulated. Working with a ferric sulfate concentration in the range 10^{-3}–10^{-5} M Fe^{3+} at pH 0–2 and at 33 °C, these workers found that the rate is independent of pH and varies significantly for specimens from different sources and that the influence of V, Co, Ni, Mn, Co, and Ce at 10^{-4} M sulfate is minimal to nil. The rate-controlling mechanism is related to adsorption of ferric and ferrous iron on the pyrite surface. It was assumed that the adsorption process is more rapid than the oxidation step. It was proposed that the rate of reaction is proportional to the fraction of pyrite surface occupied by ferric ions; this led to a working equation

$$\frac{d[Fe^{3+}]}{dt} = K\frac{[Fe^{3+}]}{\sum[Fe]} \quad (90)$$

The experiments were conducted with a gross excess of ferric ion over the E_h range 700–600 mV. If the system was allowed to equilibrate between the pyrite and the ferrous–ferric solution, the E_h would drop to an unsteady value in the vicinity of 0.250–300 mV. The instability was partly due to the imposition of other redox couples arising from minor impurities and partly to the side reaction

$$FeS_2 \rightarrow Fe^{2+} + 2S^0 + 2e \quad (91)$$

$$E_h = 0.421 + 0.0296 \log [Fe^{2+}] \quad (92)$$

Mathews and Robins[356] studied the reaction by sampling and analyzing for ferric ion and total iron during each experimental run. The reaction was studied over a pH range 1.5–0, with initial Fe^{3+} concentrations of ~0.01 M, and over a temperature range 30–70 °C. In addition, the effects of slurry density D, surface area S, carrier anion, and Cu^{2+} were studied. The overall stoichiometry of eq 92 was confirmed and the final rate equation expressed as

$$-\frac{d[Fe^{3+}]}{dt} = K\frac{DS[Fe^{3+}]}{\sum[Fe][H]^{0.44}} \quad (93)$$

where $K = 2.29 \times 10^{-9}$ $M^{0.56}$ s^{-1} and the activation energy is 85 kJ M^{-1}. It was concluded that there is a common rate expression for sulfate or chloride media, and the addition of 0.025 M Cu^{2+} only increases the rate marginally. No evidence was reported for a sulfur side reaction. This contrasted with the results of Tseft and Tatarinova,[357] who investigated the pressure leaching of pyrite and chalcopyrite at 220–240 °C with a number of oxidants, including ferric chloride and ferric sulfate. Ferric chloride is a more effective leaching agent under these conditions. In addition, pyrite is not readily soluble; it was suggested that this was perhaps due to the presence of a passivating elemental sulfur film.[358]

Smith and Shumate[16] noted a difference in reaction rates when leaching pyrite at ambient temperature with ferric chloride or ferric sulfate. They concluded that the role of the anion produces a pseudorelationship between the rate and pH and that the real controlling factor is the relative complexing strength of the sulfate and chloride anions for the ferric ion. These authors found that the experimental data could be fitted to the following theoretical rate equation:

$$\frac{d[FeS_2]}{dt} = \frac{K_1 - K_2([Fe^{2+}]/Fe^{3+})^{1/2}}{[Fe^{3+}]^{-1/2} + K_3 + K_4([Fe^{2+}]/[Fe^{3+}])^{1/2}} \quad (94)$$

Lowson[359] reported on the oxidation of pyrite by ferric ion under acid conditions and with a nitrogen atmosphere. The cell potential and hence the redox potential vary linearly with time, and the following rate equation can be derived directly from the Nernst equation and the experimental observations without having to assume a particular mechanism:

$$-\frac{d[Fe^{3+}]}{dt} = K\frac{[Fe^{3+}][Fe^{2+}]}{\sum Fe} \quad (95)$$

The kinetics were observed to be a function of pH and surface area.

The unusual form of the rate equations is due to the two-phase heterogeneous reaction at a solid surface.[355] Smith and co-workers[16,360] considered a "dual-site" adsorption model in which ferric and ferrous ions are in competition as adsorbers. The adsorbed ferric ion is reduced to ferrous ion by electron transfer from one of the reactive sites of the dual site. The resulting ferrous ion is then on a single site and accordingly desorbs. While this mechanism is possible, no consideration has been given to the corresponding anodic dissolution of the sulfur. There have been no electrochemical studies of the system apart from some initial work reported by Smith and Shumate.[16] It is concluded that the kinetics and mechanism for the oxidation of pyrite by ferric ion are poorly described and warrant further work.

V. Electrochemical Dissolution of Pyrite

A. Nonoxidative Dissolution

The dissolution of a solid may occur through an oxidative or nonoxidative process. Oxidative dissolution may be defined as when one or more of the solute species exists in a different oxidation state in the solid and solution phase. Nonoxidative dissolution occurs when the formal oxidation state of the solute species is identical in both the solution and solid phases.[361] Although the literature favors an oxidative dissolution for pyrite, the nonoxidative process readily occurs for ferrous sulfide. Historically, this was the basis for the production of hydrogen sulfide

$$FeS + H_2SO_4 \rightarrow FeSO_4 + H_2S \quad (96)$$

employing the legendary Kipp apparatus. The nonoxidative dissolution process for sulfides has been reviewed[362,363] and proposed as a means of leaching metals from sulfide ores.[364] It has been suggested that the rate of oxidative dissolution of zinc sulfide ore may, in certain circumstances, be limited by nonoxidative dissolution reactions.[350,365] The kinetics and mechanism of the nonoxidative dissolution of the iron sulfides have been studied recently by a number of workers,[361,363,366-369] but nothing has been published on the nonoxidative dissolution of pyrite. The process would require the formation of the persulfide ion S_2^- and the hydride, hydrogen persulfide, H_2S_2. Although it is possible to make hydrogen persulfide, and higher members of the polysulfide series, hydrogen polysulfides have a great tendency to decompose with the release of sulfur. The reaction is accelerated by hydroxide.[370] The dissolution of pyrite is therefore considered to be wholly oxidative.

B. Oxidative Dissolution

Oxidative and electrochemical dissolution are synonymous. Recognition of the electrochemical nature of pyrite is traceable to the work of Fox,[371] who showed that minerals, and particularly pyrite, can exhibit a potential difference of up to 1 V with the surrounding country rock; this is known as a self-potential. This phenomenon has been used extensively by geophysicists as a prospecting technique and was reviewed by Sato and Mooney.[372] Gottschalk and Bühler[373] proposed an electrochemical mechanism for the oxidation and secondary enrichment of sulfide ore deposits, and Rosetti and Cesini[374] discussed the electrochemical effects between metal sulfides and mine drainage waters. An electrochemical mechanism for the hydrometallurgical leaching of pyrite was proposed by Woodcock[199] and others,[375,377] and electrochemical leaching under potentiostatic control has been suggested as a possible hydrometallurgical route by Ammou-Chokroum.[376]

The overall process is a summation of cathodic and anodic reactions that are occurring at the pyrite surface. The principal cathodic reaction is a four-electron oxygen reduction process:[378]

$$O_2 + 4H^+ + 4e^- \rightarrow 2H_2O \quad (97)$$

$$E_{O_2} = 1.23 - 0.0592pH + 0.0148 \log P_{O_2} \quad (98)$$

The anodic process is a more complex collection of oxidation reactions, the dominant one being

$$FeS_2 + 8H_2O \rightarrow Fe^{3+} + 2SO_4^{2-} + 16H^+ + 15e \quad (99)$$

$$E_{FeS_2} = 0.389 - 0.963pH + 0.0039 \log [Fe^{3+}] + 0.0079 \log [SO_4^{2-}] \quad (100)$$

The actual potential exhibited by pyrite in solution, referred to as the open circuit or rest potential E_r, is a summation of the reversible potentials of the individual reactions taking into account the sign and kinetics of these reactions.[379] This summation may be illustrated by an Evans diagram,[380] which, although developed for corrosion, has a wider applicability. Depending on the dominant reaction, the total system may be under anodic, cathodic, mixed, or resistance control. The open circuit potential of pyrite is approximately midway between the reversible potentials of the dominant cathodic and anodic reactions, and reasonable Tafel slopes may be obtained from polarization curves on either side of the open circuit potential. The narrow band gap of pyrite and high surface concentration of electrons and positive holes are conducive to efficient anodic and cathodic reactions;[381] consequently, pyrite is under mixed potential control.

TABLE XII. Open Circuit Reduction Potentials for Pyrite

E_h, V	gas	pH	media	temp, °C	ref
0.64	Air	~0	1 M $HClO_4$	Ambient	383
0.63	Air	1	HCl	25	382[a]
0.50	Air	1	H_2SO_4	18	464
0.60	N_2	~0	1.5 M H_2SO_4	25	410
0.75	O_2 20 atm	~0	1 N H_2SO_4	175	183
0.65	N_2	~1	1 M H_2SO_4	25	178
0.62	Air	~0	1 M $HClO_4$	25	12
0.699	O_2 12 atm	~0	1 M $HClO_4$	110	12
0.674	O_2 2.7 atm	~0	1 M $HClO_4$	110	12
0.36	O_2	7	0.1 M KNO_3	25	384
0.35	Air	7	0.1 M KNO_3	25	384
0.25	N_2	7	0.1 M KNO_3	25	384

[a] Part II.

C. Open-Circuit Potential

The potential of the principal cathodic reaction is a function of pH and oxygen pressure, whereas the potential of the principal anodic reaction is a function of pH, ferric ion, and sulfate. These functional relationships are reflected in the value for the observed open-circuit potential listed in Table XII. The open-circuit potential has a linear variation with pH over the pH range 2–12 in perchlorate[382,383] and nitrate media[384,385] but becomes independent of pH below 2.[382] The slope is approximately 0.055 V/pH, which is similar to the Nernstian slope for the variation of the potentials of the individual anodic or cathodic reactions with pH. A similar linear relationship between E_h and pH was observed with powdered electrodes.[386,387] Changing from air to oxygen saturation increases the open-circuit potential but nitrogen saturation decreases the open-circuit potential as is indicated by eq 98.[382,384]

The following relationships were obtained for the open-circuit potential of pyrite in 1 N H_2SO_4 at 25 °C with Fe^{2+}, Fe^{3+}, and the redox couple Fe^{3+}/Fe^{2+}:[388]

Fe^{2+} $$E_h = 0.58 \text{ V} \quad (101)$$

Fe^{3+} $$E_h = 0.929 + 0.058 \log [Fe^{3+}] \quad (102)$$

Fe^{3+}/Fe^{2+} $$E_h = 0.673 + 0.055 \log [Fe^{3+}/Fe^{2+}] \quad (103)$$

Eq 101 and 102 are the extreme cases of the general relationship (eq 103). The Nernstian slope indicates that the Fe^{3+}/Fe^{2+} redox couple can be a significant contributor to the open-circuit potential under heap leach conditions.[389] The open-circuit potential is independent of the semiconducting characteristics of the material.[383,390] Open-circuit potentials have also been reported by Rechenberg[391] and Yashina et al.[392]

The Wagner–Traud mixed potential mechanism was derived for an ideal homogeneous surface that allows the anodic and cathodic reactions to occur simultaneously over the entire surface. A real surface departs from this ideal and, in the extreme case, will consist of a heterogeneous composite of local anodic and cathodic cells. Such a mechanism appears to be appropriate for some sulfide–xanthate–oxygen systems.[385] However, in either extreme case, the open-circuit potential is still a mixed potential whose value is determined by the individual reversible potentials and kinetics of the contributing half-cell reactions, so the net current density is zero.

In an ore body or waste heap pyrite is invariably in contact with a range of mineral sulfides. Sato[382] laid down the ground rules for determining open-circuit and self potentials of minerals for these field situations. Provided that the conditions are carefully defined, it is possible to arrange the minerals according to their measured potentials in a series analogous to the electrochemical series of metals. Sato and Mooney[372] prepared a short list of maximum potential differences that can occur between a mineral and the ore body at depth which is acting as an inert electrode:

graphite	C	0.78 V
pyrite	FeS_2	0.73 V
covellite	CuS	0.75 V
chalcocite	Cu_2S	0.50 V
galena	PbS	0.33 V

This list should only be used in conjunction with Sato and Mooney's careful discussion of the role of pH and the oxidizing–reducing environment. It indicates the type of galvanic couples that may occur naturally. Similar lists have been produced by other workers,[393] and the approach has been applied to possible pyrite flotation systems,[394] pyrite–copper sulfide galvanic couples,[395] and geophysical prospecting.[396] The operation of the chalcocite–pyrite couple with pyrite as the anode has been studied by Makarov et al.[397] In dilute sulfuric acid solutions, the couple operates under anodic control over the temperature range 25–40 °C. In solutions having concentrations greater than 0.1 N, control changes to cathodic control above 40 °C. The galvanic couple zinc–pyrite in dilute sulfuric acid was studied by Masuko and Hisamatsu;[375] in this case, pyrite was the cathode and the reductive dissolution generated H_2S.

D. Cathodic Reduction Reactions

The cathodic current obtained by cathodic polarization away from the open-circuit potential is a summation of a number of possible cathodic reductions. Sometimes the net cathodic current may be dominated by a particular reaction, but this dominance depends on the environment and degree of polarization. The following reductions may contribute to the net cathodic current:

(a) Hydrogen Ion Reduction.

$$2H^+ + 2e^- \rightarrow H_2\uparrow \quad (104)$$

$$E_h = 0.0 - 0.0592\text{pH} - 0.0296 \log P_{H_2} \text{ V} \quad (105)$$

At high cathodic polarization, this reaction may be replaced by the water decomposition reaction:

$$2H_2O + 2e^- \rightarrow H_2 + 2OH^- \quad (106)$$

but algebraic manipulation will show that thermodynamically these two reactions are equivalent.

(b) Molecular Oxygen Reduction. Provided that the solution is saturated with oxygen,

$$O_2 + 4H^+ + 4e^- = 2H_2O \quad (107)$$

$$E_h = + 1.229 - 0.0592\text{pH} - 0.0148 \log P_{O_2} \quad (108)$$

The above reaction is usually considered to apply to acid media, with

$$O_2 + 2H_2O + 4e^- = 4OH^- \quad (109)$$

applying to alkaline media.[398] Once again, simple algebraic manipulation will show that thermodynamically these two reactions are equivalent.

(c) Peroxide Formation.

$$O_2 + 2H^+ + 2e^- = H_2O_2 \quad (110)$$

$$E_h = +0.695 - 0.0592pH + 0.0296 \log \frac{P_{O_2}}{[H_2O_2]} \text{ V} \quad (111)$$

The above reaction applies to acid media. The equivalent reaction in alkaline solution has a different voltage relationship owing to the formation of the hydrogen peroxide ion:

$$O_2 + H_2O + 2e^- = OH^- + HO_2^- \quad (112)$$

$$E_h = +0.349 - 0.0296pH + 0.0296 \log \frac{P_{O_2}}{[HO_2^-]} \text{ V} \quad (113)$$

(d) Peroxide Reduction.

$$H_2O_2 + 2H^+ + 2e^- = 2H_2O \quad (114)$$

$$E_h = +1.763 - 0.0592pH + 0.0296 \log [H_2O_2] \text{ V} \quad (115)$$

Again, the above reaction applies to acid media in which H_2O_2 is the dominant species. Formation of HO_2^- under alkaline conditions yields the following equations:

$$HO_2^- + H_2O + 2e^- = 3OH^- \quad (116)$$

$$E_h = +2.109 - 0.0887pH + 0.0296 \log [HO_2^-] \text{ V} \quad (117)$$

The E_h–pH relationships were calculated from data assembled by Lowson[399] for the potential–pH temperature diagrams for water. These diagrams define the stability regions for the various ions. The values are essentially equivalent to those quoted by Damjanovic[398] with slight variations in the last significant figures owing to the use of the more recent thermodynamic compilations.[400] There is a common pH dependence for oxygen reduction, peroxide formation, and peroxide reduction reactions in acid media.[398] When alkali media are used, this common factor is lost and, above pH 11.7, the HO_2^- ion becomes the dominating peroxide species.[399]

The remaining reduction reaction is that of pyrite itself. Thermodynamically the most favorable reaction would be

$$FeS_2 + 4H^+ + 2e^- \rightarrow Fe^{2+} + 2H_2S \quad (118)$$

$$E_h = +0.057 - 0.0592 \log [H_2S] - 0.0296 \log [Fe^{2+}] - 0.118pH \text{ V} \quad (119)$$

Examination of the potential–pH diagram for the iron–sulfur–water system indicates that oxidation of pyrite with hydrogen reduction as the cathodic reaction is thermodynamically unfavorable. Similarly, inspection of the potential–pH diagram for the water system indicates that peroxide, either as H_2O_2 or HO_2^-, is thermodynamically unstable within the stability regime for water. Assuming that pyrite does not undergo a disproportion reaction by acting as cathode and anode, the selection of cathodic reduction reactions at the open-circuit potential is reduced to one, namely the oxygen reduction reaction.

Drawing on the extensive field work on fuel cells, Tributsch and Gerischer[381] separated the overall four-electron oxygen reduction into a series of one-electron steps. The primary step was the transfer of mobile electrons from the semiconductor to the O_2 molecule and subsequent stabilization of the product ion O_2^- by water:

$$O_2 + e^- = O_{2\,aq}^- \quad (120)$$

Depending on the pH of the solution, the O_2^- radical ion may form the O_2H radical

$$O_{2\,aq}^- + H^+ = O_2H_{aq} \quad (121)$$

Both radicals have a high electron affinity and can absorb another electron from the solid:

$$O_{2\,aq}^- + H_2O + e^- = O_2H_{aq}^- + OH_{aq}^- \quad (122)$$

or

$$O_2H + e^- = O_2H_{aq}^- \quad (123)$$

The O_2H^- ion is the first hydrolysis product of H_2O_2 and so equilibrates to the stable intermediate H_2O_2:

$$O_2H_{aq}^- + H_{aq}^+ = H_2O_{2aq} \quad (124)$$

Pyrite is a catalyst for the reduction of hydrogen peroxide;[401] accordingly, further reduction occurs through the steps

$$H_2O_{2aq} + e^- = OH^- + OH_{aq} \quad (125)$$

$$OH_{aq} + e^- = OH_{aq}^- \quad (126)$$

to form the final product water by

$$OH_{aq}^- + H_{aq}^+ = H_2O \quad (127)$$

Cyclic voltammetry with a rotating-disc electrode has indicated that at any pH and at low cathodic overpotential the cathodic current is independent of rotation speed and, therefore, the polarization is in an activation controlled region.[378] The corresponding Tafel slope for this region is ~−130 mV per decade with an exchange current to 1.0×10^{-11} A cm^{-2} in 1 M H_2SO_4, 9.0×10^{-12} A cm^{-2} in 1 M $HClO_4$, and 4×10^{-12} A cm^{-12} in 1 M HCl.

The Tafel slope drops from ~−130 mV per decade at ~pH 0 to ~−67 mV per decade at ~pH 12. On increasing the overpotential, the current rises to a limiting value that is both a function of the square root of the speed of rotation and oxygen concentration. This indicates that the reaction is now under pure mass-transfer control. Analysis has revealed that the overall reaction is first order with respect to oxygen and is a four-electron process.[184,378,383] The onset of mass-transfer control is independent of pH up to pH 7 but then becomes more positive with increasing pH. This indicates that for acid media, eq 120 is the rate-determining step; raising the pH into the alkaline region transfers the rate-determining step from eq 120 to the formation of hydrogen peroxide via eq 122–124.

Under certain cyclic voltammetry conditions, a two-stage process could be identified, and hydrogen peroxide was quantitatively measured as an intermediate product. Increasing the rotation speed would increase the rate of transfer of this product from the electrode to the bulk solution before it has had time to react. Consequently, to obtain the four-electron process limiting current at high rotation speeds, it is necessary to increase the overpotential. Wroblowa, Pan, and Ra-

zumney[402] have discussed the application of rotating-ring-disc electrodes to define the fine detail of the reaction scheme. These techniques have not been applied to oxygen reduction on pyrite.

At extreme overvoltages of cathodic polarization (~ −0.3 V (SHE), −1.0 V overpotential) the oxygen reduction reaction will be replaced by the hydrogen reduction and pyrite reduction reactions.[184,383] On the basis of limited information, Biegler[403] suggested that for these conditions the reduction of pyrite would be better represented by

$$FeS_2 + 2xH^+ + 2xe^- \rightarrow FeS_{2-x} + xH_2S \quad (128)$$

However the small charges involved (only about 30 μC cm^{-2} for the best defined case) indicate that the characterization of such processes would be difficult.

The electrode kinetics are independent of the semiconductor characteristics of the material, whether it be n-type, n-type metallic, or p-type pyrite.[390,403] This is due to the limited diffusion of the electrons and the ohmic drop in the near surface layer of the conductor depleted by charge carriers.[404]

E. Anodic Oxidation Reactions

Although the cathodic reduction reaction has been clearly identified, with the possible exception of minor details on the intermediate, the mechanism for the anodic oxidation reaction remains uncertain and authors tend to preface their discussion with "the anodic oxidation of pyrite is a complex process".

In contrast to pyrite, the monosulfides have a well-defined anodic reaction:

$$MS \rightarrow M^{2+} + S + 2e^- \quad (129)$$

and application of this reaction to electrochemical refining of metals was first suggested nearly 100 years ago[405] and is applied commercially in various parts of the world.[406] The combination of the electrochemical and semiconducting properties is now being considered for solar energy conversion work.[407]

In comparison, pyrite has an unusual anodic reaction that so far can only be written as an overall reaction:

$$FeS_2 + 8H_2O \rightarrow Fe^{3+} + 2SO_4^{2-} + 16H^+ + 15e^- \quad (130)$$

There have been no reports on the electrochemistry of any of the other disulfides with the pyrite structure. A recent investigation into the electrochemistry and photochemistry of MoS_2, which has a layer structure, suggested that the photochemical oxidation proceeded by the overall reaction

$$MoS_2 + 8H_2O + 18h^+ \xrightarrow{18\,h\nu} Mo(VI) + 2SO_4^{2-} + 16H^+ \quad (131)$$

where h^+ is a semiconductor hole.[408] MoS_2 has a small band gap and the electrons and holes may be considered to be in a kinetic equilibrium of generation and recombination,[381] so the overall electrochemical reaction would be

$$H^+ + e^- = \text{intact bond} \quad (132)$$

$$MoS_2 + 8H_2O \rightarrow Mo(VI) + 2SO_4^{2-} + 16H^+ + 16e^- \quad (133)$$

The reaction is similar to pyrite oxidation.

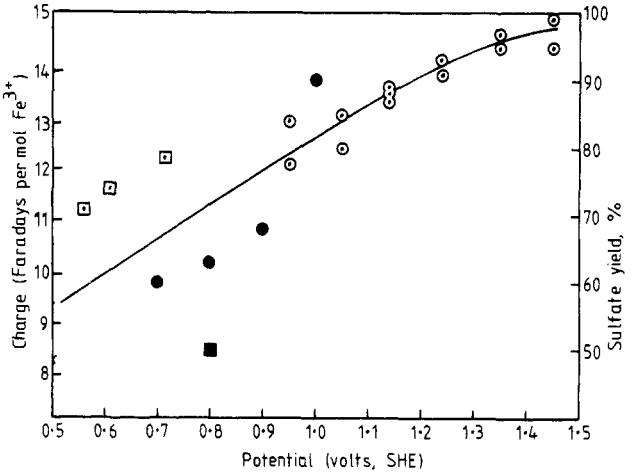

Figure 2. Stoichiometry of the pyrite anodic reaction as a function of overpotential: (⊙) 1 M H_2SO_4 at 25 °C;[178] (●) 1 M $HClO_4$ at 110 °C;[12] (□) 0.5 M H_2SO at 25 °C;[410] (■) 1 N H_2SO_4 at 145 °C.[183]

In both cases, the major products are fully oxidized metal, sulfate, and hydrogen ions. Sulfur as a product is only produced under certain conditions and is favored by a limited range in temperature,[177,179,180,185-188] a reduction in pH to below pH 1,[12,162] or applied voltage.[12,162,178,181-183]

The influence of applied voltage on the distribution of products is illustrated by Figure 2, which summarizes the results of several workers for the potentiostatic pressure leaching or potentiostatic polarization experiments at ambient temperatures in various environments. The results indicate a linear dependence between sulfate yield and, by implication, sulfur yield and applied potential. Although there is good correlation between results produced by individual authors, there is a broader scatter between results of different authors. This is to be expected in view of the widely different operating conditions and the uncertainty inherent in converting the potentials in the different environments to a common scale.

Using potentiodynamic, quasi-potentiostatic, or potentiostatic systems the anodic polarization characteristics have been determined in a range of environments: $HClO_4$, ambient temperature;[178,184,383,390] $HClO_4$, >100 °C;[183] HCl, ambient temperature;[178,388,390,409] HNO_3, ambient temperature;[388] H_2SO_4, ambient temperature;[178,388,390,410] H_2SO_4, 100 °C.[183]

Anodic polarization experiments have also been reported by Ryss and co-workers,[411-413] Yashina and co-workers,[404] and Lobanov and co-workers[414] and potential time curves for pyrite in alkali have been reported by Yashina and co-workers.[415] Potentiostatic experimental systems always contain an *iR* or ohmic potential drop. There are several methods for eliminating this effect.[416] In addition to the *iR* drop, pyrite as a semiconductor may have nonohmic and, in some cases, rectifying characteristics at either the mineral–electrolyte interface or the mineral/metal interface of the current conducting lead. The nonohmic characteristic becomes significant with increasing resistance of the mineral specimen.[417] The use of conducting epoxy resin cement[178,378] or mercury[410] to make electrical contact between the current carrying lead and the mineral has been criticized on the grounds that the technique introduces mobile ions such as Ag^+, Hg^+, and Cu^+ onto

the semiconductor interface.[417] An alternative contact method is to press-fit or tap a platinum lead into holes drilled into the mineral with a graphite-based conducting cement to achieve contact on a face shadowed with a thin layer of gold;[417] another technique is to employ two contacts, one as the normal current carrier and the second to provide additional potentiometric contact.[418]

The anodic polarization curves are independent of the semiconducting properties of the pyrite.[178,383,390] In contrast, under equilibrium conditions the semiconducting properties influence the double-layer capacitance[419] and hence the flotation properties of pyrite.[420] This may also account for the observed difference in oxidation rates for p- and n-type material under bacterial catalysis conditions.[421] In this case the p-type material leached 1.4 times faster and exhibited a 300 mV difference with the n-type after 10 days, although the initial open-circuit potentials were similar.

Springer[390] and others[383,409] obtained a Tafel slope of ~120 mV per decade at 1 M acid; the slope was independent of the nature of the acid. Meyer[410] reported that the Tafel slopes fall in the range 80–110 mV per decade, whereas Biegler and Swift[178] reported a slightly narrower range of 90–105 mV per decade and a slope that was independent of the anion solution. Tafel slopes for the electrochemical behavior of pyrite in alkali have been reported by Yashina and co-workers.[423]

Coulometry has been employed to demonstrate both the presence and absence of sulfur as a product. Peters and Majima[184] anodically polarized a pyrite specimen at a constant current of 1 mA cm^{-2} in 1 M $HClO_4$ under helium for ~6 days. The final solution was analyzed for total iron, Fe^{2+}, and SO_4^{2-}. Their results indicated that sulfur is not a product. Biegler and Swift[178] noted that anodic polarization causes the surface to darken, and with the passage of sufficient charge there is an accumulation of white or yellow material on the surface and, more significantly, in fissures where deeper corrosion has occurred. This has also been noted by the present author. Klein and Shuey[383] have attempted to identify this phenomenon by first carrying out extended anodization at 1.16 V (SHE) to produce sufficient product film. The resulting film was a blank aphanitic material which was highly magnetic but could not be positively identified. It was suggested that it may be a spinel iron oxide, either magnetite (Fe_3O_4) or maghemite (α-Fe_2O_3); a subsequent experiment with magnetite (Fe_3O_4) indicated that the surface tarnish was not magnetite, but more likely to have been maghemite or some other iron oxide.

X-ray emission spectroscopic analysis of a pyrite surface has indicated the presence of an oxygen-containing layer.[424,425] Other workers tend to favor a sulfur type film. Biegler and Swift[178] reported coulometric experiments similar to those of Peters and Majima[184] but employed a cell with separate anode and cathode compartments. Sulfate analyses were not determined; instead the product solution was analyzed for total iron and sulfur, the latter being obtained by CS_2 extraction. If sulfur is a product, then the overall process may be written as

$$FeS_2 + 8xH_2O \rightarrow Fe^{3+} + 2xSO_4^{2-} + 2(1 - x)S + 16xH^+ + (12x + 3)e^- \quad (134)$$

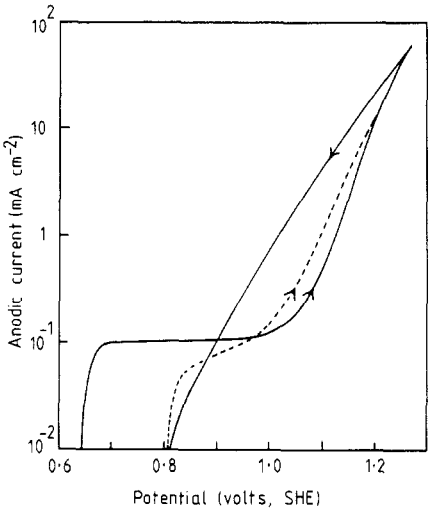

Figure 3. Anodic polarization curve for pyrite in 1 N H_2SO_4, H_2 saturated at 25 °C (author's own work; see also ref 178 and 410).

The value of x may be determined from Figure 2 for the given experimental potential and allows a theoretical sulfur yield to be obtained along with the experimental yield obtained from the CS_2 extract. The two values agreed within 20%, which is reasonable, taking into account the error range of the experiment. Meyer[410] failed to observe elemental sulfur by using scanning electron microscopy following anodic polarization. However, he did analyze his solutions for Fe^{3+} and SO_4^{2-} and found that only Fe^{3+} was formed with a varying percentage of sulfate. Koch[426] reported that the reaction product is entirely sulfate at +0.81 V. Coulometric studies of the oxidation of pyrite in sodium hydroxide solutions have been reported by Kostina and Chernyak.[427] This work was subsequently followed up by infrared studies of the reacting surfaces.[206]

Anodic polarization curves were usually prepared with polished specimens; however, Meyer[410] has reported that the polarization characteristics of polished and unpolished specimens are similar. Following polarization to high current densities, the specimens were always deeply pitted.[178,410]

The anodic polarization characteristics for H_2 saturated acid conditions are given in Figure 3. The curve has some unusual features. On sweeping for the first time from the open-circuit potential (0.55–0.65 V SHE), after holding the specimen at a cathodic potential, one observes a small peak or plateau develop over the range 0.7–0.9 V (SHE) at a current density of ~0.1 mA cm^{-2}.[178,184,410] Past 0.9 V (SHE), the current rises exponentially. Peters and Majima[184] reported that oxygen evolution occurs if the potential is raised to +1.57 V (SHE) (this may be 1.32 V (SHE)[12]); however, neither Klein and Shuey[383] nor Springer[390] was able to observe oxygen evolution at 1.2 V (SHE) and 10 mA cm^{-2}. On reversing the direction of sweep, a narrow hysteresis loop develops and there is an exponential drop in current, without any plateau, to the open-circuit potential. The absence of a plateau on the reverse sweep causes the open-circuit potential to shift by approximately +0.25 V. Subsequently, forward scans reproduce the first reverse scan. If the specimen is held at the plateau position, the current will decay. The formation of a plateau or peak is a function of scan rate. If the specimen is left under open-circuit conditions, the open-circuit potential will drift back to its original value.

The role of pH on the anodic polarization characteristics has been noted by several workers. When the pH is increased from 0 to 5, cyclic voltammograms develop larger loops in current width and voltage length.[383] In the Tafel region for anodic polarization for a given potential, the current density decreases with increasing pH or, for a given current density, the electrode potential decreases with increasing pH owing to the anodic wave shifting to more negative potentials with increasing pH.[178,410] Linear Tafel regions could not be identified when various buffer solutions of pH 4.3–8.8[178] are employed. An activation energy of 58.6 ± 2.5 kJ mol^{-1} between 0.550 and 650 mV (SHE) was determined for anodic oxidation of pyrite in 0.05 M H_2SO_4–0.5 M Na_2SO_4, Ar atmosphere, and 25–68.5 °C.[383] These low values indicate activation control.

F. The Passive Film

The anodic polarization characteristics are reminiscent of the characteristics for passivated metals and, like the passivated metal characteristics, the results for pyrite have not been fully explained. Several authors have noted that the open-circuit potential is ~0.3 V higher than the thermodynamic reversible potential for the reaction[178,410,417]

$$FeS_2 \rightarrow Fe^{2+} + 2S^0 + 2e^- \quad (135)$$

and, since the material does not actively corrode, this has generally been interpreted as evidence for the formation of a passive film. The nature of this film has yet to be described. Peters and co-workers[12,428] have pointed out that pyrite is one of the few sulfide minerals having a molar volume smaller than its sulfur content when the sulfur is in elemental form (see section IVB8). Thus, elemental sulfur protects pyrite from oxidation under conditions in which the sulfur does not oxidize. A perfect fitting film is formed if the excess sulfur is oxidized to sulfate. Increasing the percentage oxidation to sulfate lowers the protection afforded by the film.

Thermal decomposition studies of pyrite fail to provide a clue on the nature of the surface film. Under oxidizing conditions it has been suggested that pyrite thermally decomposes in two steps with the formation of FeS as an intermediate.[429] Other workers have suggested that the oxidation proceeds directly to ferrous[430] or ferric sulfate,[431] or directly to the oxide.[432–435] Ionescu, Pincovschi, and Maxim[436] considered that the mechanism of oxidation was a function of temperature, the primary product of oxidation being sulfate in the sulfate stability range and the oxide in the sulfate instability range. Under reducing conditions, pyrite is thermally decomposed to the nonstoichiometric pyrrhotite:[437]

$$FeS_2 \rightarrow FeS + {}^1/_2S_2(g) \quad (136)$$

Steam accelerates this reaction and H_2S is a product.[435,438]

$$3FeS_2 + 2H_2O \rightarrow 3FeS + 3H_2S + SO_2 \quad (137)$$

Other investigations for the low-temperature desulfurization of coal by atmospheric oxidation,[439,440] and studies of the weathering of pyrite, are contradictory, the products being listed variously as $FeSO_4$, $Fe_2(SO_4)_3$, FeO, Fe_2O_3, FeS, jarosite, H_2SO_4, or S either as single products or as complex mixtures.[441–445]

More recently, analytical methods have been developed for analyzing the S-bearing constituents in the very small amounts of oxidation products formed on sulfide minerals.[167,190,446,465] Steger and Desjardins[167] concluded that pyrite in 68% relative humidity air at 52 °C oxidizes to ferric sulfate through a thio intermediate:

$$2FeS_2 + 3O_2 \rightarrow 2FeS_2O_3 \quad (138)$$

$$FeS_2O_3 + 3O_2 \rightarrow Fe_2(SO_4)_3 + S^0 \quad (139)$$

Goldhaber[465] has reported observing the formation of tetrathionate as a metastable intermediate during the oxidation of pyrite in 0.1 M HCl at pH 6–7. Thom and Walters[447] failed to find any thio salts associated with pyrite during a study of the metal sulfide–sulfur dioxide reaction. Cyclic voltammetry has indicated that, under alkaline conditions, the pyrite surface is covered with a hydrated iron oxide film.[448]

G. The Anodic Process

The lack of understanding of the nature of the surface film is matched by an equal lack of understanding of the anodic process. Burke and Downes[173] and Stenhouse and Armstrong[186] concluded that the oxidation of iron and sulfur in pyrite proceeded, at least in part, by independent paths. Woodcock[199] suggested the initial formation and solution of the positive ion S_2^+, which is rapidly transformed to sulfate in acid or alkaline solution. Biegler and Swift[178] discounted elemental sulfur as an intermediate for the formation of sulfate since, in the leaching of sulfides that do produce elemental sulfur, the product once formed is very stable even at elevated temperatures.[350] In addition, sulfur is a very stable product of the anodic polarization of H_2S in 0.1 M H_2SO_4 in the voltage range 1.2–1.7 V (SHE);[449,450] this is the voltage range in which high sulfate yields are obtained from anodic polarization of pyrite.

Impedance studies indicate the presence of the ferrous–ferric redox couple.[451] Meyer[410] has discussed the anodic process in terms of a two-layer system. One layer is associated with the oxidation of ferrous iron to ferric as $Fe^{2+} \rightarrow Fe^{3+} + e^-$ and the other layer involves the oxidation of S_2^{2-} through thio intermediates such as $S_2O_2^{2-}$, $S_2O_3^{2-}$; a possible initial step is the formation of the as yet unknown thiosulfurous acid $S_2(OH)_2$ through the reaction

$$S_2^{2-} + 2H_2O = S_2(OH)_2 + 2H^+ + e^- \quad (140)$$

This approach has the advantage that the thio intermediates may convert to S^0 or SO_4^{2-}, depending on the operating conditions. Using cyclic voltammetry, Conway and co-workers[452] observed two almost reversible monolayer surface processes occurring on the pyrite surface in the potential range −0.2–0.454 at pH 1; the processes were not identified. The following reaction was suggested as an initial step:

$$2e^- + S_2^{2-}{}_{lattice} \rightarrow 2S^-{}_{lattice} \quad (141)$$

When the potential is increased past 0.5 V, other anodic processes occur, producing the species SO_3^{2-}, $S_2O_3^{2-}$, SO_4^{2-}, and Fe^{2+}.

Biegler and Swift[178] suggested that the initial step was the adsorption of oxygen onto the pyrite surface

through the adsorption and deprotonation of water molecules according to

$$FeS_2 + H_2O = FeS_2(OH)_{ads} + H^+ + e^- \quad (142)$$

$$FeS_2(OH)_{ads} = FeS_2(O)_{ads} + H^+ + e^- \quad (143)$$

with step 1 as rate determining. While predicting a shift in potential with pH, the equation also indicates a Tafel slope of 59 mV per decade if the Tafel constants α and β are assumed to be 0.5; this is a somewhat low value compared to the values observed in practice at ~100 mV per decade. Alternative schemes for oxygen attachment indicated even lower values for the Tafel slope. This approach is attractive because Bailey and Peters[12] demonstrated that sulfate oxygen originates from water rather than molecular oxygen in pyrite pressure leaching. However, on Biegler and Swift's own admission, the above mechanism fails to account for the formation of sulfur via the minor path.

Yashina and co-workers[453] have suggested that the electrochemical behavior of pyrite in alkaline conditions may be controlled by the diffusion limits in the solid phase and that this in turn is determined by the charge carrier concentration in the semiconductor.

VI. Summary

The chemistry and physics of iron disulfide have been reviewed with reference to the aqueous oxidation of pyrite by molecular oxygen. This reaction has technical application to the recovery of heavy metals from low grade ores by heap leaching and for the desulfurization of coal. The reaction is the source of a significant environmental hazard known as acid mine drainage, which occurs in high sulfur coal mines and heavy metal sulfide mines located in temperate and monsoonal climates. It is a cause of souring of soils and soil heave and causes problems for museum conservation of sulfide specimens.

There are two crystal forms of iron disulfide—cubic pyrite and orthorhombic marcasite. Pyrite may be further subdivided into euhedral and framboidal materials. Morphology and crystal structure influence the reaction rate in the following order: euhedral pyrite < framboidal pyrite < marcasite (most reactive). In general, such physical properties as density, thermal expansion, compressibility, magnetic susceptibility, Mössbauer spectra, and electrical and optical properties are known with a greater certainty for pyrite than for marcasite. Pyrite is a semiconductor which causes anisotropy for some physical properties. The semiconductor properties influence the reaction kinetics for systems near equilibrium conditions such as natural weathering, but do not influence the reaction kinetics for systems significantly removed from equilibrium, such as those experienced with cyclic voltammetric or potentiodynamic experiments. Thermodynamic analysis has identified a stability regime for the product jarosite, $KFe_3(SO_4)_2(OH)_6$, a complex basic ferric sulfate. This product will act as a chemical buffer and maintain the environment under acid conditions.

Three reaction paths have been identified for the aqueous oxidation of pyrite by molecular oxygen, namely, bacterial, chemical, and electrochemical. The bacterial path was not discussed. The chemical oxidation path is a sequence of three steps: (i) the oxidation of pyrite by molecular oxygen to sulfate and ferrous iron, (ii) the oxidation of ferrous iron by molecular oxygen to ferric iron, and (iii) the oxidation of pyrite by ferric iron to sulfate and ferrous iron.

Step i is represented by reaction 12. This is a het-

$$2FeS_2 + 7O_2 + 2H_2O \rightarrow 2FeSO_4 + 2H_2SO_4 \quad (12)$$

erogeneous surface reaction, and is first order with respect to oxygen partial pressure at below 0.5 MPa but becomes increasingly fractional order to oxygen partial pressure above 1 MPa. The activation energy of ~60 kJ M^{-1} indicates a chemical rather than a physical rate-determining step. The rate is a function of morphology, surface area, and, for undersaturated systems, humidity. The functional relationships for these variables have not been properly identified. There are no catalysts for the reaction. The rate of reaction increases nonlinearly as the pH is increased from 1 to 10. Below pH 1, the rate is independent of pH but the production of elemental sulfur as a side reaction becomes increasingly significant. This side reaction is enhanced by increasing the temperature to a limiting value of 150 °C. A number of reaction mechanisms have been proposed; these include the formation of an adsorbed oxygen species, formation of thio intermediates, and an electrochemical sequence. Evidence has been presented for all of these mechanisms.

The oxidation rate of ferrous iron to ferric iron is a function of the media, pH, ferrous iron concentration, oxygen concentration, temperature, and catalytic materials. Under all conditions, the reaction rate is first order with respect to oxygen partial pressure. Below pH 2, the reaction rate is independent of pH. The reaction rate is second order with respect to ferrous iron in solutions of sulfuric, nitric, and perchloric acid at room temperature. The reaction order with respect to ferrous iron is modified in sulfuric acid solutions as the temperature is raised. The reaction rate with respect to ferrous iron is first order in hyrochloric and phosphoric acid solutions and a complex function of phosphate and pyrophosphate concentrations. As the pH is raised from 2 toward 7, the reaction rate increases and becomes initially first order with respect to hydroxyl and then second order with respect to hydroxyl above pH 5. With further increases in pH beyond 7, ferrous hydroxide is precipitated and the reaction rate converts to a heterogeneous surface reaction. There are a number of catalysts for the reaction; this includes surface catalysts, such as platinum and activated charcoal, and solution catalysts, the most active of which is Cu^{2+}. A number of reaction mechanisms have been proposed involving reaction sequences, ferrous ion oxygen complexes stabilized by the media anion, oxygen anion complexes, or hydrolyzed oxygen complexes. No proposal is in full accord with all the experimental observations.

The third step of the chemical oxidation path is the oxidation of pyrite by ferric iron. This is a heterogeneous surface reaction with poorly defined kinetics. This reaction rate is independent of catalysts. The rate is a function of Fe^{2+}, Fe^{3+}, total iron concentration surface area, and pH. There is some evidence for a side reaction with elemental sulfur as a product. No mechanisms have been proposed for the surface reduction of ferric iron to ferrous iron, solution of pyritic ferrous iron, or oxidation of the S_2^{2-} moiety to sulfate.

The electrochemical path for the oxidation of pyrite by molecular oxygen is the summation of two half-cell

reactions, one for the cathode

$$O_2 + 4H^+ + 4e^- \rightarrow 2H_2O \quad (97)$$

and one for the anode

$$FeS_2 + 8H_2O \rightarrow Fe^{3+} + 2SO_4^{2-} + 16H^+ + 15e^- \quad (99)$$

Pyrite does not undergo nonoxidative dissolution. The open-circuit potential is a function of oxygen concentration and media anion. There is a Nernstian relationship for the open-circuit potential of pyrite with pH and with the Fe^{3+}/Fe^{2+} redox couple. Cyclic voltammetry has identified reaction 97 as the dominant cathodic reaction, with eq 120 as the primary and

$$O_2 + e^- = O_2^-{}_{aq} \quad (120)$$

rate-controlling step in acid media and the formation of hydrogen peroxide, eq 122 and 124, as the rate-controlling step in alkali media.

$$O_2^-{}_{aq} + H_2O + e^- = O_2H^-{}_{aq} + OH^-{}_{aq} \quad (122)$$

$$O_2H^-{}_{aq} + H^+{}_{aq} = H_2O_2{}_{aq} \quad (124)$$

Although reaction 99 is the dominant anodic reaction, there is a side reaction that produces sulfur. This side reaction is depressed as the applied voltage is increased away from the open-circuit potential. Both the anodic and cathodic current voltage characteristics are independent of the semiconductor type; however, equilibrium characteristics such as double layer capacitance are dependent on the semiconductor type. The surface is passivated by a film which has been variously reported as sulfidic or composed or iron oxides. The anodic mechanism is poorly understood, and there is no explanation for the oxidation of S_2^{2-} to SO_4^{2-} in mechanistic terms. There is limited evidence for the formation of thio intermediates, and the intermediate $2S^-$ has been suggested. Elemental sulfur is considered as a stable end product and not as an intermediate.

A necessary corollary of the chemical sequence approach is that the sum of the rates of the individual processes should equal the rate of the overall process. Mathews and Robins[175] are the only authors who have attempted the summation and obtained a negative rate of production of ferrous iron. It was suggested that the measured kinetics of individual reactions do not apply to the different environment of the overall reaction. The electrochemical path requires an external circuit for the transmitted electrons. Although such a circuit is readily available in the laboratory, it is more difficult to envisage under environmental conditions and, in the extreme case, would require the pyrite crystal to become bipolar. Both reaction paths appear to be equally applicable for the natural environment, where the kinetics are more likely to be controlled by such physical parameters as oxygen diffusion into the heap material, oxygen diffusion into the individual lumps, humidity, water flow, product removal, catalytic materials, galvanic coupling, thermal cycling, and bacteria. For this reason, heap, waste dump, and commercial operations and mathematical modeling of such systems have not been reviewed.

A number of purely chemical questions remain to be answered. These are the following: Is the Fe^{2+} ion oxidized up to Fe^{3+} before dissolution from the pyrite lattice? What is the oxidation path for S_2^{2-} to SO_4^{2-}? What are the controlling factors for the production of elemental sulfur? Under what conditions do the semiconducting properties influence the kinetics of oxidation? Can a pyrite crystal become bipolar?

VII. Acknowledgment

The text of this review has been revised following extensive discussions with workers in the UK, USA, and Canada during a recent tour of these countries. I have been well-supported by staff at the AAEC and, in particular, the secretarial staff, who undertook the many retypes, the librarians who located many of the references, and the Scientific Editing Section, who edited the text.

VIII. References

(1) Truchot, P. "Les Pyrites"; Paris, 1907.
(2) Dioscorides "De Materia Medica"; ca. 75 AD. From ref 6.
(3) Pliny The Elder, Caius Plinius Secandus. "Historia Naturalis"; ca. 77 AD. From ref 6.
(4) Theophrastus. "Περι λιθσζ"; 315 BC. From ref 6.
(5) Henckel, J. F. "Pyritologia oder Kiess-Historie"; Leipzig, 1725. From ref 6.
(6) Mellor, J. W. "A Comprehensive Treatise on Inorganic and Theoretical Chemistry: Vol. XIV. Fe(Part 3)–Cobalt": Longmans, Green and Co.: New York, 1935.
(7) Pings, W. B. *Miner. Ind. Bull. (Colo. Sch. Mines)* **1968**, *2(3)*, 1.
(8) Lowson, R. T. *Aust. A.E.C., Res. Establ. [Rep.]* **1975** *AAEC/E356.*
(9) Brierley, C. L. *CRC Crit. Rev. Microbiol.* **1978**, *6*, 207.
(10) Dugan, P. R.; Apel, W. A. *Metall. Appl. Bact. Leaching Relat. Microbiol. Phenom., [Proc. Int. Symp].* **1977** (Pub. **1978**), 223–50.
(11) Brierley, J. A.; Brierley, C. L. *Metall. Appl. Bact. Leaching Relat. Microbiol. Phenom., [Proc. Int. Symp.]* **1977** (Pub. **1978**), 477–90.
(12) Bailey, L. K.; Peters, E. *Can. Metall. Q.* **1976**, *15*, 333.
(13) Dana, J. D.; Dana, E. S. "The System of Mineralogy", 7th ed.; Palache, C., Berman, H., Frondel, C., Eds.; Wiley: New York, 1944; Vol. 1.
(14) Gait, R. I. *Mineral. Rec.* **1978**, *9*, 219.
(15) Goldschmidt, V. "Atlas der Kristallformen"; Carl Winter's Universitätsbuchhandlung: Heidelburg, 1919.
(16) Smith, E. E.; Shumate, K. S. Report by The Ohio State University Research Foundation for the Federal Water Pollution Control Administration. Program No. FWPCA. Grant No. 14010. FPS February 1970.
(17) Gray, R. J.; Schapiro, N.; Dale, G. *Trans. Soc. Min. Eng. AIME* **1963**, *226*, 113.
(18) Caruccio, F. T.; Ferm, J. C.; Horne, J.; Geidel, G.; Baganz, B. *U.S. NTIS, PB Rep.* **1977**, PB-270080.
(19) Caruccio, F. T. *Ecol. Reclam. Devastated Land, [Proc. NATO Adv. Study Inst.]* **1969** (Pub. **1973**), *1*, 193.
(20) Caruccio, F. T. *Symp. Br. Ecol. Soc.* **1975**, *15*, 197.
(21) Caruccio, F. T.; Geidel, G.; Sewell, J. M. *Pap. Symp. Coal Mine Drain Res.* **1976**, *6*, 1.
(22) Schneiderhöhn, H. *Neues Jahrb. Mineral. Geol. Beilageband* **1922**, *47*, 1.
(23) Stevens, B. P. J. "The Mineral Deposits of New South Wales"; Markham, N. L., Basden, H., Eds. Government Press: Sydney, 1975.
(24) Berner, R. "Principles of Chemical Sedimentology"; McGraw-Hill: New York, 1971.
(25) Rickard, D. T. *Lithos* **1970**, *3*, 269.
(26) Javor, B.; Mountjoy, E. *Geology* **1976**, *4*, 2.
(27) Love, L. G. *Q. J. Geol. Soc. London* **1957**, *113*, 429.
(28) Love, L. G.; Amstutz, G. C. *Fortschr. Mineral.* **1965**, *43*, 273.
(29) Czyscinski, K. S. *Diss. Abstr. Int. B* **1976**, *37*, 124.
(30) Ostwald, J.; England, B. M. *Mineral. Mag.* **1979**, *43*, 297.
(31) Raybould, J. G. *Lithos* **1973**, *6*, 175.
(32) Croxford, N. J. W. *Miner. Deposita* **1974**, *9*, 105.
(33) Chauhan, D. S. *Miner. Deposita* **1974**, *9*, 69.
(34) Caruccio, F. T. *NATO Adv. Study Inst. Ser., Ser. E7* **1978**, 127.
(35) Schneiderhöhn, H. "Anleitung zur mikroskopischen Bestimmung und Untersuchungen von Erzen und Aufbereitungsprodukten besonders in auffallenden Licht"; Berlin: Gesellschaft Deutscher Metallhütten und Bergleute, 1922.
(36) Hahn, F. V. V. *Kolloid-Z.* **1925**, 277.
(37) Bernauer, F. "Die Kolloidchemie als Hilfswissenschaft der Mineralogie und Lagerstättenlehre und ihre Anwendung auf

die metasomatischen Blei-Zink-Lager-stätten"; Berlin: Gebr. Borntraeger, 1924.
(38) Doss, B. *Z. Prakt. Geol.* **1912**, *20*, 453.
(39) Feld, W. *Z. Angew. Chem.* **1911**, *24*, 290.
(40) Allen, E. T.; Johnston, J. *J. Ind. Eng. Chem.* **1910**, *2*, 196.
(41) Allen, E. T.; Crenshaw, J. L.; Johnston, J.; Larsen, E. S. *Am. J. Sci.* **1912**, *33*, 169.
(42) Allen, E. T.; Crenshaw, J. L. *Am. J. Sci.* **1914**, *33*, 393.
(43) Berner, R. A. *J. Geol.* **1964**, *72*, 293.
(44) Rickard, D. T. *Publ.—Int. Inst. Land Reclam. Improv.* **1972**, *1*, 28.
(45) Rickard, D. T. *Am. J. Sci.* **1975**, *275*, 636.
(46) Ward, J. C. *Rev. Pure Appl. Chem.* **1970**, *20*, 175.
(47) Wyckoff, R. W. G. "Crystal Structures", 2nd ed.; New York: Wiley, 1963, Vol. 1.
(48) Finklea, S. L., III; Cathey, Le C.; Amma, E. L. *Acta Crystallogr., Sect. A* **1976**, *A32*, 529.
(49) Smith, F. G. *Am. Mineral.* **1942**, *27*, 1.
(50) Robie, R. A.; Bethke, P. M.; Beardsley, K. M. *U.S. Geol. Surv. Bull.* **1967**, No. 1248. See also ref 208, 198–208.
(51) International Critical Tables; McGraw-Hill: New York, 1933.
(52) Gupta, V. P.; Ravindra, N. M.; Srivastava, V. K. *J. Phys. Chem. Solids.* **1980**, *41*, 145.
(53) Horita, H.; Suzuki, T. *Sci. Rep. Rev. Inst., Tohoku Univ., Ser. A* **1975**, *25*, 124.
(54) Wilson, E. *Proc. R. Soc. London, Ser. A* **1921**, *98*, 274.
(55) Wilson, E. *Proc. R. Soc. London, Ser. A* **1923**, *103*, 185.
(56) Serres, A. *J. Phys. Radium.* **1953**, *14*, 689.
(57) Néel, L.; Benoit, R. *C. R. Hebd. Seances Acad. Sci.* **1953**, *237*, 444.
(58) Benoit, R. *J. Chim. Phys. Phys. Chim. Biol.* **1955**, *52*, 119.
(59) Ergun, S.; Bean, E. H. *Rep. Invest.–U.S. Bur. Mines* **1968**, *No. 7181.*
(60) Jarrett, H. S.; Cloud, W. H.; Bouchard, R. J.; Butler, S. R.; Frederick, C. G.; Gillson, J. L. *Phys. Rev. Lett.* **1968**, *21*, 617.
(61) Bither, T. A.; Bouchard, R. J.; Cloud, W. H.; Donohue, P. C.; Siemons, W. J. *Inorg. Chem.* **1968**, *7*, 2208.
(62) Miyahara, S.; Teranishi, T. *J. Appl. Phys.* **1968**, *39*, 896.
(63) Burgardt, P.; Seehra, M. S. *Solid State Commun.* **1977**, *22*, 153.
(64) Stevens, E. D.; DeLucia, M. L.; Coppens, P. *Inorg. Chem.* **1980**, *19*, 813.
(65) Konig, E. "Landolt-Börnstein, Group II: Atomic and Molecular Physics, Vol. 2: Magnetic Properties of Co-ordination and Organometallic Transition Metal Compounds"; Hellwege, K. H., Hellwege, A. M., Eds.; Springer-Verlag: Berlin, 1966.
(66) Gupta, V. P.; Ravindra, N. M. *Solid State Commun.* **1979**, *32*, 1327.
(67) Marusak, L. A.; Walker, P. L.; Mulay, L. N. *IEEE Trans. Magn.* **1976**, *MAG-12*, 889.
(68) Marusak, L. A.; Cordero-Montalvo, C.; Mulay, L. N. *Mater. Res. Bull.* **1977**, *12*, 1009.
(69) Walker, L. R.; Wertheim, G. K.; Jaccarino, V. *Phys. Rev. Lett.* **1961**, *6*, 98.
(70) Imbert, P.; Gerard, A.; Wintenberger, M. *C. R. Hebd. Seances Acad. Sci.* **1963**, *256*, 4391.
(71) Goodman, R. H. *Chem. Can.* **1966**, *18*, 31.
(72) Vaughan, R. W.; Drickamer, H. G. *J. Chem. Phys.* **1967**, *47*, 468.
(73) Morice, J.; Rees, L. V. C.; Rickard, D. T. *J. Inorg. Chem.* **1969**, *31*, 3797.
(74) Suzdalev, I. P.; Vinogradov, I. A.; Imshennik, V. K. *Fiz. Tverd. Tela (Leningrad)* **1972**, *14*, 1321.
(75) Garg, V. K.; Liu, Y. S.; Puri, S. P. *J. Appl. Phys.* **1974**, *45*, 70.
(76) Montano, P. A.; Seehra, M. S. *Solid State Commun.* **1976**, *20*, 897.
(77) Garg, R.; Vishwamitter; Gupta, V. P.; Garg, V. K. *J. Phys. Colloq. (Orsay, Fr.)* **1980**, 355.
(78) Russell, P. E.; Montano, P. A. *J. Appl. Phys.* **1978**, *49*, 4615.
(79) Hulliger, F.; Mooser, F. *J. Phys. Chem. Solids* **1965**, *26*, 429.
(80) Liu, Y. S. *Phys. Rev. B: Condens. Matter* **1979**, *20*, 71.
(81) Seehra, M. S.; Jagadeesh, M. S. *Phys. Rev. B: Condens. Matter* **1979**, *20*, 3897.
(82) Temperley, A. A.; Lefevre, H. W. *J. Phys. Chem. Solids* **1966**, *27*, 85.
(83) Garg, R.; Garg, V. K. *Appl. Phys.* **1978**, *16*, 175.
(84) Jagadeesh, M. S.; Seehra, M. S. *Phys. Lett. A* **1980**, *80A*, 59.
(85) Shuey, R. T. "Semiconducting Ore Minerals"; Elsevier: London, 1975.
(86) Marinace, J. C. *Phys. Rev.* **1954**, *96*, 593.
(87) Sasaki, A. *Mineral. J.* **1955**, *1*, 290.
(88) Horita, H. *Jpn. J. Appl. Phys.* **1971**, *10*, 1478.
(89) Kikuchi, K.; Yamada, S.; Nanjo, J.; Nomura, S.; Hara, S. *Muroran Kogyo Daigaku, Kenkyu Hokoku* **1970**, *7*, 1.
(90) Prokhorov, V. G.; Titarenko, A. D. *Zap. Vses. Mineral. Ova.* **1971**, *100*, 163.
(91) Revyakin, P. S.; Chekalova, K. A.; Zherebtsov, Yu. D. *Izv. Akad. Nauk Kaz. SSR, Ser. Geol.* **1977**, *34*, 40.
(92) Revyakin, P. S.; Revyakina, E. A. *Razved. Okhr. Nedr* **1978**, (*7*), 45.
(93) Joshi, S. K.; Mitra, S. S. *Proc. Phys. Soc. London* **1960**, *76*, 295.
(94) Robie, R. A.; Edwards, J. L. *J. Appl. Phys.* **1966**, *37*, 2659.
(95) Husk, D. E.; Seehra, M. S. *Solid State Commun.* **1978**, *27*, 1147.
(96) Wesely, A. *Physik. Z.* **1913**, *14*, 76.
(97) Saz, M. V. *Ser. Univ.—Fund. Juan March* **1980**, 120.
(98) Li, E. K.; Johnson, K. H.; Eastman, D. E.; Freeouf, J. L. *Phys. Rev. Lett.* **1974**, *32*, 470.
(99) Ohsawa, A.; Yamamoto, H.; Watanabe, H. *J. Phys. Soc. Jpn.* **1974**, *37*, 568.
(100) Wiech, G.; Koeppen, W.; Urch, D. S. *Inorg. Chim. Acta* **1972**, *6*, 376.
(101) Nemoshkalenko, V. V.; Krivitskii, V. P.; Nikolaev, L.; Shpak, A. P. *Dopov. Akad. Nauk Ukr. RSR. Ser. A* **1974**, *36*, 1112.
(102) Kolobova, K. M.; Nemnonov, S. A. *Izv. Sib. Otd. Akad. Nauk SSSR. Ser. Khim. Nauk* **1975**, 34.
(103) Horita, H. *Tohoku Daigaku Senko Seiren Kenkyusho Iho* **1977**, *33*, 9.
(104) Verble, J. L.; Wallis, R. F. *Phys. Rev.* **1969**, *182*, 783.
(105) Schlegel, A.; Wachter, P. *J. Phys. C* **1976**, *9*, 3363.
(106) Kou, W. W.; Seehra, M. S. *Phys. Rev. B: Condens. Matter* **1978**, *18*, 7062.
(107) Seehra, M. S.; Seehra, S. S. *Phys. Rev. B: Condens. Matter* **1979**, *19*, 6620.
(108) Lachinov, A. N.; Chuvyrov, A. N. *Fazov. Perekhody Svoistva Uporyadochen. Struktur* **1977**, 62.
(109) Horita, H.; Suzuki, T. *Jpn. J. Appl. Phys.* **1980**, *19*, 391.
(110) Grønvold, F.; Westrum, E. F.; Chou, C. *J. Chem. Phys.* **1959**, *30*, 528.
(111) Grønvold, F.; Westrum, E. F. *Inorg. Chem.* **1962**, *1*, 36.
(112) Grønvold, F.; Westrum, E. F. *J. Chem. Thermodyn.* **1976**, *8*, 1039.
(113) Coughlin, J. P. *J. Am. Chem. Soc.* **1950**, *72*, 5445.
(114) Mraw, S. C.; Naas, D. F. *J. Chem. Thermodyn.* **1979**, *11*, 567.
(115) Garrels, R. M.; Christ, C. L. "Solutions, Minerals, and Equilibria"; Harper and Row: New York, 1965.
(116) Hem, J. D. *J.—Am. Water Works Assoc.* **1961**, *53*, 211.
(117) Bouet, J.; Brenet, J. P. *Corrosion Sci.* **1963**, *3*, 51.
(118) Biernat, R. J.; Robins, R. G. *Electrochim. Acta* **1972**, *17*, 1261.
(119) Linkson, P. B.; Nobbs, D. M.; Robins, R. G. Extraction Metallurgy Symposium, New South Wales University, Nov 7–9, 1977.
(120) Posnjak, E.; Merwin, H. E. *J. Am. Chem. Soc.* **1922**, *44*, 1965.
(121) Robins, R. G. *J. Inorg. Nucl. Chem.* **1967**, *29*, 431.
(122) Gruner, J. W. *Econ. Geol.* **1931**, *26*, 442.
(123) Smith, F. G.; Kidd, D. J. *Am. Mineral.* **1949**, *34*, 403.
(124) Schmalz, R. F. *J. Geophys. Res.* **1959**, *46*, 575.
(125) Berner, R. A. *Geochim. Cosmochim. Acta* **1969**, *33*, 267.
(126) Breithaupt, A. *Berg. Hütt ZTG* **1857**, *5*, 68.
(127) Botinelly, T. *J. Res. U.S. Geol. Surv.* **1976**, *4*, 213.
(128) McConnell, D. *Am. J. Sci.* **1942**, *240*, 649.
(129) Larsen, E. S.; Berman, H. *U.S. Geol. Survey Bull.* **1934**, 848.
(130) McKie, D. *Mineral. Mag.* **1962**, *33*, 281.
(131) Brophy, G. P.; Scott, E. C.; Snellgrove, R. A. *Am. Mineral.* **1962**, *47*, 112.
(132) Spek, J. van der. *Versl. Landbouwkd. Onderz.* **1950**, *56*, 2.
(133) Furbish, Wm. J. *Am. Mineral.* **1963**, *48*, 703.
(134) Van Breemen, N. *Publ.—Int. Inst. Land Reclam. Improv.* **1972**, 66.
(135) Broomfield, C.; Coulter, J. K. *Adv. Agron.* **1973**, *25*, 265.
(136) Van Breemen, N.; Harmsen, K. *Soil Sci. Soc. Am. Proc.* **1975**, *39*, 1140.
(137) Harmsen, K.; Van Breemen, N. *Soil Sci. Soc. Am. Proc.* **1975**, *39*, 1148.
(138) Spanovich, M.; Fewell, R. B. *Charette Pa. J. Architecture* **1969**, *49*, 15.
(139) Quigley, R. M.; Vogan, R. W. *Can. Geotech. J.* **1970**, *7*, 106.
(140) Penner, E.; Gillott, J. E.; Eden, W. J. *Can. Geotech. J.* **1970**, *7*, 333.
(141) Penner, E.; Eden, W. J.; Grattan-Bellew, P. E. *Can. Build. Dig.* **1972**, *CBD-152*, 152/1.
(142) Quigley, R. M.; Zajic, J. E.; McKyes, E.; Yong, R. N. *Can. J. Earth Sci.* **1973**, *10*, 1005.
(143) Gillott, J. E.; Penner, E.; Eden, W. J. *Can. Geotech. J.* **1974**, *11*, 482.
(144) Turner, H. W. *Am. J. Sci.* **1898** [4], *5*, 424.
(145) De Launay, L. *C. R. Int. Geol. Conf. 10th*, **1907**, *Pt. 1*, 679.
(146) Callaghan, E. *U.S. Geol. Survey, Bull.* **1938**, *886-D*, 91.
(147) Willard, M. E.; Proctor, P. D. *Econ. Geol.* **1946**, *41*, 619.
(148) Hollingworth, S. E.; Bannister, F. A. *Mineralog. Mag.* **1950**, *29*, 1.
(149) Herbillon, A. J.; Pecrot, A.; Vielvoye, L. *Pedologie* **1966**, *16*, 5.
(150) Rossini, F. D.; Wagman, D. D.; Evans, Wm. H.; Levine, S.; Jaffe, I. *Natl. Bur. Stand. (U.S.) Cir.* **1952**, *No. 500.*
(151) Brown, J. B. *Can. Mineral.* **1970**, *10*, 696.

(152) Brown, J. B. *Miner. Deposita* **1971**, *6*, 245.
(153) Lowson, R. T. *Aust. J. Chem.* **1974**, *27*, 105.
(154) Miller, S. D. *Diss. Abstr. Int. B* **1979**, *40*, 2569.
(155) Miller, S. D. *Biogeochem. Ancient Mod. Environ., Proc. Int. Symp., 4th*, **1979** (Pub. **1980**), 537.
(156) Hem, J. D. *Geol. Surv. Water—Supply Pap. (U.S.)* **1959**, 1473.
(157) Conway, N. F.; Davy, D. R.; Lowson, R. T.; Ritchie, A. I. M. *Aust. A. E. C., Res. Establ., [Rep.]* **1975**, *AAEC/E365*, 6.
(158) Howie, F. M. P. Curation of Palaeontological Collections: Special papers in palaeontology No. 22, 1979, 103.
(159) Booth, G. H.; Sefton, G. V. *Nature (London)* **1970**, *226*, 185.
(160) Broadhurst, F. M.; Duffy, L. *Mus. J.* **1970**, *70*, 30.
(161) Howie, F. M. P. personal communication, 1980.
(162) McKay, D. R.; Halpern, J. *Trans. Met. Soc. AIME* **1959**, *212*, 301.
(163) Singer, P. C.; Stumm, W. *Prepr. Pap.—Am. Chem. Soc., Div. Fuel. Chem.* **1969**, *13*, 80.
(164) Singer, P. C.; Stumm, W. *Science (Washington, D.C.)* **1970**, *167*, 1121.
(165) Stumm, W.; Morgan, J. J. "Aquatic Chemistry; An Introduction Emphasizing Chemical Equilibriums in Natural Waters"; Wiley-Interscience: New York, 1970.
(166) Temple, K. L.; Delchamps, E. W. *Appl. Microbiol.* **1953**, *1*, 255.
(167) Steger, H. F.; Desjardins, L. E. *Chem. Geol.* **1978**, *23*, 225.
(168) Sorokin, Yu. I. *Tr., Inst. Biol. Vnutr. Vod, Akad. Nauk SSSR* **1967**, *15*, 75.
(169) Schedel, M.; Trueper, H. G. *Arch. Microbiol.* **1980**, *124*, 205.
(170) Burghardt, C. A. *Chem. News J. Phys. Sci.* **1878**, *37*, 49.
(171) Forman, F. *Econ. Geol.* **1929**, *24*, 811.
(172) Nelson, H. W.; Snow, R. D.; Keyes, D. B. *Ind. Eng. Chem.* **1933**, *25*, 1355.
(173) Burke, S. P.; Downs, R. *Am. Inst. Mining Met. Engrs. Tech. Pub.* **1937**, *No. 769*.
(174) Cornelius, R. J.; Woodcock, J. T. *Proc. Australasian Inst. Mining Metall.* **1958**, 65.
(175) Mathews, C. T.; Robins, R. G. *Aust. Chem. Eng.* **1974**, *15*, 19.
(176) Gmelin. *Handb. Chem.* **1851**, 5, 234.
(177) Bergholm, A. *Jernkontorets Ann.* **1955**, *139*, 531.
(178) Biegler, T.; Swift, D. A. *Electrochim. Acta* **1979**, *24*, 415.
(179) Gerlach, J.; Haehne, H.; Pawlek, F. *Z. Erzbergbau Metallhuettenwes.* **1966**, *19*, 66.
(180) Kim, J. W.; Choi, K. J. *Kumsok Hakkoe Chi.* **1968**, *6*, 83.
(181) Nagai, T.; Kiuchi, H. *Nippon Kogyo Kaishi* **1974**, *90*, 653.
(182) Nagai, T.; Kiuchi, H. *Nippon Kogyo Kaishi* **1975**, *91*, 473.
(183) Nagai, T.; Kiuchi, H. *Nippon Kogyo Kaishi* **1975**, *91*, 547. (English translation ORNL-tr-4296).
(184) Peters, E.; Majima, H. *Can. Metall. Q.* **1968**, *7*, 111.
(185) Warren, I. H. *Aust. J. Appl. Sci.* **1956**, *7*, 346.
(186) Stenhouse, J. F.; Armstrong, W. H. *Trans.—Can. Inst. Min. Metall. Min. Soc. N.S.* **1952**, 49.
(187) Downes, K. W.; Bruce, R. W. *Trans.—Can. Inst. Mining Metall. Min. Soc. N.S.* **1955**, 127.
(188) Sherman, M. I.; Strickland, J. D. H. *J. Met.* **1957**, *209*, 1386.
(189) Majima, H.; Peters, E. *Proc.—IUPAC Conf., Sydney, Australia*, **1969**.
(190) Steger, H. F.; Desjardins, L. E. *Talanta* **1977**, *24*, 675.
(191) Phillips, D. H.; Johnson, H. J. *Ind. Eng. Chem.* **1959**, *51*, 83.
(192) Whipple, G. C.; Whipple, M. C. *J. Am. Chem. Soc.* **1911**, *33*, 362.
(193) Pray, H. A. Report BMI-7-25. 1950.
(194) Pray, H. A.; Schweickert, C. E.; Minnich, B. H. *Ind. Eng. Chem.* **1952**, *44*, 1146.
(195) Linke, W. F. "Solubilities of Inorganic and Metal Organic Compounds", 4th ed.; American Chemical Society: Washington, D.C., 1965, Vol. 2, p 1229.
(196) Dresher, Wm. H.; Wadsworth, M. E.; Fassell, W. M. *J. Met.* **1956**, *8*, 794.
(197) Tamura, H.; Goto, K.; Nagayama, M. *J. Inorg. Nucl. Chem.* **1976**, *38*, 113.
(198) Majima, H.; Peters, E. *Trans. Metall. Soc. AIME* **1966**, *236*, 1409.
(199) Woodcock, J. T. *Proc. Australas. Inst. Min. Metall. Proc.* **1961**, *198*, 47.
(200) Clark, S. C. *J. San. Eng. Div. Am. Soc. Civ. Eng.* **1966**, *92*, 127.
(201) Glasstone, S.; Laidler, K. J.; Eyring, H. "The Theory of Rate Processes"; McGraw-Hill: London, 1941.
(202) Leathen, W. W.; Braley, S. A.; McIntyre, L. D. *Appl. Microbiol.* **1953**, *1*, 61.
(203) Pugh, C. E. *Diss. Abstr. Int. B* **1979**, *39*, 4788.
(204) Gray, P. M. J. *CSIRO Div. Ind. Chem. Int. Rep.* 1954.
(205) Bunn, R. L. *Diss. Abstr. Int.* **1978**, *38*, 5489.
(206) Kostina, G. M.; Chernyak, A. S. *Zh. Prikl. Khim. (Leningrad)* **1979**, *52*, 766.
(207) Berzelius, J. J. *Schweigger's J.* **1819**, *26*, 67; **1822**, *36*, 311. *Ann. Chim. Phys.* **1821**, *9*, 440. *Lehrb. Chemise, Dresden* **1826**, *2*, 365. *Arsberat.- Kemi* **1829**, *8*, 129. From ref 6.
(208) Weast, R. C. "Handbook of Chemistry and Physics", 53rd ed.; Chemical Rubber Co.: Cleveland, Ohio, 1972: (a) p B192; (b) p B99.
(209) Kim, H. W. M.Sc. Thesis, The Ohio State University, 1964.
(210) Morth, A. H.; Smith, E. E. *Am. Chem. Soc., Div. Fuel Chem., Prepr.* **1966**, *10*, 83.
(211) Diev, N. P.; Pavlov, F. N. *Priroda (Moscow)* **1956**, *45*, 82.
(212) Goodman, A., personal communication, 1981.
(213) Iordan, E. F.; Pavlov, F. N.; Diev. N. P. *Trudy Inst. Khim. Metall., Akad. Nauk SSSR, Ural. Fil.* **1955**, *No. 3*, 18.
(214) Mukai, S.; Ito, F.; Nakahiro, Y. *Suiyo. Kaishi* **1966**, *16*, 65.
(215) Lorenz, W. C.; Tarpley, E. C. *Rept. Invest.—U.S., Bur. Mines*, Report 6247, 1963.
(216) Bryner, L. C.; Walker, R. B.; Palmer, R. *Trans. Soc. Min. Eng. AIME* **1967**, *238*, 56.
(217) Walsh, F. M.; Stone, R. L.; Engelmann, W. H. *Pap. Symp. Underground Min.* **1979**, 139.
(218) Habashi, F.; Bauer, E. L. *Ind. Eng. Chem., Fundam.* **1966**, *5*, 469.
(219) McBain, J. W. *J. Phys. Chem.* **1901**, *5*, 623.
(220) Boselli, J. *C. R. Hebd. Seances Acad. Sci.* **1911**, *152*, 602.
(221) Ennos, F. R. *Proc. Cam. Philos. Soc.* **1913**, *17*, 182.
(222) Mikhelson, E. M. *J. Gen. Chem. USSR (Engl. Transl.)* **1931**, *1*, 905.
(223) Lamb, A. B.; Elder, L. W. *J. Am. Chem. Soc.* **1931**, *23*, 137.
(224) Liepina, L.; Macejevskis, B. *Dockl. Akad. Nauk SSSR* **1967**, *173*, 1336.
(225) Fenyi, G.; Ibos-Burkus, J. *Proc. Conf. Appl. Chem., Unit Oper. Processes, 3rd* **1977**, 305.
(226) Mathews, C. T.; Robins, R. G. *Proc., Australas. Inst. Mining Metall.*, **1972**, *No. 242*, 47.
(227) Pound, R. *J. Phys. Chem.* **1939**, *43*, 955.
(228) Macejevskis, B.; Vlasova, A.; Liepina, L. *Latv. PSR Zinat. Akad. Vestis* **1961**, *No. 2*, 123.
(229) Green, W. F.; *J. Phys. Chem.* **1908**, *12*, 389.
(230) Macejevskis, B.; Liepina, L. *Uch. Zap. Rizh. Politekh. Inst.* **1965**, *16*, 199.
(231) Huffman, R. E.; Davidson, N. *J. Am. Chem. Soc.* **1956**, *78*, 4836.
(232) Astanina, A. N.; Rudenko, A. P. *Zh. Fiz. Khim.* **1971**, *45*, 352.
(233) George, P. *J. Chem. Soc.* **1954**, 4349.
(234) Chernaya, S. S.; Matseevskii, B. P. *Latv. PSR Zinat. Akad. Vestis, Khim. Ser.* **1980**, 435.
(235) Dokuchaeva, A. N.; Matseevskii, B. P.; Liepina, L. *Latv. PSR Zinat. Akad. Vestis, Khim. Ser.* **1965**, 533.
(236) Belopol'skii, A. P.; Urusov, V. V. *Zh. Prikl. Khim. (Leningrad)* **1948**, *21*, 903.
(237) Macejevskis, B.; Liepina, L. *Latv. PSR Zinat. Akad. Vestis* **1960**, *No. 10*, 19.
(238) Macejevskis, B.; Liepina, L. *Latv. PSR Zinat. Akad. Vestis* **1960**, *No. 9*, 109.
(239) Vucurovic, D. M.; Vracar, R. Z.; Ilic, I. B. *Glasnik Hem. Drustva, Beograd* **1964**, *29 (3–4)*, 81.
(240) Hotta, H.; Suzuki, N. *Bull. Chem. Soc. Jpn.* **1963**, *36*, 717.
(241) Matseevskii, B. P.; Markov, I. B.; Chernaya, S. S. *Latv. PSR Zinat. Akad. Vestis, Khim. Ser.* **1979**, 399.
(242) Saprygin, A. F.; Gusar, L. S. *Zh. Prikl. Khim. (Leningrad)* **1974**, *47*, 1690.
(243) Smith, J. H. C.; Spoehr, H. A. *J. Am. Chem. Soc.* **1926**, *48*, 107.
(244) Macejevskis, B.; Dokuchaeva, A. N.; Liepina, L. *Latv. PSR Zinat. Akad. Vestis, Kim. Ser.* **1965**, 453.
(245) Astanina, A. N.; Rudenko, A. P. *Zh. Fiz. Khim.* **1971**, *45*, 345.
(246) Agde, G.; Schimmel, F. *Z. Anorg. Allg. Chem.* **1935**, *225*, 29.
(247) Nicol, D. I. *Rep.—Natl. Inst. Metall., (S. Afr.)* **1975**, 1711.
(248) Tiwari, B. L.; Kolbe, J.; Hayden, H. W., Jr. *Metall. Trans., B* **1979**, *10B*, 607.
(249) Spoehr, H. A. *J. Am. Chem. Soc.* **1924**, *46*, 1494.
(250) Cher, M.; Davidson, N. *J. Am. Chem. Soc.* **1955**, *77*, 793.
(251) King, J.; Davidson, N. *J. Am. Chem. Soc.* **1958**, *80*, 1542.
(252) Sokol'skii, D. V.; Dorfman, Ya. A.; Rakitskaya, T. L. *Kinet. Katal.* **1973**, *14*, 608.
(253) Utsumi, S.; Muroshim, K. *Nippon Kagaku Zasshi* **1965**, *86*, 593.
(254) Kurimura, Y.; Kuriyama, H. *Bull. Chem. Soc. Jpn.* **1969**, *42*, 2238.
(255) Posner, A. M. *Trans. Faraday Soc.* **1953**, *49*, 382.
(256) Nikishova, N. I.; Sysoeva, V. V. *Zh. Prikl. Khim. (Leningrad)* **1971**, *44*, 648.
(257) Matseevskii, B. P.; Chernaya, S. S. *Latv. PSR Zinat. Akad. Vestis, Khim. Ser.* **1980**, 439.
(258) Yano, T.; Suetaka, T.; Umehara, T.; Konishi, K.; Horiuchi, A. *Nippon Kagaku Kaishi* **1974**, 1375.
(259) Colborn, R. P.; Nicol, M. J. *J. S. Afr. Inst. Min. Metall.* **1973**, *73*, 281.
(260) Nikishova, N. K.; Rotinyan, A. L.; Sysoeva, V. V. *Zh. Prikl. Khim. (Leningrad)* **1974**, *47*, 2228.
(261) Iwai, M.; Majima, H.; Izaki, T. *Denki Kagaku oyobi Kogyo Butsuri Kagaku* **1979**, *47*, 409.

(262) Cornog, J.; Hershberger, A. *Proc. Iowa Acad. Sci.* **1929**, *36*, 264.
(263) Holluta, J.; Koelle, W. *GWF, Gas—Wasserfach* **1964**, *105*, 471.
(264) Sysoeva, V. V.; Rotinyan, A. L. *Zh. Prikl. Khim. (Leningrad)* **1971**, *44*, 254.
(265) Nikishova, N. I.; Osinenkova, I. G.; Rotinyan, A. L.; Sysoeva, V. V. *Zh. Prikl. Khim. (Leningrad)* **1974**, *47*, 1196.
(266) Markov, I. B.; Matseevskii, B. P. *Latv. PSR Zinat. Akad. Vestis, Khim. Ser.* **1976**, 550.
(267) Sysoeva, V. V.; Nikishova, N. I. *Zh. Prikl. Khim. (Leningrad)* **1971**, *44*, 2436.
(268) Wilmoth, R. C.; Kennedy, J. L.; Hill, R. D. *Prepr. Pap. Symp. Coal Mine Drain Res., 5th* **1974**, 246.
(269) Just, G. *Ber.* **1907**, *40*, 3695.
(270) Just, G. *Z. Phys. Chem.* **1908**, *63*, 385.
(271) Karpora, I. F. *J. Gen. Chem. USSR (Engl. Transl.)* **1937**, *7*, 2613.
(272) Abel, E. *Z. Elektrochem.* **1955**, *59*, 903.
(273) Tödt, F.; Stoklossa, K. *Z. Elektrochem.* **1954**, *58*, 354.
(274) Holluta, J.; Eberhardt, M. *Vom Wasser* **1957**, *24*, 79.
(275) Stumm, W.; Lee, G. F. *Ind. Eng. Chem.* **1961**, *53*, 143.
(276) Schenk, J. E.; Weber, W. J. *J.—Am. Water Works Assoc.* **1968**, *60*, 199.
(277) Stumm, W. Symposium on Acid Mine Drainage Research, Pittsburgh, PA, 1965, pp 51–63.
(278) Kim, A. G. 2nd Symposium on Coal Mine Drainage Research, Pittsburgh, PA, 1968, pp 40–45.
(279) Stauffer, T. E.; Lovell, H. L. *Am. Chem. Soc., Div. Fuel Chem., Prepr.* **1969**, *13*, 88.
(280) Goto, K.; Tamura, H.; Nagayama, M. *Denki Kagaku* **1971**, *39*, 690.
(281) Theis, T. L. Ph.D. Dissertation, Notre Dame University, Notre Dame, IN, 1972.
(282) Suc, N. V. *Khoc Hoc Ky Huat* **1974**, 17.
(283) Kester, D. R.; Byrne, R. H., Jr.; Liang, Y. J. *ACS Symp. Ser.* **1975**, *No. 18*, 56.
(284) Murray, J. W.; Gill, G. *Geochim. Cosmochim. Acta* **1978**, *42*, 9.
(285) Sung, W.; Morgan, J. J. *Environ. Sci. Technol.* **1980**, *14*, 561.
(286) Gluud, W.; Reise, W. *GWF, Gas—Wasserfach* **1929**, *72*, 1251.
(287) Herman, J. *C. R. Hebd. Seances Acad. Sci.* **1936**, *202*, 419.
(288) Roig, E.; Hazel, J. F.; McNabb, W. M. *J. Am. Chem. Soc.* **1958**, *80*, 1874.
(289) Ioshpa, I. E.; Ivanov, V. G. *Tr. Gor'k Politekh. Inst. im. A. A. Zhdanova* **1971**, *27*, 89.
(290) Prasad, T. P.; Suryanarayana, A. *J. Appl. Chem. Biotechnol.* **1973**, *23*, 711.
(291) Emets, A. A.; Bogdanov, V. I. *Tr. Novocherk. Politekh. Inst. im. Sugo Ordzhankidze* **1972**, 28.
(292) Macejevskis, B.; Liepina, L. *Latv. PSR Zinat. Akad. Vestis* **1960**, *No. 6*, 85.
(293) Macejevskis, B.; Liepina, L. *Latv. PSR Zinat. Akad. Vestis* **1960**, *No. 1*, 89.
(294) Gorshkov, A. S.; Reibakh, M. S. *Zh. Prikl. Khim. (Leningrad)* **1974**, *47*, 649.
(295) Prasad, T. P.; Ramasastry, V. V. *J. Appl. Chem. Biotechnol.* **1974**, *24*, 769.
(296) Varinsikii, T.; Laska, M. *Ann. Chim. Anal. Chim. Appl.* **1909**, *14*, 45.
(297) Pound, J. R. *J. Soc. Chem. Ind., London* **1936**, *55*, 327.
(298) Stumm, W.; Lee, G. F. *Schweiz. Z. Hydrol.* **1960**, *22*, 295.
(299) Thomas, G.; Ingraham, T. R. *Unit Process Hydromet.* **1965**, *1*, 67.
(300) Saito, I. *Kogai Shigen Kenkyusho Iho* **1976**, *6*, 1.
(301) Posner, A. M. *Trans. Faraday Soc.* **1953**, *49*, 389.
(302) Polzer, W. L. *Prin. Appl. Water Chem., Proc. Rudolfs Res. Conf., 4th* **1965**, 505.
(303) Weber, W. J.; Stumm, W. *J. Inorg. Nucl. Chem.* **1965**, *27*, 237.
(304) Stankevicius, V. *Zh. Prikl. Khim. (Leningrad)* **1972**, *45*, 1615.
(305) Starkenstein, E.; Steiger, R. *Arch. Exp. Pathol. Pharmakol.* **1933**, *172*, 104.
(306) Okura, T.; Goto, K. *Kogyo Kagaku Zasshi* **1955**, *58*, 239.
(307) Okura, T.; Goto, K. *Yoshui to Haisui* **1961**, *3*, 803.
(308) Saito, J.; Koshino, Y.; Kondo, G. *Nippon Kagaku Zasshi* **1963**, *66*, 99.
(309) Goto, T.; Unohara, N. *Kogyo Yosui* **1967**, 68.
(310) Frank, W. H. *GWF Gas—Wasserfach* **1968**, *109*, 198.
(311) Bond, D. C.; Bernard, G. G. *Ind. Eng. Chem.* **1952**, *44*, 2435.
(312) Takai, Y. *J. Jap. Wat. Works Assn.* **1967**, *394*, 19.
(313) Takai, Y. *J. Jap. Wat. Works Assn.* **1967**, *396*, 14.
(314) Takai, Y. *J. Jap. Water Works Assn.* **1973**, *466*, 5.
(315) Tamura, H.; Goto, K.; Nagayama, M. *Corros. Sci.* **1976**, *16*, 197.
(316) Meyerhof, O. *Arch. Ges. Physiol.* **1923**, *200*, 1.
(317) Meyerhof, O. "Chemical Dynamics of Life Phenomena"; Lippincott: Philadelphia, 1924.
(318) Posnjak, E. *Am. Inst. Mining Met. Eng.* **1926**, *1615D*.
(319) Quartaroll, A. *Gazz. Chim. Ital.* **1925**, *55*, 252.
(320) Reinders, W.; Vles, S. I. *Recl. Trav. Chim. Pays-Bas* **1925**, *44*, 29.
(321) Banerji, P. K. *Proc. Asiat. Soc. Bengal* **1922**, *18*, 71.
(322) Dokuchaeva, A. N.; Liepina, L.; Macejevskis, B. *Latv. PSR Zinat. Akad. Vestis, Kim. Ser.* **1969**, 164.
(323) Kuz'minykh, I. N.; Babushkina, M. D. *Zh. Prikl. Khim.* **1955**, *28*, 565.
(324) Dokuchaeva, A. N.; Liepina, L.; Macejevskis, B. *Latv. PSR Zinat. Akad. Vestis, Khim. Ser.* **1973**, 434.
(325) Kobe, K. A.; Dickey, W. *Ind. Eng. Chem.* **1945**, *37*, 429.
(326) Dokuchaeva, A. N.; Liepina, L.; Macejevskis, B. P. *Latv. PSR Zinat. Akad. Vestis, Kim. Ser.* **1969**, 167.
(327) Verhoeff, J. A. *Chem. Weekbl.* **1924**, *21*, 469.
(328) Levin, P. I.; Pronina, E. S. *Sb. Nauchn. Tr.—Vses. Nauchno—Issled. Gornometall. Inst. Tsvetn. Met.* **1958**, *3*, 98.
(329) Epatko, Yu. M.; Vorob'eva, K. A. *Polezn. Iskop. Ukr.* **1966**, 250.
(330) Singer, P. C.; Stumm, W. *Pap. Symp. Coal Mine Drain. Res. 2nd*, **1968**, 12–34.
(331) Yamamoto, Y. *Tokyohyritu Kogyo-syo-reikwan Kwagaku Kenkyu Hokoku (Rep. Chem. Res. Prefectural Inst. Advancement Ind., Tokyo)* **1940**, *2*, 21.
(332) Gilroy, D.; Mayne, J. E. O. *Brit. Corrosion J.* **1965**, *1*, 107.
(333) Chrētien, A.; Rohmer, R. *Ann. Chim. (Paris)* **1943**, *18*, 267.
(334) Reedy, J. H.; Machin, J. S. *Ind. Eng. Chem.* **1923**, *15*, 1271.
(335) Grant, R. F.; Wetherbee, H. E. U.S. Patent 1 606 470, 1927; *Chem. Abstr.* **1927**, *21*, 160 3.
(336) Leak, V. G.; Fine, M. M. *Ind. Eng. Chem. Fundam.* **1969**, *8*, 411.
(337) Kurimura, Y.; Ochiai, R.; Matsuura, N. *Bull. Chem. Soc. Jpn.* **1968**, *41*, 2234.
(338) Kauffmann, W. *Water (Holland)* **1948**, *32*, 217.
(339) Thomas, R.; Williams, E. T. *J. Chem. Soc.* **1921**, *119*, 749.
(340) Astanina, A. N.; Rudenko, A. P.; Kuznetsova, N. A. *Zh. Fiz. Khim.* **1972**, *46*, 369.
(341) Astanina, A. N.; Larina, N. A.; Rudenko, A. P. *Vestn. Mosk. Univ., Ser. 2: Khim.* **1977**, *18*, 244.
(342) Weiss, J. *Naturwissenschaften* **1935**, *23*, 64.
(343) Weiss, J. *Experientia* **1953**, *9*, 61.
(344) Evans, M. G.; George, P.; Uri, N. *Trans. Faraday Soc.* **1949**, *45*, 230.
(345) Abel, E. *Monatsh. Chem.* **1955**, *86*, 1036.
(346) Abel, E. *Monatsh. Chem.* **1956**, *87*, 113.
(347) Macejevskis, B.; Liepina, L. *Katal. Reakts. Zhidk. Faze., Tr. Vses. Konf., 2nd* **1966**, 486.
(348) Goto, K.; Tamura, H.; Nagayama, M. *Inorg. Chem.* **1970**, *9*, 963.
(349) Macejevskis, B.; Liepina, L. *Izv. Sib. Otd. Akad. Nauk SSSR, Ser. Khim. Nauk* **1968**, 32.
(350) Dutrizac, J. E.; MacDonald, R. J. C. *Miner. Sci. Eng.* **1974**, *6*, 59.
(351) Agarawal, J. C.; Giberti, R. A.; Irminger, P. F.; Petrovic, L. F.; Sareen, S. S. *Min. Congr. J.* **1975**, 40.
(352) Meyers, R. A. *Hydrocarbon Process.* **1975**, *54*, 93.
(353) King, W. E., Jr.; Lewis, J. A. *Ind. Eng. Chem. Process Des. Dev.* **1980**, *19*, 719.
(354) Thomas, G.; Whalley, B. J. P. *Can. J. Chem. Eng.* **1958**, *36*, 37.
(355) Garrels, R. M.; Thompson, M. E. *Am. J. Sci.* **1960**, *258A*, 56.
(356) Mathews, C. T.; Robins, R. G. *Aust. Chem. Eng.* **1972**, *13*, 21.
(357) Tseft, A. L.; Tatarinova, A. A. *Vestn. Akad. Nauk Kaz. SSR* **1958**, *14*, 32.
(358) Sasmojo, S. *Diss. Abstr. Int. B* **1970**, *31*, 656.
(359) Lowson, R. T. 6th RACI National Convention, Surfers Paradise, Australia, Nov 5–10, 1978.
(360) Smith, E. E.; Svanks, K.; Halko, E. *Am. Chem. Soc., Div. Fuel Chem., Prepr.* **1969**, *13*, 68.
(361) Nicol, M. J.; Scott, P. D. *J. S. Afr. Inst. Min. Metall.* **1979**, *79*, 298.
(362) Parsons, H. W.; Ingraham, T. R. Ottawa, Department of Energy, Mines and Resources, Inf. Circ. IC242, June 1970.
(363) Scott, P. D.; Nicol, M. J. *Rep.—Natl. Inst. Metall. (S. Afr.)* **1976**, 1858.
(364) Subramanian, K. N.; Stratigakos, E. S.; Jennings, P. H. *Can. Metall. Q.* **1972**, *11*, 425.
(365) Scott, P. D.; Nicol, M. J. *Rep.—Natl. Inst. Metall. (S. Afr.)* **1978**, 1949.
(366) Ingraham, T. R.; Parsons, H. W.; Cabri, L. J. *Can. Metall. Q.* **1972**, *11*, 407.
(367) Jibiki, K. *Diss. Abstr. Int. B* **1975**, *35*, 5454.
(368) Van Weert, G.; Mah, K.; Piret, N. L. *CIM Bull.* **1974**, *67*, 97.
(369) Tewari, P. H.; Campbell, A. B. *J. Phys. Chem.* **1976**, *80*, 1844.
(370) Kleinberg, J.; Argersinger, W. J., Jr.; Griswold, E. "Inorganic Chemistry"; D. C. Heath: Boston, 1960.
(371) Fox, F. M. *Philos. Trans. Royal Soc. London* **1830**, 399.
(372) Sato, M.; Mooney, H. D. *Geophysics* **1960**, *25*, 226.
(373) Gottschalk, V. H.; Bühler, H. A. *Econ. Geol.* **1915**, *7*, 15.

(374) Rosetti, V.; Cesini, A. M. *Period. Mineral.* **1957**, *26*, 63.
(375) Masuko, N.; Hisamatsu, Y. *Nippon Kogyo Kaishi* **1967**, *83*, 153.
(376) Ammou-Chokroum, M. *Bull. Mineral.* **1979**, *102*, 708.
(377) Baev, A. V.; Orlov, A. I. *Izv. Vyssh. Uchebn. Zaved., Tsvetn. Metall.* **1975** (*5*), 18.
(378) Biegler, T.; Rand, D. A. J.; Woods, R. *J. Electroanal. Chem. Interfacial Electrochem.* **1975**, *60*, 151.
(379) Wagner, C.; Traud, W. *Z. Elektrochem.* **1938**, *44*, 391.
(380) Evans, U. R. "The Corrosion and Oxidation of Metals: Scientific Principles and Practical Applications"; St. Martin's Press: New York, 1960.
(381) Tributsch, H.; Gerischer, H. *J. Appl. Chem. Biotechnol.* **1976**, *26*, 747.
(382) Sato, M. *Econ. Geol.* **1960**, *55*; part I, 928; part II, 1202.
(383) Klein, J. D.; Shuey, R. T. *Geophysics* **1978**, *43*, 1222.
(384) Ahmed, S. M. *Int. J. Miner. Process.* **1978**, *5*, 163.
(385) Ahmed, S. M. *Int. J. Miner. Process.* **1978**, *5*, 175.
(386) Petrov, I. V. *Tr. Vses. Nauchno-Issled. Proektn. Inst. Mekh. Obrab. Polezn. Iskop.* **1973**, *138*, 54.
(387) Sirunyan, R. M.; Abramyan, S. A.; Sagradyan, A. L.; Pogosyan, K. A.; Isaakyan, R. I. *Izv. Akad. Nauk Arm. SSR, Nauki Zemle* **1978**, *31*, 93.
(388) Kato, T.; Oki, T. *Nippon Kinzoku Gakkaishi* **1973**, *37*, 529.
(389) Loshkarev, A. G.; Yudina, E. A. *Tr. Sverdl. Gorn. Inst. im. V. V. Vakhrusheva* **1975**, *107*, 112.
(390) Springer, G. *Trans.—Inst. Mining Metall., Sect. C* **1970**, *79*, C11.
(391) Rechenberg, H. *Neues Jahrb. Mineral., Montsh.* **1951**, 88.
(392) Yashina, G. M.; Eliseev, N. I.; Bobov, S. S. *Izv. Vyssh. Uchebn. Zaved., Gorn, Zh.* **1978**, *21*, 124.
(393) Khudyakov, I. F.; Yaroslavtsev, A. S. *Tr. Ural. Politekh. Inst. im. S. M. Kirova* **1967**, *155*, 30.
(394) Yashina, G. M.; Vorob'eva, N. P.; Levin, A. I. *Elektron. Obrab. Mater.* **1980**, 53.
(395) Ospanov, Kh. K. *Izv. Akad. Nauk. Kaz. SSR, Ser. Khim.* **1977**, *27*, 1.
(396) Bitterlich, W.; Woebking, H. *Aufschluss* **1970**, *21*, 267.
(397) Makarov, G. V.; Nasipkalieva, Sh. K.; Buketov, E. A.; Minaeva, V. A. *Izv. Akad. Nauk Kaz. SSR, Ser. Khim.* **1979**, *29*, 31.
(398) Damjanovic, A. *Mod. Aspects Electrochem.* **1969**, 369.
(399) Lowson, R. T. *Aust. A.E.C., Res. Establ.* [*Rep.*] **1972**, *AAEC/E219*, Part 2.
(400) Wagman, D. D.; Evans, W. H.; Parker, V. B.; Halow, I.; Bailey, S. M.; Schumm, R. H. *NBS Tech. Note* (*U.S.*) **1969**, *No. 270-4*.
(401) Schumb, W. C.; Satterfield, C. N.; Wentworth, R. L. *ACS Monogr.* **1955**, **No. 128**.
(402) Wroblowa, H. S.; Pan, Y.; Razumney, G. *J. Electroanal. Chem. Interfacial Electrochem.* **1976**, *69*, 195.
(403) Biegler, T. *J. Electroanal. Chem. Interfacial Electrochem.* **1976**, *70*, 265.
(404) Yashina, G. M.; Olerskaya, N. L.; Smolenskaya, E. A. *Tr., Ural. Nauchno-Issled. Proektn. Inst. Mednoi Promsti.* **1975**, *18*, 137.
(405) Marchese, E. German Patent 22 429, 1882.
(406) Habashi, F. *Miner. Sci. Eng.* **1971**, *3*, 3.
(407) Gerischer, H. *Surf. Sci.* **1969**, *13*, 265.
(408) Tributsch, H.; Bennett, J. C. *J. Electroanal. Chem. Interfacial Electrochem.* **1977**, *81*, 97.
(409) Kunori, S.; Ishii, F. *Nippon Kogyo Kaishi* **1963**, *79*, 35.
(410) Meyer, R. E. *J. Electroanal. Chem. Interfacial Electrochem.* **1979**, *101*, 59.
(411) Ryss, Yu. S.; Ovchinnikova, T. M. *Metod. Tekh. Razved.* **1969**, *65*, 5.
(412) Ryss, Yu. S.; Chamaev, V. N. *Metod. Tekh. Razved.* **1975**, *101*, 30.
(413) Bernakevich, A. V.; Ryss, Yu. S.; Chamaev, V. N. *Metod. Tekh. Razved.* **1976**, *103*, 5.
(414) Lobanov, V. G.; Tyurin, N. G.; Sverdlov, S. S. *Fiz. Khim. Elektrokhim. Rasplavl. Tverd. Elektrolitov, Tezisy Dokl. Vses. Soveshch. 7th* **1979**, *3*, 100.
(415) Yashina, G. M.; Bobov, S. S.; Smolenskaya, E. A. *Korroz. Zashch. Neftegazov. Promsti.* **1980**, 5.
(416) Britz, D. *J. Electroanal. Chem. Interfacial Electrochem.* **1978**, *88*, 309.
(417) Peters, E. *Trends Electrochem. Plen. Invited Contrib. Aust. Electrochem. Conf., 4th* **1976**, (Pub. **1977**), 267.
(418) Hepel, T.; Hepel, M. *J. Electroanal. Chem. Interfacial Electrochem.* **1980**, *112*, 365.
(419) Eliseev, N. I.; Yashina, G. M.; Olerskaya, N. L.; Chanturiya, V. A. *Obogashch. Rud* (*Irkutsk*) **1976**, *4*, 53.
(420) Eliseev, N. I.; Yashina, G. M.; Boriskov, F. F.; Vorob'eva, N. P.; Averbukh, A. V.; Chanturiya, V. A. *Sovrem. Sostoyanie Perspekt. Razvit. Teor. Flotatsii* **1979**, 232.
(421) Yakhontova, L. K.; Sergeev, V. M.; Karavaiko, G. I.; Sukhantseva, V. S. *Ekol. Geokhim. Deyat. Mikroorg.* **1976**, 99.
(422) Karavaiko, G. I.; Pivovaroa, T. A. *GBF Monogr. Ser.* **1977**, *No. 4*.
(423) Yashina, G. M.; Smirnova, E. N.; Olerskaya, N. L.; Levin, A. I. *Izv. Vyssh. Uchebn. Zaved., Khim. Khim. Tekhnol.* **1977**, *20*, 1579.
(424) Clifford, R. K.; Purdy, K. L.; Miller, J. D. *AIChE Symp. Ser.* **1975**, *71*(*150*), 138.
(425) Michell, D.; Woods, R. *Aust. J. Chem.* **1978**, *31*, 27.
(426) Koch, D. "Modern Aspects of Electrochemistry", No. 10. Bockris, J. O. M., Conway, B. E., Ed.; Plenum Press: New York, 1975, Chapter 4.
(427) Kostina, G. M.; Chernyak, A. S. *Zh. Prikl. Khim.* (*Leningrad*) **1977**, *50*, 2701.
(428) Peters, E. *Metall. Trans., B* **1976**, *7B*, 505.
(429) Everhart, J. O.; Van der Beck, R. R. *Am. Ceram. Soc. Bull.* **1953**, *32*, 239.
(430) Banerjee, A. C. *J. Chem. Soc. D* **1971**, 1006.
(431) Safiullin, N. S.; Gitis, E. B. *Zh. Prikl. Khim.* (*Leningrad*) **1968**, *41*, 1686.
(432) Schwab, G. M.; Philinis, J. *J. Am. Chem. Soc.* **1947**, *69*, 2588.
(433) Kopp, O. C.; Kerr, P. F. *Am. Mineral.* **1958**, *43*, 1079.
(434) Schorr, J. R.; Everhart, J. O. *J. Am. Ceram. Soc.* **1969**, *52*, 351.
(435) Blachere, J. R. *J. Am. Ceram. Soc.* **1966**, *49*, 590.
(436) Ionescu, T.; Pincovschi, E.; Maxim, I. *Z. Anorg. Allg. Chem.* **1968**, *356*, 207.
(437) Hiller, J. E.; Probsthain, K. *Geologie* (*Berlin*) **1956**, *5*, 607.
(438) Thompson, F. C.; Tilling, N. *J. Soc. Chem. Ind., London* **1924**, *43*, 37T.
(439) Sinha, R. K.; Walker, P. L., Jr. *Fuel* **1972**, *51*, 125.
(440) Frost, D. C.; Leeder, W. R.; Tapping, R. L. *Fuel* **1974**, *53*, 206.
(441) Saksela, M. *Geologi* **1952**, *4*, 23.
(442) Frenzel, G. *Fortschr. Mineral.* **1957**, *35*, 23.
(443) Nambu, M. *Sci. Rep. Res. Inst., Tohoku Univ. Ser.*, ***1957***, *A9*, 215.
(444) Mapstone, G. E. *Chem. Ind.* (*London*) **1954**, 577.
(445) Chatterjee, N. N. *Q. J. Geol., Min. Metall. Soc. India* **1942**, *14*, 1.
(446) Makhija, R.; Hitchen, A. *Anal. Chim. Acta* **1979**, *105*, 375.
(447) Thom, G. C.; Waters, P. F.; Hadermann, A. F. *Hydrometallurgy* **1978**, *3*, 373.
(448) Janetski, N. D.; Woodburn, S. I.; Woods, R. *Int. J. Miner. Process.* **1977**, *4*, 227.
(449) Najdeker, E.; Bishop, E. *J. Electroanal. Chem. Interfacial Electrochem.* **1973**, *41*, 79.
(450) Ramasubramanian, N. *J. Electroanal. Chem. Interfacial Electrochem.* **1975**, *64*, 21.
(451) Zhavoronkova, V. V.; Kormil'tsev, V. V.; Ulitin, R. V. *Izv. Vyssh. Uchebn. Zaved., Geol. Razved.* **1967**, *10*, 119.
(452) Conway, B. E.; Ku, J. C. H.; Ho, F. C. *J. Colloid Interface Sci.* **1980**, *75*, 357.
(453) Yashina, G. M.; Olerskaya, N. L.; Eliseev, N. I. *Izv. Vyssh. Uchebn. Zaved., Gorn. Zh.* **1977**, *20*, 143.
(454) Case, G. D.; Farrior, W. L.; Green, D. A.; Stewart, G. W. Report METC/RI-79/3, 1979.
(455) Otsuka, R. Synopsis Graduate School of Science and Engineering, Waseda University (Japan) **1957**, *6*, 57.
(456) Fukui, J. *J. Phys. Soc. Jpn.* **1970**, *31*, 1277.
(457) Kelley, K. K. *Bull.—U.S., Bur. Mines* **1960**, No. 584.
(458) Naumov, G. B.; Ryzhenko, B. N.; Khodakovskii, I. "Handbook of Thermodynamic Data"; English Translation PB-226722/7GA, 1974.
(459) Mills, K. C. "Thermodynamic Data for Inorganic Sulfides, Selenides, and Tellurides"; Butterworth: London, 1974.
(460) Biernat, R. J.; Robins, R. G. *Electrochim. Acta* **1969**, *14*, 809.
(461) Puzei, N. V.; Zubritskii, I. A.; Muzychenko, L. A.; Rossovskii, S. N.; Fioshin, M. Ya. *Khim. Promst.* (*Moscow*) **1977**, 126.
(462) Gosh, M. M. "Aqueous-Environmental Chemistry of Metals"; Rubin, A. J., Ed.; Ann Arbor Science Publishers: Ann Arbor, Mich. 1974.
(463) Morgan, J. J.; Birkner, F. B. *J. Sanit. Eng. Div., Am. Soc. Civ. Eng.* **1966**, *92*, 137.
(464) Wrabetz, K. E. *Z. Elektrochem.* **1956**, *60*, 722.
(465) Goldhaber, M. B. *Geol. Surv. Open-File Rep.* (*U.S.*) **1980**, 80.